November 16, 2018
Jet Propulsion Laboratory,
California Institute of Technology,
MS-233-300,
4800 Oak Grove Drive.
Pasadena, CA-91109.

Biogeosciences,
Subject: Revision of Manuscript bg-2018-303

Dear Dr. Yakir:

Thank you for serving as the editor for our manuscript "Optimal inverse Estimation of Ecosystem Parameters from Observations of Carbon and Energy Fluxes", for possible publication in Biogeosciences. As suggested, I and the co-authors submit the revision of our manuscript in accordance with the reviewer comments.

We have provided our detailed responses to all the individual reviewer comments and made major and significant changes to our manuscript. Our primary changes to the manuscript are as follows:

1. We have now included 2 MODIS reflectance bands in our inversion framework. The results indicate that reflectance constrains LAI better which in turn reduced the fluctuations in Vcmax and BBslope leading to more realistic parameter estimates. We have demonstrated the improvement in results with simulations of our study sites. This is a substantial step forward and adds to uniqueness of the study in using SCOPE in the inversion framework.
2. More analysis and discussion are presented as to the inclusion of MODIS reflectance along with flux data in the revised manuscript. We have also highlighted the possible connection to seasonal variability in leaf nitrogen and fractional allocation to Rubisco to explain the seasonal variability of parameters from the retrievals (Vcmax, BBslope) and their ranges from available literature.
3. The model inter-comparison of previous and newer implementation of Photosynthesis is simplified, the result and discussion section are also streamlined as suggested by moving some details and figures to the supplementary information.

Our changes to the manuscript are indicated with a different color (and font) for both added and removed text, we have either specifically mentioned the changes in this letter or indicated their locations in the difference version attached to this letter for the other substantial changes. We believe that these changes to the manuscript as per the reviewer's suggestions have helped to greatly improve the manuscript. Thanks again for the valuable suggestions and attention to the manuscript.

Sincerely,
Debsunder Dutta

Response to Reviewer 1 Comments

MAIN COMMENTS

The article presents a methodology to estimate parameters of a land-surface carbon and energy balance model (SCOPE) through a Bayesian non-linear inversion framework. First, the biochemical model of photosynthesis is modified to resemble the model implemented in the land-surface model CLM4.5. Then, the values of three important parameters: Vcmax, BBslope (the slope of the empirical function relating net assimilation to stomatal conductance) and LAI are computed for one growing season for three locations characterized by different vegetation types, a C4 crop, a C3 deciduous forest and a C3 evergreen forest. The methodology leads to estimate the seasonality of the analyzed parameters (Fig. 9, 14 and 18) and improve model performance in reproducing carbon and energy fluxes (Fig. 12 and 16).

The article is generally well written, although with a large number of imprecisions (see detailed comments). From my evaluation the technical aspects of the inversion algorithm to estimate the parameters are rigorously implemented. However, I have a number of concerns which are detailed in the major comments below.

The authors thank the referee for the careful and detailed review of the manuscript. We consider the work presented in the manuscript as significant as it presents a framework to incorporate different types of observations at different scales and temporal resolutions in detailed process-based models to characterize explanatory dynamics of the ecosystem parameterizations which are either very uncertain or poorly represented in models.

The major objective here was to set up the inversion framework with SCOPE and demonstrate the usefulness in retrieving the temporal parameter variability. SCOPE is a detailed model about canopy physiological processes and energy balance and it can simulate the fluxes, spectral reflectance, SIF and many other variables thus offering a much greater potential.

We have optimized three key ecosystem parameters by allowing the parameters to take any value in the real positive space, and in-spite of allowing such a large range we found the optimized parameters to lie within physically feasible values. This may be possible due to detailed and accurate representation of canopy processes within the SCOPE model used in the study. The novelty also lies in the windowed approach and allowing the system (parameters) to evolve over long durations. We have mainly used the GPP and LE fluxes as constraining observations but in the revised manuscript we have now included MODIS reflectance as well and included more examples which demonstrated significant enhancements in LAI and perhaps Vcmax retrievals. The incorporation of MODIS reflectance is a substantial step forward as it makes use of the uniqueness of SCOPE, i.e. the coupling of a carbon cycle model with canopy radiative transfer and full modeling of spectrally resolved reflectance as a function of ecosystem structure. Following the comments, we have substantially revised the manuscript and streamlined the presentation of some material in supplementary information. Your comments thus greatly helped improve the overall content as well as readability.

(i) The algorithm of the Bayesian inversion framework is designed to provide robust numerical results and optimize the model parameters to reduce the mismatch between observations and simulations. However, the same results are likely less meaningful from a plant physiological point of view. This is important given the premises of the authors in giving a physiological interpretation of the parameters (Page 2, LL 7-9). When I see (a) Vcmax changing from less than 10 to 80 throughout the growing season (Fig. 9 and 14), (b) LAI decreasing from 5-6 to less than 4 in the second part of the growing season for a

crop, which is expected, at the very least, to maintain the same LAI until harvest (Fig. 9), or (c) a threefold variability in BBslope, I tend to think, there is a considerable adjustment of model structural issues rather than an estimation of meaningful ecosystem parameters. This is hinted by the authors when they say that they do not include evaporation from interception or have a simplified soil evaporation (Page 20, LL 2-4). Surely, Vcmax or photosynthetic capacity have been observed to change seasonally even considerably in a single tree (e.g., Wilson et al 2001; Misson et al 2006; Bauerle et al 2012; Wu et al 2017) but not in a range that cover almost the entire variability of Vcmax globally (Kattge et al 2009). What would be the physiological explanation for such a variation in Vcmax? The seasonality of leaf nitrogen content is surely much less pronounced. I think what we see in the seasonality of parameters is largely a compensation of model structural inadequacy (e.g., the jumps in correspondence to major rainfall events) and only partially a real seasonality. Better constraints should be placed on the potential range of the parameters. Furthermore, some of these "parameter" as the seasonality of LAI could be tested against ground or remote sensing observations to support or disprove the values obtained in the optimization. It is also not surprising that model results are improved (even though it is not clear how much, since R2 results with the non-optimized model are not reported) since now the parameter space is significantly larger, being parameters allowed to vary seasonally.

The paper presents a Bayesian non-linear inversion framework with a relatively complex process-based canopy radiative transfer and energy balance model (SCOPE) to estimate three key ecosystem parameters. One of the advantages of the framework is the flexibility to incorporate different observations in the measurement vector and different variables in the state vector along with a full posterior error characterization of the state vector. It may be noted that the estimated parameters and their seasonality (in comparison to real seasonality) will include uncertainties in the process representation in the model, the uncertainty in forcing and matching observations. We also note that we retrieve the "effective Vcmax_25", while carbon cycle models typically include a stress-factor ([0-1]), which scales Vcmax to account for stress factors, which might downregulate photosynthesis. This is an important aspect, as our inversion might eventually enable us to decouple and fit the stress-factor independently under the assumption of a relatively stable "true Vcmax".

In addition, we now also incorporated MODIS reflectances in our inversion scheme, which greatly reduces the variability in Vcmax and LAI and should alleviate these main concerns. We believe that parameters retrieved for the examples now represent reasonable temporal/seasonal variability. Thanks to the reviewer for the insightful references we have included these in the manuscript. The reference literature indicates global variability in Vcmax is perhaps much larger in the range of 0-150 or 200 (Gronedijk et al 2011, Archontoulis 2012), than what we have found for our study sites.

Groenendijk, M., et al. "Seasonal variation of photosynthetic model parameters and leaf area index from global Fluxnet eddy covariance data." Journal of Geophysical Research: Biogeosciences 116.G4 (2011).

Archontoulis, S. V., et al. "Leaf photosynthesis and respiration of three bioenergy crops in relation to temperature and leaf nitrogen: how conserved are biochemical model parameters among crop species?." Journal of Experimental Botany 63.2 (2011): 895-911.

Literature does support similar ranges of variability of Vcmax in the growing season (for different crop types) as we have found in our inversion results. Changes in leaf nitrogen and more importantly its allocation to Rubisco can cause substantial seasonal variability (e.g. Wilson et al 2000). There may be other biochemical reasons for increasing the photosynthetic capacity which are not parameterized in FvCB equations or even beyond scope of the current study (model structural issues). We have incorporated them in the discussion as suggested later by the reviewer in minor comments.

Section 7 (revised manuscript)

"There is strong evidence from measurements that under normal conditions both LAI and photosynthetic parameters have seasonal variability (Wang et al., 2008; Wilson and Baldocchi, 2000; Wilson et al., 2000), which correlate with energy fluxes. Our model inversion results are in alignment and agree well with these findings. From our results, we find considerable seasonal variability in Vcmax and BBslope (to some extent). Previously, many studies have reported measured Vcmax values of similar ranges such as, 0-70 μ mols m−2 s−1 (Wilson et al., 2000) for deciduous trees and 0-80 μ mols m−2 s−1 as annual variability in tall Japanese red pine forests (Han et al., 2004). In addition, most of the Vcmax variability is found in systems, which have seasonally variable or constant Nitrogen (N) content (Wilson et al., 2000). These changes may be mostly attributed to substantial in-season changes in the fraction of total N allocated to Rubisco as well as changes in leaf mass per area (Wilson et al., 2000). In addition, most models including SCOPE have no other method of imposing environmental stress than reducing Vcmax by a stress factor [0,1]. The effect of reductions in Vcmax are a reduction in assimilation, which also suppresses transpiration (that is stress might also change BBslope). Thus, we are fitting an 'effective' Vcmax parameter, which factors in effects from true changes in Rubisco content as well as the impact of environmental stress."

Throughout the description of results, we have now included both prior and posterior R2 values as well as the chi-2 error statistic which now do a much better job of comparing the results and demonstrating the improvement.

(ii) A major issue is also the use of a single year for the three locations. In this way, the robustness of such estimates across different years remain untested. In my view, an important test, would be to use the constant and seasonal parameters over few other years and see if the prediction are better in the case of seasonally variable parameters. Saying that they are better when they are optimized is completely expected and trivial. Finally, I am glad the author consider uncertainty in the flux-tower data (Sε), which is a very important aspect given the considerable uncertainties in flux-tower observations, however, how they do (Page 16, Line 2-3) is not very clear nor justified.

We initially used a single year to demonstrate the approach across three different ecosystems representing both C3 and C4 photosynthetic pathways. The three sites tested have different climates as well and we believe that the inversions across these sites test the approach and demonstrate that it is able to capture the seasonality of the parameters. As we have shown with our examples that the predictions are better with optimized parameters over their prior constant values across different ecosystems, we are certain this will be true (to different degree) when tested for other years as well.

Following reviewer comments, we have now incorporated MODIS reflectance bands and added a couple of more inversion retrieval examples. We have included a different years – 2009 (normal) and 2007 (drought) for the Ozark site as well as added another simulation for the Mead1 site for the year 2010, now including the MODIS reflectance bands. We find the reflectance acts as a much better constraint for LAI and in turn reduces fluctuations in Vcmax and BBslope to provide more realistic parameter estimates. The posterior simulations also show similar or better improvement in prediction of fluxes over their constant priors. These results have been presented in detail in the modified manuscript sections 6.3.2, 6.4.2 and 6.4.3.

The observation (flux tower) uncertainties are indeed incorporated in the Bayesian framework. In the absence of a formal error estimate from the flux-tower data itself, we currently use an average 10% uncertainty, which might be an underestimate in some cases. However, we can easily change this Sε

uncertainty in our retrievals and are open to suggestions from the flux-tower community. This point is further elaborated in the minor comments.

(iii) I also have doubts about the overall novelty of the study. Several other studies have been published using Bayesian approaches to parameter estimation with inverse methods in ecosystem or land-surface models (e.g., Mackay et al 2012, Xu et al 2006; Wu et al 2009; Wolf et al 2006). For instance, the authors do a remarkable job in highlighting the subtle differences of their work with respect to Wolf et al 2006 (Page 3, LL 15-21). Surely, in this article, the model is different, the optimized parameters are different and the inversion methodology has some peculiarity but overall the idea and scope is not much dissimilar from the ones of previous studies. If the novelty is on technical aspects of the methodology, then "Biogeosciences" may not be the most appropriate venue.

The inversion framework presented here provides a generalized Bayesian non-linear inversion approach for studying the temporal dynamics of the parameterizations from observations using process-based models. We have used SCOPE here because it is fairly sophisticated canopy model which uses spectrally resolved irradiance and also produces spectral reflectance and fluorescence along with water and CO2 fluxes which are coupled through leaf photosynthesis and stomatal conductance. Along with parameter estimations the framework provides posterior error estimates of the parameters. It is important to reconcile the estimated parameters along with their posterior uncertainties measures together for physiologically explaining the temporal variability in conjunction with forcing and observations. We do agree that we haven't yet really exploited the capabilities of SCOPE in our original manuscript as the inversions presented could have been performed with a much simpler ecosystem model. Thus, we have now added MODIS reflectance data in our inversion framework (discussed with many examples in section 6 of revised manuscript), which is the first step towards making full use of the SCOPE capabilities, i.e. spectrally resolved canopy radiative transfer (including fluorescence) in the short-wave as well as thermal infrared. This addition on our revised manuscript should set our manuscript apart from previously published research.

A major novelty of the study is that the framework is flexible to adapt to temporal or spectral observations easily (which is not a feature of most available Carbon cycle models currently) and the moving window approach is well adapted for capturing the temporal variability in the parameter space. There are very limited number of studies which are aimed towards capturing the temporal dynamics of the parameters (Wolf 2006 considers temporal variability of the parameters, and differences with the current work are already indicated in the literature review). In comparison most Monte-Carlo approaches (Mackay et al 2012, Xu et al 2006; Wu et al 2009) considers time invariance of the parameters and at the max gives a range of the parameters. These Monte Carlo methods also does not provide any definite error characterization as the Bayesian methods. This study presents a methodology by elegantly combining different ecosystem observations together to jointly estimate the temporal dynamics of ecosystem parameters using non-linear optimal approaches with process-based models. It is important to characterize the temporal variability of important ecosystem parameters in carbon-cycle or ecosystem models. The windowed approach provides an elegant approach to capturing the temporal dynamics in important ecosystem parameters and potentially more insight into stress events.

As mentioned, we have now modified the framework to assimilate observations of MODIS reflectance bands and match these with the spectral reflectance simulated by SCOPE model. A couple of retrieval examples for different ecosystems and years are presented. The assimilation of reflectance better constrains LAI and in turn Vcmax and BBslope. The posterior error reduction on parameters is improved as well. This is presented in detail in section 6 in the revised version of the manuscript.

(iv) Finally, some of the presented material is redundant. There is an entire manuscript part in comparing new and old implementations of the biochemical model of photosynthesis (Section 2.3 Fig. 2, 3, 4 and 5), which is just relevant for the SCOPE model users, since it is quite obvious that if one substitutes temperature functions in the bio- chemical photosynthesis module, he/she might obtain different results. These types of analyses are carried out by any model developer all the time, without the necessity to write 5 pages of peer-reviewed paper about it. Figure 11 is also very technical and I think it would be more appropriate for an appendix or supplementary material than for a main text. The results described for the three sites are also separated and many explanatory sentences are repeated. Their presentation can be largely streamlined, combining Figure 8, 13 and 17, Figure 9, 14 and 18, and Figure 10, 15 and 19 and removing the repetitive parts, highlighting differences among the case studies, rather than iterating the overall result presentation.

We agree with the reviewer in reorganizing some parts into a supplementary material. We would like to however keep some discussion related to the newer implementation of photosynthesis in the main text. We have modified the entire photosynthesis module together with its temperature dependence functions at the leaf element level (which is at the heart of energy balance) as well as a new A-Ci-gs iteration implementation. The comparisons are all shown al the canopy level, and the main message from the figures 2 and associated text carry is that the results are consistent after the major model changes but there are many subtle and noticeable differences as well indicating room for improvement in terms of optimizing the different parameters representing the processes (lines 3-7, page 11).

Following the reviewer suggestions, we have largely streamlined the manuscript, we have moved parts of the manuscript on comparing old and new photosynthesis implementations to the supplementary information along with previous figs 2, 4 and 5. We have also now removed previous Fig. 11 as suggested. The results section is streamlined and compactly presented with more analysis. Previous version figures 13 and 17 have been moved to the appendix as well.

DETAILED COMMENTS

Page 2 LL 5. See also Wramneby et al 2008; Pappas et al 2013.

Thank you for the references, and we have incorporated them in the manuscript.

Page 2 LL 18-19. Which model do you refer to? LSM, Ecosystem/Vegetation models or the biochemical models of photosynthesis? The first they also require shortwave radiation and precipitation as input and information about soil depth and properties, at the very least.

We refer to the ecosystem/vegetation models, which model the canopy processes to estimate the carbon and water fluxes (calculated as a byproduct of photosynthesis). SCOPE does require the specification of shortwave from which the PAR/APAR is computed. Below ground and surface processes are not simulated with SCOPE, only canopy radiative transfer and energy balance.

Modified page 2,3 lines 28-30, 1-2 on the revised manuscript states this:

"Further, the process based canopy models require some environmental drivers such as incoming shortwave and longwave radiation, air temperature, relative humidity, wind speed, and ambient CO2 concentration, along with a number of leaf and canopy parameters to simulate the fluxes of carbon in terms of gross primary production (GPP), flux of water or latent energy (LE), sensible heat (H), net radiation and others."

Page 2. LL 26. Rate-limiting, strictly speaking, refers only to Jmax not Rd.

Thank you, we have modified the sentence on page 3, line 7 to clarify this.

Page 2. LL 33-34. LAI in most of Terrestrial Biosphere Models is a prognostic variable not a parameter. As you correctly wrote in Page 3, LL 13-14. I think, this needs to be stated here.

Agreed, we have stated this in page 3, lines 14-15 here to make this point clear.

Page 3. LL 2. LAI can be also estimated from destructive observations.

Agreed and true. We have included this in the manuscript. We would like to note that in the present modeling exercise we characterize the dynamics of LAI over ecosystems and in-destructive methods seems to be the most suitable observations for comparison.

Page 3. LL 12 and Page 4 LL 12. SCOPE can model "spectrally resolved" radiation, but it remains unclear throughout the manuscript how many wavebands and which ones are considered?

A little description about wavelength ranges are already present in the SCOPE model description. The SCOPE model calculates outgoing spectrum of radiation from 0.4 to 50 μm. It resolves top of canopy incoming/outgoing radiation and reflectance in the spectral range of 0.4 to 2.5 μm @ 1nm wavebands. Further it also computes the spectrally resolved fluorescence emission in the range of 650 to 850 nm @ 1nm wavebands. It is clarified further that SCOPE considers the fully spectrally resolved radiation in the revised manuscript as follows:

P5 LL 15-17

"SCOPE resolves top of canopy incoming/outgoing shortwave radiation and reflectance in the spectral range of 400 to 2500 nm at 1nm wavelength bands. Further, it also computes the spectrally resolved fluorescence emission in the range of 650 to 850 nm at 1nm wavelength bands."

Page 3. LL 22 See also Mackay et al 2012.

Thank you, we have included the study in the introductory paragraph.

Page 3. LL 25. I would write "often the associated computational costs. . ."

Agreed we modified the sentence as suggested.

Page 3. LL 26-31. While I completely agree that modeling SIF and comparing SIF with observations is very important, since SIF is not explicitly used in this manuscript, such a long paragraph in the introduction, deviates from the main focus of the article.

An important feature of the inversion framework we develop is the ability to bring in different data streams to investigate the dynamics of ecosystem parameters and fluxes. This is particularly relevant when we use this framework with SCOPE as it can model the fully spectrally resolved canopy reflectance as well as the fully resolved SIF emission spectrum. Although initially we have focused on carbon and water fluxes as the main input data streams for the inversion we have now revised the manuscript to include simulations with satellite (MODIS) reflectance bands to demonstrate some of this capability. We

believe this is a unique advantage of using SCOPE in enabling use of data from different sensors. We feel that the description of this potential fits well in the introduction, as more SIF and spectrally resolved observations become available this framework can be utilized to better constrain and/or retrieve the dynamics of more ecosystem parameters.

Page 4. LL 26-28. So, in the end, how many prognostic temperatures do you resolve in the system? E.g., 2 temperatures for each layer for how many layers?

In SCOPE we resolve the sunlit and shaded temperatures for 60 vertical layers in the canopy. The vertical canopy is divided into 60 layers (standard implementation in SCOPE) to add up to total LAI.

Page 4. LL 28. Since you brought this up and this is not an easy problem to solve. Are iterations repeated until convergence? Which tolerance is used for convergence? If not, how many iterations are used?

Internally within SCOPE the tolerance used is the energy balance within the canopy, the iterations are repeated till convergence. The convergence criteria is an energy balance closure error <= 1.0 W/m^2. If the convergence does not occur within 100 iterations, the iterations are terminated and the energy balance error is stated.

Page 5. LL 10-16. I found this part explaining differences with CLM4.5 at least awkward. As a reader I want to know what you do now, not what was different from CLM4.5 in the previous model version.

We have presented that in the existing SCOPE version the implementation of Photosynthesis and its temperature dependence are in line with the older CLM4.0. However, we update the biochemical module to make the Photosynthesis and particularly its temperature dependence fully consistent with a major Earth System Model component CLM4.5 which is improved and broadly accepted by the community. Temperature dependence was a major improvement in CLM4.5 which we have implemented in the current SCOPE version. The important and major changes made to the SCOPE model are then further listed.

Page 5. LL 20-21. Please move to an earlier part of the section the explanation of what CLM is.

We agree with the reviewer and have now included the brief description of CLM (4.5) earlier in the section where CLM is mentioned for the first time. The modifications are found in P6LL 5-15(revised).

Page 6. LL 1. There is no mention of the parameter “intrinsic quantum use efficiency” or “quantum yield of photosystem II” depending how it is expressed. While it is considered constant by most biochemical models, this could also exhibit some variability (e.g., Skillman 2008) and could have been integrated in the optimization framework.

The quantum efficiency/yield of PSII for C3 photosynthesis is mentioned in the details (Appendix equation A6). As mentioned by the reviewer the value of max PSII yield is currently assumed to be constant as 0.85 in SCOPE biochemical module and could potentially be included in the optimization framework (also like temperature dependence parameters, etc). In the present work we would like to demonstrate our approach with the three important parameters and later on work with expanded or more targeted parameter space.

Page 6. LL 4-5. As before, please delete the second part of the sentence “in the earlier SCOPE version it was implemented as potential ETR x CO2 per electron”, this is not relevant here.

Thank you, we have deleted this part of the sentence.

Page 6. LL 15-20. Cs is not defined, but it must be the CO2 concentration on the leaf-surface, otherwise a leaf boundary layer resistance would be necessary in Eq. (1) and (2).

Thanks for the comment, yes Cs represents the CO2 concentration on the leaf surface we have included this in the description.

Page 6. LL 26. Iterative methods to solve the A – Ci – gs system were already included in ecohydrological models, (e.g., Ivanov et al 2008 and other land-surface models before that).

Thanks again, we have included this reference in the manuscript. In the present study we have included a Newton-Raphson scheme in SCOPE for the convergence of the A-Ci-gs convergence. This iteration was absent (or some complex unpublished scheme was present) in previous SCOPE versions.

Page 7. LL 1. This is repetitive, it has been already stated a few times.

We have removed this sentence.

Page 7, LL 6-7 and Figure 1, Caption. It is not clear what ±σ variability means. It is the variability in the parameters of the temperature functions, how σ is defined? Is the standard deviation of which parameter? What data from Leuning 2002 are considered/used for the plots? Are the temperature parameters rather than data taken from Leuning, 2002?

The parameters referred here (Fig 1) are the activation energy, deactivation energy, entropy in the temperature response functions of Vcmax (Appendix eqns B1, B2). The mean values and standard deviation (σ) are all computed from actual data of the parameters provided in the Leuning 2002 paper, the response functions are then plotted in figure 1 with these parameters. We have made the wording clearer in the caption (P8) and text (P8, LL8) to explain this part.

Page 7. Line 16. The two sites are not defined yet, their description is arriving much later in the manuscript, while it should be made upfront.

We agree that the site descriptions appear a little later in the inversion result sections, this is also clearly indicated in the parenthesis in the manuscript text. As also pointed out later the results shown in this section does not relate much to the explaining the physiological behavior of plants but rather as a comparison to show model improvement/consistency. The simulations with the SCOPE although required real observations and we show some actual comparison of GPP with tower values to show the model behavior after making changes to the model. We felt the actual meteorological/crop settings would be more relevant when looking at parameter optimization/ flux results and hence would like to present these at a later stage (result section) in the manuscript.

Page 8. Line 5, Figure 5 and Page 11 Line 4-6. Which version has been calibrated to the data? It is not surprising that the newer implementation is closer to observations, if Vcmax or other parameters have been optimized for the newer version. For instance, in Figure 5b you could likely adjust the value of Vcmax to obtain an opposite behavior, where the old model is unbiased and the new one is.

The results presented in figures 5 and 2 (earlier version) only indicate the improvement/change in carbon and water fluxes due to changes/improvement made to the SCOPE model, specifically the

implementations in modeling photosynthesis, its temperature dependence functions and the A-Ci-gs iterations. For these results same parameterization is used (not optimized yet but using reasonable values) and shows the difference in results obtained from old version and new modified version of the SCOPE model. We have now moved these figures to the supplementary information, with these figures we have demonstrated that with same parameterization but with improved process representation (photosynthesis, temperature dependence, etc) the model does a better job in capturing the fluxes.

Page 8. Line 9-10 and Figure 3 and 4 caption. I do not think you are showing any result for the Missouri Ozark site or Nebraska-Mead-1, you just use the meteorological forcing and C3 vegetation type derived for these sites to run the two version of the biochemical model and make a comparison. Strictly speaking you could have done a test varying temperature, VPD, and PAR for C3 and C4 vegetation without referring to any specific site. However, I do not find this part generally insightful for a journal article.

We partially agree, figures 3 and 4 (previous version) just illustrate the difference between two (old and new) model implementations, but we would like to argue that these results are a part of the model comparisons which also includes figures 2 and 5 (previous version) where we show site specific data such as GPP and LE comparisons. We therefore believe that it may be relevant to show the comparisons with real site-specific meteorological forcing data as well. Also, it may be erroneous to generate all the meteorological forcing synthetically as it may generate combinations of forcing variables (such as T, VPD or RH) which are unphysical and this may also lead to unphysical model outputs when driven with these forcing. Finally, we believe that the comparisons are necessary and important, we have modified the entire photosynthesis module together with its temperature dependence functions (which is the heart of energy balance) as well as a new A-Ci-gs iteration implementation. It is therefore important to show the model works (and probably shows improvement!) after the modifications. The modifications are done at leaf element level but the comparisons are shown at the canopy level. The messages figures 2-5 (previous version) conveyed are that the results are consistent after the major model changes but there are many subtle and noticeable differences as well indicating room for improvement in terms of optimizing the different parameters representing the processes (lines 4-7, page 11 revised version). The description of this part has now been greatly streamlined (section 2.2, revised version) and figures 2, 4 and 5 from previous version have been moved to the supplementary information.

Page 13. Line 4. The Jacobian depends on the linearization point, X_l, which is somehow approximated for any optimization window. This is discussed later but maybe it should be stated here already.

We have already briefly stated that the Jacobian for SCOPE is estimated numerically here (page 12, LL12-15, revised version), the formulation of moving window are stated later and therefore the method of setting up and estimating the Jacobians are also stated along with it.

Page 13. Line 14-15. It is fine to have a more in-depth treatment in the appendix, but at least you need to define the terms, Ki (the Jacobian matrix) is never defined at this stage of the article.

Thank you, we have defined Ki here at this step.

Page 14, Figure 6, and also Page 22, LL 5-6. Some of the derivative values are a bit surprising. Why LE is decreasing with increasing LAI? Is due to self-shading effects? This is generally counterintuitive. Even more difficult to understand is why LE decreases with increasing Vcmax. Higher photosynthesis should lead to higher stomatal conductance and thus higher LE, especially in a model like SCOPE. These unexpected behaviors need justification.

Thank you, the decrease in LE with an increase in LAI is indeed due to self-shading effects. In general, the nature of the Jacobians also depends on the meteorological conditions (temperature, VPD, RH etc) and their integration from leaf element level to canopy level is non-linear as such we expect the Jacobians to be diverse and maybe counterintuitive. We have clarified these in the text:

P14, LL 5-8, revised version

"*The decrease in LE is attributed to less radiation reaching the soil and corresponding increase in soil aerodynamic resistance. In this case the canopy resistance goes up but does not compensate for the decreased soil evaporation and results in low sensitivities."*

P15, LL 1-4, revised version

"It can be noted that the nature of these sensitivities at the canopy level are sometimes counter-intuitive from their leaf-level mechanisms and may vary depending on environmental conditions, such as incoming PAR as well as air temperature and vapor pressure deficit. This also creates diversity in the Jacobians over the diurnal cycle, which allows us to derive more than 2 parameters from 2 sets of measurements."

Page 15. Figure 7 caption. You need to specify what is "m" and what is intended here for ΔX. Plus, it should be better stated what the measurement vector refers to, since the derivative must be computed with model outputs.

Thank you, we have modified the figure caption to reflect and better explain the above-mentioned points.

Page 16. Line 2-3. The observational error matrix $S\varepsilon$ is quite important given the general uncertainty of flux-tower observations. However, from such a brief description "using noise standard deviation as 10% of observations" is not clear how this is computed. Does it mean that you assume an uncertainty of 10%? This is likely quite a low number in the context of flux-tower observations (e.g., Leuning et al 2012).

Thank you, our Bayesian inversion framework includes both observation noise and parameter prior errors which can be adjusted as per different site conditions to better optimize the retrievals. We assume that the flux observations have uncertainty of 10%. The actual uncertainty of flux observations is hard to characterize and also not available readily that is why we have made this assumption. The surface energy balance closure error has been generally reported to be around 10-30% (Wilson et. al, 2002, Von Randow et. al, 2004, Sanchez et. al 2010) and is found to be dependent on time-scales due to differences in energy storage terms in ecosystems (Reed, et. al 2018) (Leuning et. al. 2012 specifies closure for ~8% of sites sites with half hourly datasets). However, the important point we demonstrate here is the feasibility of the approach in parameter retrieval with full posterior error characterization using suitable apriori uncertainties.

Reed, David E., et al. "Time dependency of eddy covariance site energy balance." Agricultural and Forest Meteorology 249 (2018): 467-478.
Wilson, Kell, et al. "Energy balance closure at FLUXNET sites." Agricultural and Forest Meteorology 113.1 (2002): 223-243.
Sánchez, J. M., V. Caselles, and E. M. Rubio. "Analysis of the energy balance closure over a FLUXNET boreal forest in Finland." Hydrology and Earth System Sciences 14.8 (2010): 1487-1497.
von Randow, Coauthors, et al. "Comparative measurements and seasonal variations in energy and carbon exchange over forest and pasture in South West Amazonia." Theoretical and Applied Climatology 78.1-3 (2004): 5-26.

Page 16. Line 5. Which iteration step? The current one? This is relevant since K depends on where it is computed.

Yes, the Jacobian matrix K is computed at every iteration step, we modified the text to make this clear.

Page 16. Line 6-7. I am not sure I can see very well the concatenation between observations Y and modeled values F(X) in Figure 7. I just see ΔY.

The concatenation is performed for different variables (GPP, LE, etc) represented in different colors in the figure 4 (revised version), it is done for both observations (tower fluxes) and modeled values separately, ΔY represents the difference in observations and modeled values. We have clarified this in the figure caption (Pg. 15) and also the associated text.

Page 16. Line 20-22. I agree with the authors that 3-days sounds as a reasonable length for separating the time scales of parameter variability and meteorological forcing. But, what does it happen if you modify the time window and instead of 3 days you select 7 days or 15 days? Do you get similar seasonality of parameters? This is a test, which could be relevant in the scope of this article.

For the present problem 3-day sounds a reasonable length of the time-window, some early and initial testing with daily, 2-day windows also captured the seasonality. Windows of 7 or 15 days may be a little too long especially if there are artifacts in the forcing or observations data (as we have seen in many cases) it will make our parameter estimations poorer. The results will also depend on the parameter set we are optimizing, for the current set (Vcmax, BBslope, LAI) 3 days seems an appropriate window. We have not tried longer time-windows in our setup yet but assume they will work equally well if the boundary conditions (T/VPD, etc) don't change dramatically over the time-window. This might be something to test in the future.

Page 16. Line 24. I do not find where this is mentioned in Section 5.

This point is briefly mentioned in P16, Sec 5.3 (Details are in Rodgers 2000 which is referred in the article).

The detailed criterion is:

The strategy to update γ is that we compute R which is the ratio of the true change in cost function to the expected change in cost function.

- If R > 0.75 reduce γ (factor of 2), update X.
- If R < 0.25 increase γ (factor of 10), do not update X.

Page 17. Equation (17). The subscript "jj" is undefined.

Since S or Sa is a matrix, the index "jj" refers to the diagonal elements here, have clarified this point in the text (P17, LL12).

Page 18. Figure 8. Did you see that incoming shortwave radiation is reconstructed and actually almost equal for the first 60 days? Afterwards, fortunately, you do not use this period because it is not in the growing season, but such type of artifacts, which are frequent in Fluxnet data, could jeopardize your procedure. This may need a mention.

Thank you, artifacts in the flux data influence the inversion and optimization greatly and affects the results. We added the following lines of discussion (section 7, P35 LL2-4) on this point.

"Apart from observations, it should also be noted that filtering and quality control may be necessary for the meteorological and/or forcing fluxes as artifacts in the data can influence the inversion and optimization and greatly affects the results."

Page 18. Line 8. Why did you select a single year? I think it would be rather important to see how seasonality of parameters is retrieved in different years.

We used a single year to demonstrate the approach across three different ecosystems representing both C3 and C4 photosynthetic pathways. The three sites tested have different climates as well and we believe that the simulations across sites does test the approach and demonstrate that it is able to capture the seasonality of the parameters. It is also almost certain that seasonally variable parameters over constant values will show improvement in prediction over any other years as well. We selected the year 2010 because it was a normal (wet) year without any significant crop stresses.

With the reviewer's suggestions we have now demonstrated the parameter retrievals at the Ozark site with for two different years 2009 (normal year) and 2007 (with a late summer drought) utilizing only flux observations as well as flux and MODIS reflectance. *These results and comparisons are presented in detail in section 6.4 pages 24-30 of the revised manuscript.*

Page 19. Line 8-9, Please provide references for such changes in BBslope, LAI and Vcmax if they are found to be reasonable, which I do not think it is the case for BBslope and Vcmax.

As reported earlier the incorporation of MODIS reflectance constrains the parameters better. We believe the temporal variability in Vcmax (and order of magnitude) presented in the manuscript is very much feasible. This is already stated above in response previously and we have cited the proper references as well following the suggestions.

Wilson et al 2000 reported values of 0-70 μmols m^{-2} s^{-1} for Vcmax (Fig 2) for the deciduous trees also similar large ranges are reported in figs 3-5.

Han et al 2004 reported measurements of Vcmax over an entire year in the range of 0-80 μmols m^{-2} s^{-1} (Fig. 3)

Gronedijk et al 2011 presented the seasonality of Vcmax over cold, warm and temperature regions for grassland, savanna, broadleaf deciduous and evergreen forests. The ranges over a year vary from 0-150 μmols m^{-2} s^{-1} (fig, 5).

Archontoulis 2012 also presented Vcmax experimental values for crops ranging from 25 to 150 μmols m^{-2} s^{-1}.

It may also be possible to have large variability in BBslope values Wolf et al 2006 showed that seasonal variability in BBslope could vary from 15 to 25 (fig 7a).

We have discussed this in the manuscript, P34, LL 11-16.

Page 20. Line 12 and captions of Figure 10 and also Figure 15 and Figure 19. If it is a "correlation coefficient", why the symbol r2 is used, this is typically reserved for the "coefficient of determination", and not for the correlation coefficient, which is typically indicated by r.

The correlation mentioned here is the correlation in terms of two random variables (x,y), this is defined as COV(x,y)/(σx σy). We have changed it to more standard symbol such as ρ throughout the manuscript.

Page 21. Figure 11. The x-label with the indexes is not defined in the figure caption but only in the main text.

The x-label is an index representing the sequence (of values) after the observations are concatenated. We have indicated the meaning of the indices in the caption.

Page 22. LL 7 and LL 10 and Figure 12 caption. How much is it this "net improvement"? The value of R2 for the previous parameter set is not reported, values are only reported for the optimized model.

We have computed the value of R2 for the unoptimized parameter set and added them for every example in the paper which makes the improvement clear. In addition, we have also reported the chi-square statistic for comparing the results.

Page 23. LL 12. It is quite well-known that the growing season is longer for a deciduous forest than for a crop. I would suggest eliminating "we find".

Thanks, we have made the correction.

Page 24, LL 13 and Page 29, LL 6-7. What could justify a threefold change of BBslope in a single growing season? This is theoretically an intrinsic property of the stomatal regulation, I can see how can change during leaf development (very first part of the growing season) or if water stress occur, but I do not see what can justify such a large variability throughout the entire season.

The BBsope results previously presented (just with flux observations) does not show three-fold change everywhere. For the deciduous site at Ozark the BBslope for year 2010 changes between DOY 100 and 250 were very subtle and small with the values varying between 5-7. The newer simulations and comparisons with MODIS data indicate that BBslope is much better constrained in our case the improvement is clear for the mid-season spike for the Mead1 site, discussion is presented in section 6.3.2. The BBslope is now also better constrained for the Ozark site for two different simulation years as presented in section 6.4 of the revised manuscript.

For the Evergreen forests the three-fold variability could be representative of the stomatal activity after a dominant cold season and it could be a model structural issue as well (as now described therein section 6.5.2). Finally, it may be possible for large variability in BBslope values Wolf et al 2006 (Fig 7a) showed that seasonal variability in BBslope could vary from 15 to 25, this point is mentioned in the discussion section.

Page 25. LL 13-16. The value of R2 for the previous parameter set is not reported, values are only reported for the optimized model. How much the results were improved remains unverifiable, although clear from Figure 16.

Thank you, yes, we have added the value of R2 for the unoptimized case as well to make the improvement clearer.

Page 27. LL 2-6. Please consider that at Niwot Ridge snow-cover is affecting energy exchange and potentially GPP for a large fraction of the year. It is true that you focus only in the snow free-period, but this confounding element needs to be stated somewhere.

Thank you, this point stated in the manuscript where the Niwot ridge site is discussed (P31, LL10).

Page 27. LL 10. The constraint on LAI from observation is a very good addition to the modeling exercise, I would have liked to see this type of constraints placed also for other sites, or parameters, whenever available.

Thank you, the constraint on LAI for Niwot ridge was available from literature, in comparison constraints on Vcmax or BBslope are much harder to obtain. We have now added MODIS data as well to enable better constraints at the other sites.

Page 29. LL 16 and Page 30 LL 4-5. I am sorry, but I am thinking you mostly retrieve "model parameters" and not "ecosystem parameters", and I also tend to think you are "overfitting" the SCOPE model rather than constraining it. The advantage of using seasonality of parameters for predictive simulations (e.g., in other years or other conditions) remain to be tested.

We would like to argue that the retrieved model parameters which are representative of ecosystem parameters. We have utilized the fluxes at ecosystem level from flux towers in process-based canopy models (assuming homogeneity in ecosystems). The results obtained from the inversion are thus representative of the ecosystem parameters with certain uncertainty. Some information about overfitting may be examined from the chi2 values computed during the inversion (which are not presented in the manuscript) but the reduction in chi2 values (posterior simulation) after optimization indicate that these points may not be overfitted. The method is also further tested for different climatic conditions and vegetation types across different ecosystems.

Page 29. LL 22. Yes, LAI and Vcmax have seasonal variability but for Vcmax unlikely in the order of magnitude that is presented here.

The optimized parameters also include the uncertainty associated with observations as well as errors in the process representations of other unoptimized parameterizations in the model. The variability of Vcmax we have obtained is not highly unlikely (as mentioned in the previous comments and supported with references), our optimization and inversion framework also account for full posterior error characterization and test of independence (correlation coefficients). The results of optimized Vcmax must also be therefore interpreted with these uncertainty measures. As presented earlier the variability in Vcmax may be due to seasonal variability in relocating nitrogen to Rubisco and further other stress factors which may be lumped into the Vcmax values. Please note that the addition of MODIS reflectances has now greatly reduced the variability in LAI and Vcmax. These points are mentioned in the discussion of the manuscript (P34, LL16-24).

Page 29. LL 27-30. While interesting the discussion on SIF is out of place, since SIF is not used or treated in this article.

We have already extended our work by incorporating satellite reflectance in the inversions. We would like to mention SIF here because it is an important output from SCOPE model (spectrally resolved) and

the inversion framework is easily adaptable to incorporate these observations which is an important future research direction.

Page 30. LL 16. Optimality approaches (e.g., Medlyn et al 2011, Katul et al 2010) do not typically comprise soil-moisture dependences, which therefore need to be included as additional parameterizations.

We agree and indicated this point in the discussion, P35, LL10-14.

Page 30. LL 18. Rather than "better solution", I would say it can provide "optimized model parameters."

We have changed the wording as suggested.

Page 30. LL 19-25. All this paragraph is emphasizing the technical aspects of the "optimal inverse estimation of the parameters", I am wondering if this is the most effective way of concluding the manuscript.

We have revised this to include some physiological aspects into the discussion and the forward outlook of our work. (P36 LL 13-15).

Page 31. LL 7-8. This sentence is quite repetitive.

We have removed the sentence.

Page 34. LL 9. I would suggest to write "will allow us".

Thank you we have made the change.

Response to Reviewer 2

The present study attempts to develop an optimal inversion framework to use SCOPE for estimating Vcmax, m, and LAI by against measurements of carbon and energy flux from EC towers. They demonstrated the applicability of their approach in terms of capturing the seasonal variability of these key ecosystem parameters.

The current work may provide additional information on estimating key ecosystem parameters from field data. Compared to the literatures, however, the novelty of the current study is not clear. There are so many papers which estimates the key ecosystem parameters from models and EC flux tower data (e.g., Mackay et al 2012, Xu et al 2006; Wu et al 2009; Wolf et al 2006; Wang et al., 2010). What is the main novelty for this work? If it is the technical approach of an optimal inversion framework, then it may go some other technical journal. Even for the inversion framework, I didn't see too much improvements compared to previous work.

My general impression is that this work is a rather technical description on the inversion framework of using SCOPE. I understood the rather detailed information by the authors, but the manuscript is really too long and some parts are too lengthy. I think some parts could be simplified.

We thank the reviewer for the comments on the manuscript. In this study we try to set up an inversion framework with the SCOPE model which is a fairly sophisticated canopy radiative transfer and energy balance model. SCOPE uses spectrally resolved irradiance and also produces spectral reflectance and

fluorescence along with water and CO2 fluxes which are coupled through leaf photosynthesis and stomatal conductance. As also indicated by reviewer 3, a major novelty of this study is breaking up the seasonal assimilation into smaller time windows and together with a fully Bayesian non-linear optimal estimation approach allows us to get posterior estimates of state vector comprising a number of important ecosystem parameters together will its full uncertainty characterization.

To address the novelty comment further we have now modified the framework to assimilate MODIS reflectance bands and match these with the spectral reflectance simulated by SCOPE model for optimal parameter estimation. We admit that our original manuscript didn't really make use of the complexity of the SCOPE model and the benefit of modeling spectrally resolved reflectance (and fluorescence, thermal emissions). A couple of retrieval examples are now presented as well for different ecosystems. The results using 2 MODIS bands indicate much better constraints on LAI and in turn on Vcmax and BBslope (which partially interfered with LAI before). This constraint further reduces the fluctuations in the retrievals due to observational noise in the fluxes. The posterior error reduction is also improved as a result. More discussion about the results of parameter retrieval and further intercomparison within sites and year are presented as well. More discussion of physiology and ecosystem functioning as revealed with parameter estimations are included as well. Finally following the comments of all the reviewers, we have streamlined the presentation and included supporting information in the supplementary.

Response to Reviewer 3 (Peter Rayner)

This paper demonstrates a method for assimilating site-level flux observations into a terrestrial biosphere model. Its novelty lies in breaking the assimilation into short windows to capture high-frequency variations in the parameters it estimates. given the variety of journals within the Copernicus family, I wonder whether this article is better suited to GMD than BG (see comments below) but this is mainly a question for the editor. The paper is also clearly written, verging on the tutorial at times.

I have one significant concern with the paper and one general request for more analysis. My concern is the analysis of the results. This is quite thin. The only commentary I can see on the results in the discussion section is: "There is strong evidence from measurements that under normal conditions LAI and photosynthetic parameters have seasonal variability [Wang et al., 2008; Wilson and Baldocchi, 2000; Wilson et al., 2000] which correlate with observations of energy fluxes. Our model inversion results are in alignment and agree well with these observations." this seems quite a poor scientific return from a difficult and well-executed piece of work. I would recommend particularly using the posterior simulation to look at some other observables. Do you do a better job matching the high SIF values over the corn site? If so, why, e.g. which parameter, Vcmax or LAI is mainly responsible? What temporal resolution of the parameters is necessary to capture the important variations? I suspect these questions only scratch the surface. I stress that this is potentially a good paper. What it does it does well but I believe it needs more scientific content before publication. If the authors wish to maintain it near its present form I believe it is better suited as a demonstration of a new methodology and hence to GMD.

My request is to delve a little deeper into why the system works better at some places than others. I note there seems less analysis of the Niwot Ridge results which were, in general, also less successful (lower correlation for example). Remember that a less successful assimilation is *not* a failure but rather a useful probe into model performance. It says definitively "we have a problem here and it isn't the choice of parameters". This is even clearer in this case where the parameters are allowed to vary in time.

We thank Peter Rayner for his valuable and insightful comments. The comments have helped us to improve our manuscript greatly. We have addressed the concerns raised and made major revisions to the

manuscript following the comments of all the reviewers. BG will be a great outlet for readers interested in the coupled carbon and water dynamics in ecosystems. The developed moving window inversion framework would serve as a valuable tool for the exploration of different and rather difficult to measure ecosystem parameters using a number of observational data streams. This study is an initial step towards this objective, we thus hope that this journal is appropriate, especially given our substantial improvements in the revised version.

We have added significantly more analysis to the manuscript. We have now incorporated MODIS spectral reflectance bands in the inversion framework for two of our examples. The results are promising and suggest much better constraint on LAI, which in turn reduced fluctuations in Vcmax and BBslope. The retrieved parameters are more realistic and the sensitivity of the inversion towards sudden fluctuations in tower observations is reduced (sec 6.3 and 6.4). Within and inter site comparison of the retrievals is also presented when reflectance data is assimilated in the inversion framework.

We have also further added more posterior simulation results and discussed the effect of optimization results for the different sites for different years with and without using MODIS data with flux observations. As suggested we have gone deeper to better explain retrieval results and their fluctuations from the simulations. Discussion about effects of nitrogen variability and Rubisco allocation on Vcmax seasonal variability is also presented (Sec 7). We have also analyzed the results of posterior simulations from Niwot ridge as suggested. Further, we have streamlined our work by moving some material to the supplementary information.

Minor comments

P14 In fact the Jacobian doesn't quite show the problem is non-linear, it could be that all the variation is a result of different forcing.

We would like to clarify that the Jacobian shows the response slope at different times of the day due to a small perturbation in the variables of the state vector. Most importantly, we find the Jacobian to change with subsequent iterations, which is a clear sign of non-linearity.

P16L3 The choice of observational error is quite important in DA, hopefully this is checked later.

Yes, we have included the observational error in the inversion scheme. We assume that the flux observations have uncertainty of 10%. The actual uncertainty of flux observations is hard to characterize and also not available readily, which is why we have made this simplified assumption. The surface energy balance closure error has been generally reported to be around 10-30% (Wilson et. al, 2002, Von Randow et. al, 2004, Sanchez et. al 2010) and is found to be dependent on time-scales due to differences in energy storage terms in ecosystems (Reed, et. al 2018). However, the important point we demonstrate here is the feasibility of the approach in parameter retrieval with full posterior error characterization using suitable a-priori uncertainties. We have included some discussion to state this point and the scope of characterizing the observation noise better in the framework (P35, LL 3-7).

Reed, David E., et al. "Time dependency of eddy covariance site energy balance." Agricultural and Forest Meteorology 249 (2018): 467-478.
Wilson, Kell, et al. "Energy balance closure at FLUXNET sites." Agricultural and Forest Meteorology 113.1 (2002): 223-243.
Sánchez, J. M., V. Caselles, and E. M. Rubio. "Analysis of the energy balance closure over a FLUXNET boreal forest in Finland." Hydrology and Earth System Sciences 14.8 (2010): 1487-1497.
von Randow, Coauthors, et al. "Comparative measurements and seasonal variations in energy and carbon exchange over forest and pasture in South West Amazonia." Theoretical and Applied Climatology 78.1-3 (2004): 5-26.

P16L10 I doubt the size of observational vector has much impact on computational efficiency, can you comment why it would?

Thanks for the comment, by size of the observational vector we meant the number of days and the number of time points (half hourly/hourly) for constructing the concatenated observation vector. This will have a direct impact because it will increase the number of time points (instances) for the forward model runs this will also increase with the number of parameters. This will significantly increase the computational time.

P16L20 The choice of time resolution is also important and yours seems very short. This is likely to lead to parameters which can vary fairly rapidly in time but which are also quite uncertain as they are constrained by fewer observations. Hopefully you can comment on whether parameters change significantly, i.e outside their uncertainty limits.

Thanks for the comments, we believe that the 3-day window sounds short but reasonable, as variations in environmental stress can happen on synaptic time-scales. It might eventually be better to group the season into blocks with similar "drivers", e.g. VPD, temperature, PAR, but for now, we tried to find a consistent window length, which would allow us to discern short-term fluctuations.
We had performed some initial testing with other window sizes (not shown), which showed that a 3-day window is appropriate. Regarding the rapid and abrupt changing of parameters, we could observe this in particular when flux observations appeared to be quite noisy. The addition of more constraint in these cases is extremely beneficial as we have now clearly demonstrated with the inclusion of MODIS reflectance data, which has greatly improved our results for the Mead-1 site (revised ver Fig. 7). The measure of error reduction has also significantly improved with the inclusion of reflectance data (revised ver Fig.8 with associated changes in sec 6.3 and 6.4).

P16 Eq. 12, this should have a term from the prior included I think. Unless there's no prior.

Thank you, the full chi-square error we are minimizing in the optimization does have a term from prior error included. However, in order to test the convergence for each iteration in the retrieval windows (and stopping criteria) we use the mentioned criterion to test the difference between the fit and measurements (excluding the prior). This is clarified in the manuscript P16, LL23-26.

P19L7 "reasonable and realistic" is a little vague, perhaps some references would help.

We agree and have removed this sentence and we have included references in the discussion of results (sec 7) for our examples which support the values of Vcmax and other parameters obtained in this study.

P20L10 be careful about describing correlations as describing how parameters move since these are uncertainty not signal correlations. the sentence above makes it clear you understand this difference but many of your readers will be less clear.

Thank you for this comment/warning. Yes, we agree that the error correlation has to be considered as a posterior inversion property and not be confused with actual physical behavior of the variables. These are a result of the inverse retrievals and gives us an indication whether the variable pairs are independent or have a positive or negative association in the retrievals. The actual association in nature between the variables may or may not be similar. We have further clarified this in the manuscript (P23, LL10-12 and in subsequent results descriptions in section 6.).

P20L14 but here you do confuse signal and error, this correlation does NOT indicate they are changing in sync

We agree the relationship between the variables is only valid in the context of the retrievals and this may or may not be the true association between the variables we find in nature and this association may change depending on different environmental stresses and conditions. We will probably have more confidence regarding the true nature of correlation between the variables if under different retrieval schemes/constraints the error correlations are found to be similar. We are able to include some discussion when we incorporate the MODIS reflectance in the error covariances and compare the error correlations between the two cases (sections 6.4.2 and sections 6.4.3). MODIS reflectance data greatly helps to reduce error correlation, in particular between Vcmax and LAI.

P20 in general you seem to be quoting r^2 but claim this can be negative. You probably mean r.

This was also mentioned by the other reviewer, we have now changed all instances in the text and figure to ρ for the correlation coefficient.

P21 I'm not sure that the figures showing your algorithm works are necessary, especially in a journal like biogeosciences where you should focus more on the science and less on the algorithm.

Thank you, we as also mentioned by the other reviewer we have streamlined the presentation and moved some parts to the supplementary information and appendix. We have now removed figure 11 in the revision.

P22L3 as noted earlier the diurnality is not a measure of nonlinearity.

Thank you, as we mentioned we think the variability throughout the day and subsequent evolution when multiple days are concatenated together makes the problem non-linear. In most cases the variability seems diurnal but in some cases K matrix becomes a highly variable and represents a non-linear 3-d surface which varies with different environmental conditions.

P22L10 don't quote improved correlation as a measure of fit, you could have a great correlation and terrible performance if, for example, diurnal variations had great phase and terrible amplitudes. rms is a better though not perfect statistic.

Thank you, we have now presented the coefficient of determination for both prior and posterior simulations for all the examples, together with this we have also now presented the chi2 error statistic as a measure to represent the improvement in performance.

P25 See earlier comments on signal and error correlation.

Thank you, we have again clarified this part in the manuscript (P23, LL10-13, P28 LL 9-14).

P25 can you explain further why a strong negative correlation means you need to optimise both, the step from "you can't see them separately" to "you must do both of them" isn't so clear to me.

Thank you, in this context we simply mean that from the retrieval framework perspective the results indicate there is a strong negative linear association between the two variables. As such these are not independent and therefore not ideal to be optimized independently. We agree that the logic as written was faulty and we have removed this from the text.

P25 I hope you go on to compare the performance at the two sites, one of them seems much harder than the other.

We have now included the MODIS datasets and provided a substantial comparison of the results of parameter retrievals using only flux observations to that using both flux and reflectance observations for both the Mead and Ozark study sites for multiple years. The variability in all the three parameters greatly reduced due to the addition of reflectance for the Mead site and at the Ozark site this change made the parameters to be more realistic in addition the posterior simulations suggested a significant improvement in LE fluxes over the other year. These are presented in detail in section 6 in the revised manuscript.

P27 I'm betting you originally tried to fit LAI at NWR and couldn't. That's not a failure, it's interesting information so is probably worth discussing. You're only fitting in 3 day windows so neither site really knows about the evolution of LAI from one window to the next so why does one work well and the other not, provided I'm guessing correctly.

Thank you, yes this is the unique advantage of using a fully Bayesian framework, we found out approximately the true expected value of LAI for NR and prescribed an extremely low prior error on it and thus our windowed simulations maintain it as nearly constant values, this is also a nice test about the mechanism of the inversion. We did some tests where the LAI was allowed to vary and it did indeed try to match mainly the GPP and LE variability. In terms of physiology the changes in GPP (and LE) in SCOPE is mostly attributed to LAI and Vcmax (and BBslope). In Niwot ridge due to cold climates there is other plant physiological signaling which stops the photosynthesis without apparent changes in LAI (or Vcmax) like the deciduous forests. This is thus probably a model structural issue which SCOPE is not able to capture just as a stress factor in Vcmax. We have added this part in the NR discussion of results, section 6.5.2.

P29L13 This site analysis doesn't seem as well developed as the others, e.g. quality of fit etc.

We have now included the results of posterior and prior simulations and discussed the fits after optimizing the parameters, section 6.5.2.

P29L30 do you mean changes in the temperature dependencies or more simply that there *is* a temperature dependence?

Thank you, we mean changes in temperature dependency due to changes in activation, deactivation and entropy parameters which are incorporated carefully into the modified version of SCOPE in this study and which the current inversion framework is fully equipped to optimize. As discussed this is although a future scope of work (P36 LL9-12).

P30L20 In what sense is the approach "stepwise"? This term was previously used by Bacour et al. (2015), doi:10.1002/2015JG002966) to describe optimising for one observable then using its posterior parameters as priors for the next observable. They would describe your method as "all at once", what do *you* mean by stepwise?

We meant stepwise in the context of a within window optimization, in a sense that the LM algorithm takes a stepwise change in the parameter space considering the prior and the observation errors to achieve optimal solutions. As pointed when we look at the broader scheme of things seasonally the optimization seems to be all at once for each time window. We have slightly modified the sentence to better present this.

Optimal Inverse Estimation of Ecosystem Parameters from Observations of Carbon and Energy Fluxes

Debsunder Dutta[1], David S. Schimel[1], Ying Sun[3], Christiaan van der Tol[4], and Christian Frankenberg[1,2]

[1]Jet Propulsion Laboratory, California Institute of Technology, Pasadena, CA, United States.
[2]Division of Geological and Planetary Sciences, California Institute of Technology, Pasadena, CA, , United States.
[3]School of Integrative Plant Science, Soil and Crop Sciences Section, Cornell University, Ithaca, NY, United States.
[4]Faculty of Geo-Information Science and Earth Observation (ITC), University of Twente, Enschede, The Netherlands.

Correspondence: Debsunder Dutta (Debsunder.Dutta@jpl.nasa.gov); Christian Frankenberg (cfranken@caltech.edu)

Abstract. Canopy structural and leaf photosynthesis parameterizations such as maximum carboxylation capacity (V_{cmax}), slope of the Ball-Berry stomatal conductance model (BB_{slope}) and leaf area index (LAI) are crucial for modeling [..[1]]plant physiological processes and canopy radiative transfer. These parameters are large sources of uncertainty in predictions of carbon and water fluxes. In this study, we develop an optimal moving window non-linear Bayesian inversion framework to use the Soil Canopy Observation Photochemistry and Energy fluxes (SCOPE) model for [..[2]]constraining V_{cmax}, BB_{slope} and LAI [..[3]]with observations of coupled carbon and energy fluxes [..[4]]and spectral reflectance from satellites. We adapted SCOPE to follow the biochemical implementation of the Community Land Model and applied [..[5]]the inversion framework for parameter retrievals of plant species having both the C_3 and C_4 photosynthetic pathways across three ecosystems. We present comparative analysis of parameter retrievals using observations of (i) Gross Primary Productivity (GPP) and Latent Energy (LE) fluxes [..[6]]and (ii) improvement in results when using flux observations along with reflectance. Our results demonstrate the applicability of the approach in terms of capturing the seasonal variability and posterior error reduction (40-90%) of key ecosystem parameters. The optimized parameters capture the diurnal and seasonal variability in the GPP and LE fluxes well when compared to flux tower observations ($0.95 > R^2 > 0.79$). This study thus demonstrates the feasibility of parameter inversions using SCOPE, which can be easily adapted to incorporate additional data sources such as spectrally resolved reflectance and [..[7]]fluorescence and thermal emissions.

[1]removed: the
[2]removed: estimating
[3]removed: by constraining
[4]removed: from eddy covariance towers
[5]removed: a moving window Bayesian non-linear inversion framework using SCOPE to invert the ecosystem parameters V_{cmax}, BB_{slope} and LAI that best match flux-tower observations of
[6]removed: . We applied this inversion framework to plant species having both the C_3 and C_4 photosynthetic pathways across three different ecosystems
[7]removed: solar induced chlorophyll fluorescence

1 Introduction

Terrestrial ecosystems play a very important role in regulating the carbon exchange over land surfaces(Schimel, 1995; Falkowski et al., 2000). Although they are known to be important sinks in buffering the increasing anthropogenic CO_2 emissions (Friedlingstein et al., 2006; Sitch et al., 2015), there is a large variability and heterogeneity in the carbon exchange mechanisms which are tightly correlated with inter-annual climatic variations (Cox et al., 2013; Liu et al., 2017). Moreover, terrestrial ecosystems also control the exchange of energy, water and momentum between the atmosphere and the land-surface, thus regulating climate-ecosystem (carbon) feedbacks leading to amplification or dampening of regional and global climate change (Heimann and Reichstein, 2008). Measurements and modeling of carbon and water vapor fluxes over terrestrial ecosystems are therefore [..[8]]important to better understand these issues and account for the regional and global carbon and water budgets (Baldocchi et al., 1996, 2001; Sitch et al., 2003, 2008). Terrestrial ecosystem models have been used to study the carbon and water fluxes (McGuire et al., 2001; Sitch et al., 2003; Cramer et al., 2001; Kucharik et al., 2000), however there are large uncertainties in fluxes associated with poorly quantified model parameters [..[9]](Wramneby et al., 2008; Pappas et al., 2013; Knorr and Heimann, 2001; Zaehle et al., 2005; Rogers et al., 2017). Some of these parameters have temporal and spatial variability and are hard to measure directly over large scales (Simioni et al., 2004; Wilson et al., 2000; Dutta et al., 2017). For the majority of model implementations these parameters and their temperature dependence are represented as a single constant value according to plant functional types with little or no seasonal variability. In this study, we present an inversion approach which can be implemented with ecosystem models involving canopy physiological processes to better estimate the seasonal variability in photosynthesis and canopy structural parameters, which in turn can reduce the uncertainty in estimation of carbon and water fluxes over ecosystems.

The micrometeorological data from flux towers is extremely useful in understanding the biogeochemistry and thermodynamics of ecosystems (Baldocchi et al., 2000; McGuire et al., 2002). A number of approaches have been developed to model and estimate photosynthesis, respiration, energy balance, stomatal behavior, radiation transfer and turbulent gas exchange across the plant canopy on the basis of data from flux tower experiments (van der Tol et al., 2009; Running and Coughlan, 1988; Oleson et al., 2010). Detailed canopy models are often resolved into multiple layers, thus providing a better treatment of radiation regime and energy balance across the canopy (van der Tol et al., 2009; Wang and Leuning, 1998; Dai et al., 2004). At the heart of these models lies the leaf level biochemical model of photosynthesis and carbon fixation (Farquhar et al., 1980) together with a stomatal conductance (most often the widely used Ball-Berry) model (Collatz et al., 1991b). The fluxes of carbon and water are tightly coupled through stomatal regulation and photosynthesis (Baldocchi, 1994; Collatz et al., 1992). [..[10]]Further, the process based canopy models require some environmental drivers such as incoming [..[11]]shortwave and longwave radiation, air temperature, relative humidity, wind speed, and ambient CO_2 concentration, along with a [..[12]]number of leaf and

[8] removed: extremely
[9] removed: (Knorr and Heimann, 2001; Zaehle et al., 2005; Rogers et al., 2017)
[10] removed: These
[11] removed: photosynthetically active radiation(PAR)
[12] removed: few

canopy parameters to simulate the fluxes of carbon in terms of gross primary production (GPP), flux of water or latent energy (LE), sensible heat (H), net radiation and others.

One of the most important ecosystem descriptors is the maximum rate of carboxylation (V_{cmax}), which is directly related to the concentration of the enzyme Rubisco. V_{cmax} is a key parameter in the [..[13]]Michaelis-Menten kinetics for an enzyme-catalyzed reaction of the substrates CO_2 or O_2 with ribulose-1,5-bisphosphate, representing the enzyme-limited photosynthesis rate (Farquhar et al., 1980). Other rate-limiting photosynthesis parameters such as maximum electron transport rate (J_{max}) [..[14]]are generally parameterized with respect to V_{cmax}. The Ball-Berry equation calculates the stomatal conductance (g_s) for water vapor as a function of net assimilation, relative humidity, leaf surface CO_2 concentration, minimum conductance and a proportionality constant called the Ball-Berry slope (BB_{slope}) [..[15]](Ball et al., 1987; Wullschleger, 1993; Beerling and Quick, 1995; Tanaka et al., 2002). The BB_{slope} [..[16]]plays a crucial role in regulating the stomatal conductance and water use efficiency, and thus the surface energy fluxes in terms of partitioning the turbulent energy into LE and H fluxes. Thus, it is a crucial parameter regulating the tradeoff between carbon gain and water loss, e.g. during drought conditions (Monteith and Unsworth, 2007). The Leaf Area Index (LAI) is a canopy structural and key ecosystem [..[17]]variable in most Terrestrial Biosphere Models, which determines interception of radiation as well as photosynthesis and energy exchange across the canopy (Chen et al., 1997). The parameters V_{cmax} and BB_{slope} can be determined experimentally from leaf level gas exchange measurements and generated A-C_i curves (Wullschleger, 1993; Tanaka et al., 2002; Xu and Baldocchi, 2003). LAI can be estimated from destructive and non-destructive optical methods (Myneni et al., 1997; Dutta et al., 2017; Chen et al., 1997), as well as inversion approaches on spectrally resolved reflectance data from satellite and airborne platforms (Houborg et al., 2007; Jacquemoud et al., 1995). However, these measurements are much more complex and labor intensive, being measured [..[18]]less frequently than flux tower observations.

Inversion of detailed process-based models using observations of carbon and energy fluxes could thus yield these key ecosystem parameters. Process based models such as the Soil Canopy Observation, Photochemistry and Energy fluxes (SCOPE) (van der Tol et al., 2009) can simulate the radiative transfer and the fluxes of carbon and energy vertically resolved within the canopy. Our hypothesis is that the inversion of detailed vertically resolved canopy model such as SCOPE with multiple layers consisting of sunlit and shaded fractions together with fully spectrally resolved radiation regime and energy balance computations (van der Tol et al., 2009) is able to retrieve the ecosystem parameters accurately using observations of carbon and energy fluxes, and in the future remote sensing data, as SCOPE can model the spectrally resolved short-wave reflectance, thermal emission and solar induced chlorophyll fluorescence. [..[19]]

[13] removed: equation representing the
[14] removed: and dark respiration (R_d)
[15] removed: (Wullschleger, 1993; Beerling and Quick, 1995; Tanaka et al., 2002)
[16] removed: is also one of the most important ecosystem parameters as it
[17] removed: parameter
[18] removed: much
[19] removed: It can be noted that LAI is a parameter in SCOPE, not a state variable as in dynamic vegetation models.

A few studies have used inversion approaches to extract ecosystem parameters from flux [..[20]](Reichstein et al., 2003; Schulze et al., 1994) and refectance (Quaife et al., 2008) measurements but not yet to constrain all three key parameters (V_{cmax}, BB_{slope} and LAI) simultaneous using the fluxes of water and carbon[..[21]]. A previous study by Wolf et. al (Wolf et al., 2006) used deterministic linear least-squares inversion method to estimate the key ecosystem parameters (V_{cmax}, BB_{slope}, LAI and respiration rate) using the net ecosystem exchange (NEE) and sensible and latent heat fluxes. The approach assumed a simple model of radiation driven photosynthesis, respiration and energy balance using a two component (sunlit and shaded) canopy. The optimization used total energy (H+LE) to fit LAI values, the NEE to fit V_{cmax} and respiration rate and energy difference (H-LE) to fit BB_{slope}. In comparison to deterministic [..[22]]approach, stochastic Monte-Carlo [..[23]]approaches (Knorr and Kattge, 2005; Xu et al., 2006; Ricciuto et al., 2008; Mackay et al., 2012) constrain a number of parameters (including the photosynthetic parameters) using eddy covariance observations but assuming them to be time invariant[..[24]]. These studies considers multiple temporal resolutions such as seasonal or half-yearly and present a range of parameters without providing a definite error characterization as Bayesian methods (Wu et al., 2009). Moreover, since the stochastic methods sample the probability distribution in parameter space, they are better suited to non-linear models but often the associated computational costs can be prohibitive.

In this study, we develop an inversion framework for estimating the temporal dynamics of key ecosystem parameters using the SCOPE model representing detailed plant physiological processes including Sun Induced chlorophyll Fluorescence (SIF). SIF is chlorophyll re-emission during photosynthesis and acts as a direct probe into photosynthesis measurable from space and is strongly correlated with flux based GPP estimates at canopy to ecosystem scales (Frankenberg et al., 2011; Flexas et al., 2002). Thus, the SCOPE based inversion approach has the flexibility and advantage of incorporating tower-based observations of fluxes including SIF as well as spectrally resolved reflectance and thermal emissions for optimal estimation of a wide range of ecosystem parameters. [..[25]]In this paper, we first focus on the conceptual framework of parameter inversion using SCOPE followed by parameter retrieval examples, with specific objectives as follows:

1. Implementation of photosynthesis model and its temperature dependencies consistent with a well-accepted major Earth system model (Community Land Model CLM 4.5) in SCOPE.

2. Development of a Bayesian non-linear inversion framework using SCOPE to estimate ecosystem parameters using eddy covariance flux observations.

3. Demonstrating the retrieval and posterior error reduction of key ecosystem parameters using (i) observations of carbon and water fluxes and (ii) combining flux observations together with satellite reflectance across different ecosystems.

[20] removed: measurements (Reichstein et al., 2003)
[21] removed: (Schulze et al., 1994)
[22] removed: approaches the
[23] removed: approach (Knorr and Kattge, 2005; Xu et al., 2006; Ricciuto et al., 2008) constrains
[24] removed: , including the photosynthetic parameters
[25] removed: However, in

The rest of the paper is organized as follows. Section 2 provides a brief overview of the SCOPE model and the new implementation of photosynthesis and its temperature dependencies. Section 2.2 provides a comparison of the old and new photosynthesis implementations in SCOPE. Sections 3, 4 and 5 describes the formulation of the inverse problem followed by linearization of the forward model and mechanisms of the retrieval algorithm. Section 6 describes the results of the inversion framework across three different ecosystems and finally Section 7 provides a discussion summary and conclusions.

2 SCOPE Model

The Soil, Canopy, Observation, Photochemistry and Energy fluxes (SCOPE) (van der Tol et al., 2009) is an integrated 1-D vertical radiative transfer and energy balance model. The model utilizes the spectrally resolved visible to thermal (0.4 to 50 μm) infrared irradiation at the canopy top to derive the fluxes of water, energy, carbon dioxide and vertical profiles of temperature as a function of canopy structure and weather variables. The four most important SCOPE modules represent (i) radiative transfer of incident solar radiation and generated fluorescence within the leaf (Fluspect), (ii) radiative transfer of incident direct and indirect solar radiation (0.4 - 50 μm), (iii) radiative transfer of internally generated thermal radiation by vegetation and soil (Verhoef et al., 2007), (iv) an energy balance module [..[26]]and (v) radiative transfer module for computing the top of canopy radiance spectrum of fluorescence from leaf level chlorophyll fluorescence.

[..[27]]SCOPE resolves top of canopy [..[28]]incoming/outgoing shortwave radiation and reflectance in the spectral range of 400 to 2500 nm at 1nm wavelength bands. Further, it also computes the spectrally resolved fluorescence emission in the range of 650 to 850 nm at 1nm wavelength bands.

One important aspect is that SCOPE relaxes the assumption of constant temperatures for the sunlit and shaded fractions of the leaves across the different canopy layers. This is true when we consider different orientations, and their vertical positions in the canopy. Therefore, an iterative solution scheme is implemented in SCOPE as stomatal conductance affects leaf temperature, which in turn affects photosynthesis (and thus again stomatal conductance). Thus, the fully integrated thermal radiative transfer and [..[29]]energy balance modules allow feedback between leaf temperatures, photosynthesis, chlorophyll fluorescence, and radiative fluxes.

[..[30]]

[26] removed: (EBAL)

[27] removed: The leaf radiative transfer model computes the leaf reflectance, transmittance, bi-directional fluorescence emission, and the absorbed PAR per pigment. The solar radiative transfer model computes the

[28] removed: (TOC) outgoing radiance spectrum as well as net radiance and absorbed PAR per surface elements, the thermal radiative transfer module computes the TOC outgoing thermal radiation and net radiation per surface element for heterogeneous leaf and surface temperatures generated internally by soil and vegetation, the EBAL computes the latent, sensible and soil heat per element as well as photosynthesis, fluorescence and skin temperatures, finally the fluorescence radiative transfer module computes the outgoing top of canopy radiance spectrum of fluorescence

[29] removed: EBAL

[30] removed: Within the heart of the EBAL module (and also essentially SCOPE) is the biochemical module for the computation of photosynthesis and chlorophyll fluorescence at the leaf level. Photosynthesis and stomatal regulation is one of the most important physiological processes which controls each of the outgoing fluxes and radiances. Therefore, its computation and temperature dependence are crucial for accurate estimation of the canopy net fluxes.

2.1 The SCOPE Biochemical Module

The SCOPE biochemical module is a submodule of the [..[31]]energy balance routine, which provides an iterative solution of the photosynthesis, energy balance, net radiation and heterogeneous skin temperatures for a particular net external forcing. The main functions of the biochemical module include leaf temperature dependent computation of photosynthesis and fluorescence. Some of the photosynthesis parameterizations in the current version of the SCOPE model (V1.7) are outdated and more in line with previous versions of the [..[32]]Community Land surface Model (CLM version 4) or based on a mix of other model implementations. CLM is a community-developed land model which focus on the modeling of land surface processes including biogeophysics, carbon cycle, vegetation dynamics and river routing. Specifically, the main modifications in the more recent CLM (version 4.5, CLM4.5) (Lawrence et al., 2011; Oleson et al., 2013) include updates to the canopy radiation scheme and canopy scaling of leaf processes, co-limitations on photosynthesis, revisions to photosynthetic parameters (Bonan et al., 2011), temperature acclimation of photosynthesis and improved stability of the iterative solution in the photosynthesis and stomatal conductance model (Sun et al., 2012). CLM4.5 implements a multi-layer canopy modeling framework with coupled photosynthesis (Farquhar et al., 1980) and Ball-Berry stomatal conductance models similar to the SCOPE framework.

The main inconsistencies of SCOPE (V1.7) with the CLM4.5 parameterizations are as follows:

1. Similar, generic temperature response functions are implemented for both C_3 and C_4 species excepting V_{cmax} and further it uses a Q_{10} based exponential function with same functional parameters for computing the temperature response of the various photosynthetic parameters.

2. There is no J_{max} (maximum potential electron transport rate (ETR)) or its temperature dependence in the computation of light limited C_3 photosynthesis rate.

3. The net assimilation, internal CO_2 concentration and stomatal conductance ($A - C_i - g_s$) iterative solution method is not quite robust or was lacking in the previous versions with the V1.7 implementation being complicated and unpublished.

We therefore attempt to improve the SCOPE biochemical module by implementing the photosynthesis and temperature dependence of the photosynthetic parameters according to well established and widely used [..[33]]CLM4.5[..[34]].

[31] removed: EBAL routine

[32] removed: community land surface model (CLM4

[33] removed: Community Land Model (CLM V4.5 or

[34] removed:) (Lawrence et al., 2011; Oleson et al., 2013). The CLM is a community-developed land model which focus on the modeling of land surface processes including biogeophysics, carbon cycle, vegetation dynamics and river routing. CLM is the land surface component of the Community Earth System Modeling framework. Specifically, the main modifications in CLM4.5 include updates to the canopy radiation scheme and canopy scaling of leaf processes, co-limitations on photosynthesis, revisions to photosynthetic parameters (Bonan et al., 2011), temperature acclimation of photosynthesis and improved stability of the iterative solution in the photosynthesis and stomatal conductance model (Sun et al., 2012). CLM4.5 implements a multi-layer canopy modeling framework with coupled photosynthesis(Farquhar et al., 1980) and Ball-Berry stomatal conductance models similar to the SCOPE framework. We therefore make the implementation of photosynthesis and its temperature dependence in SCOPE fully consistent with CLM4.5

All the detailed implementation steps and equations for modeling the photosynthesis and temperature dependence primarily as per (Bonan et al., 2011) is presented in detail in the appendix A [..[35]]and B. Within the inverse framework described later, we only invert V_{cmax} at the reference temperature of 25° and apply the given temperature dependencies. Any systematic difference in the temperature function could thus alias into the derived V_{cmax}. Overall, the major new updates made to the model (biochemical module) are as follows:

1. Computing the electron limited photosynthesis rate A_j using the potential ETR J, which is obtained by solving the smaller root of equation A5 comprising the light utilized in photosystem II (I_{PSII}) and the maximum potential ETR (J_{max}).

2. The light limited photosynthesis rate for C_4 is given by equation A3[..[36]].

3. The temperature dependence of photosynthetic parameters (Bonan et al., 2011) now uses the activation, deactivation energies and entropy terms in the temperature response and high temperature inhibition functions (Leuning, 2002) (see appendix B for details). The temperature response of C_3 (Leuning, 2002; Bernacchi et al., 2001) and C_4 photosynthesis is represented by equations B1 - B5.

4. Finally we also incorporate a new simplified implementation of $A - C_i - g_s$ iterations (Sun et al., 2012) and include the computation of oxidative photosynthesis (Bernacchi et al., 2001) within the photosynthesis model. See appendix B1 for details.

2.2 [..[37]]

[..[38]]

[..[39]]

[..[40]]

[..[41]]In the [..[42]]

[35] removed: . The

[36] removed: , in the earlier SCOPE version it was implemented as potential ETR x CO_2 per electron

[37] removed: A-Ci-g_s Iterations

[38] removed: The final solution for photosynthesis requires an iterative solution of the coupled equations representing (i) the Farquhar, von Caemmerer and Berry (FvCB) model (Farquhar et al., 1980) for the photosynthesis rate (A), (ii) Fick's law of diffusion (Eqn. B6) for internal CO_2 (C_i) concentration and (iii) Ball-Berry stomatal conductance model (Ball et al., 1987) (Eqn. B7) for stomatal conductance (g_s) to obtain stable converging solutions.

[41] removed: In Eqn. B7, BB_{slope} represents the Ball-Berry slope, r_h the relative humidity and g_0

[42] removed: Ball-Berry intercept. In the absence of an initial specification of C_i, we make the assumption that $g_0 = 0$ in Eqn. B7, then combining equations B6, B7, the initial estimate of C_i is given as:

[..[43]]

[..[44]]

[..[45]]following section, we demonstrate the photosynthesis results with [..[46]]the newer photosynthesis and temperature dependence implementation as well as its comparison with the previous version (V1.7) in SCOPE for different ecosystems.

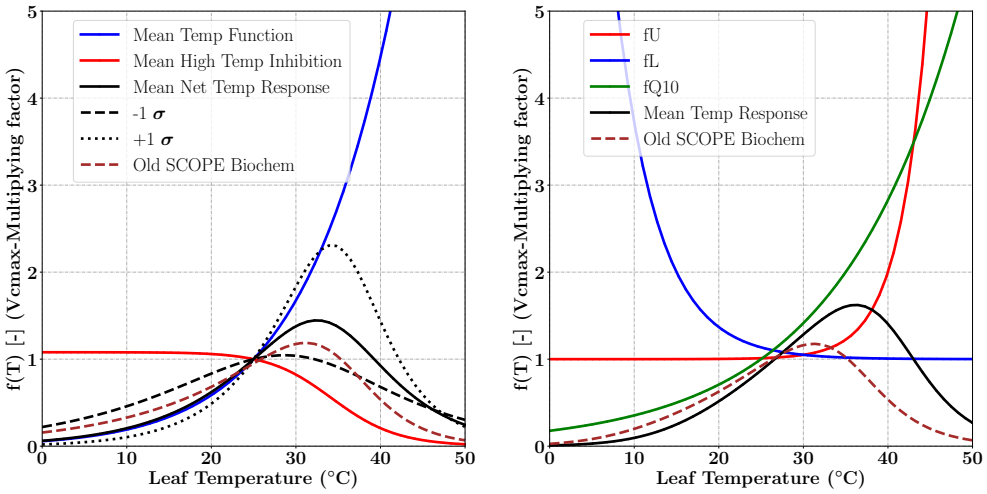

Figure 1. Temperature response functions of V_{cmax} for C_3 (left) and C_4 (right) plants. For the C_3 species the mean and $\pm 1\sigma$ variability (shown as broken black lines) in the net temperature response [..[47]]is computed using data [..[48]]presented in (Leuning, 2002) [..[49]]is shown [..[50]]in the left panel. The temperature range corresponding to maximum V_{cmax} response for both the C_3 and C_4 pathways is between 30-40 °C. The overall temperature response from the previous version (V1.7) is shown as brown dashed line.

2.2 Comparison of [..[51]]Current and [..[52]]Previous Photosynthesis Implementations in SCOPE

Figure 1 shows the temperature response functions for V_{cmax} for both C_3 (left) and C_4 (right) photosynthetic pathways. The functions of mean temperature response, high temperature inhibition and the 1σ variance as per the different photosynthesis pathway dependent parameterization (e.g. activation energy, deactivation energy, entropy) is shown according to [..[53]

[44] removed: where f_{Ci}^{min} is the assumed minimum fractional leaf boundary layer CO_2 (assumed as 0.3 for C_3 and 0.1 for C_4 species). This initial estimate of C_i is used to again estimate the photosynthesis based on the FvCB model (Farquhar et al., 1980), followed by estimation of stomatal conductance using the Ball-Berry model Eqn. B7. Finally, the Newton-Raphson method is used to obtain a forward estimation of the new value of internal CO_2 concentration (Sun et al., 2012). The updated C_i is further used in the $A - g_s - C_i$ until convergence.

[45] removed: In the current SCOPE implementation we replaced the photosynthesis model to be fully consistent with CLM4.5. In the

[46] removed: this new

[51] removed: Old

[52] removed: New

[53] removed: (Leuning, 2002)

]Leuning (2002). The new temperature dependency parameterizations follow the temperature functions and high temperature inhibition for C_3 and the Q_{10} functions for the C_4 pathways. We have also shown the temperature dependence of V_{cmax} from the previous [..[54]](old) implementation of SCOPE model (V1.70). The differences in the net response at both lower and higher than optimal temperature can be clearly identified in the figure for both C_3 and C_4 species. It can be observed that the difference in temperature response is more for C_4 , clearly the maximum is in the leaf temperature range $30 - 40°C$, however it continues into the higher temperatures as well. Moreover, it can be noted that the overall shapes of the response functions are nearly identical (with some lag) for the different parameters for the previous SCOPE implementation compared to the newer implementation as per CLM4.5 (Bonan et al., 2011).

[..[56]]A number of analyses were performed to study the differences in net response of canopy level [..[57]]carbon and energy fluxes for both C_3 and C_4 species [..[58]]from the SCOPE model due to modification in photosynthesis implementation (old and new[..[59]]) and its temperature dependence [see supplementary information Sec S1.]

Figure 2 shows the comparison between the old and new SCOPE versions as the ratio of overall canopy GPP[..[60]], which is defined as [..[61]]$f_{GPP} = \frac{GPP_{new}}{GPP_{old}}$[..[62]]. This ratio is further represented as a function of the three most important forcing variables PAR, canopy temperature and VPD. The results for the Missouri Ozark site (see section 6.4.1 for site details) with C_3 plant species for the year 2009 are presented in Fig. 2. For this analysis, the SCOPE model simulations are computed for the entire growing season and the f_{GPP} values are binned according to the PAR-Temperature (for specific VPD ranges) and PAR-VPD (for specific temperature ranges) as 2-D histograms[..[63]], of which only the mean ($f_{GPP_{mean}}$) is represented in figure 2. [..[64]]

We find that over the larger parts of the domain of random variables, f_{GPP} is around 1 and the maximum change in overall GPP is around 25%. From Figure 2, it can be observed that in the case of C_3 species, for the combinations of higher canopy temperature and low VPD values (panel-a), the new GPP values remain the same or are reduced by about 5%. Although from Fig. 1 we find an increase in the V_{cmax} response at $> 25°C$ temperature, which may indicate photosynthesis being limited by light instead of the enzyme rubisco. For the combination of low canopy temperature and lower VPD values (panel-c),

[54] removed: implementation

[56] removed: To study the overall or net response from the SCOPE model in terms

[57] removed: fluxes, we tested the old and new model version

[58] removed: at two different sites. Figure **??** shows the comparison of SCOPE model predictions for both model versions using C_4 plants. The results shown are for corn (C_4) crops at the Mead-1 Ameriflux site in Lincoln, Nebraska (see section 6.3.1 for some more site information). The environmental forcings and SCOPE parameterizations were kept identical for the

[59] removed: SCOPE runs. The only difference is the replacement of the old biochemical module with our new photosynthesis implementation. The top panel shows the environmental forcing for a few clear days in the growing season. There is considerable variability in temperature and VPD.The middle and lower panels represent the comparisons in diurnal GPP and LE fluxes. It is observed that with the given parameterization the newer implementation better captures the diurnal variability as compared to the actual tower observations at relatively higher average canopy temperatures.

[60] removed: computed using the new implementation of photosynthesis to the old implementation. The ratio

[61] removed: (

[62] removed:)

[63] removed: . Each of these bins have multiple data points and essentially follow a distribution

[64] removed: Finally contour plots are developed with these mean values to demonstrate the effect of paired random variables PAR-canopy temperature (shown in the left column) and PAR-VPD (shown in the left column) on $f_{GPP_{mean}}$.

[..[55]]

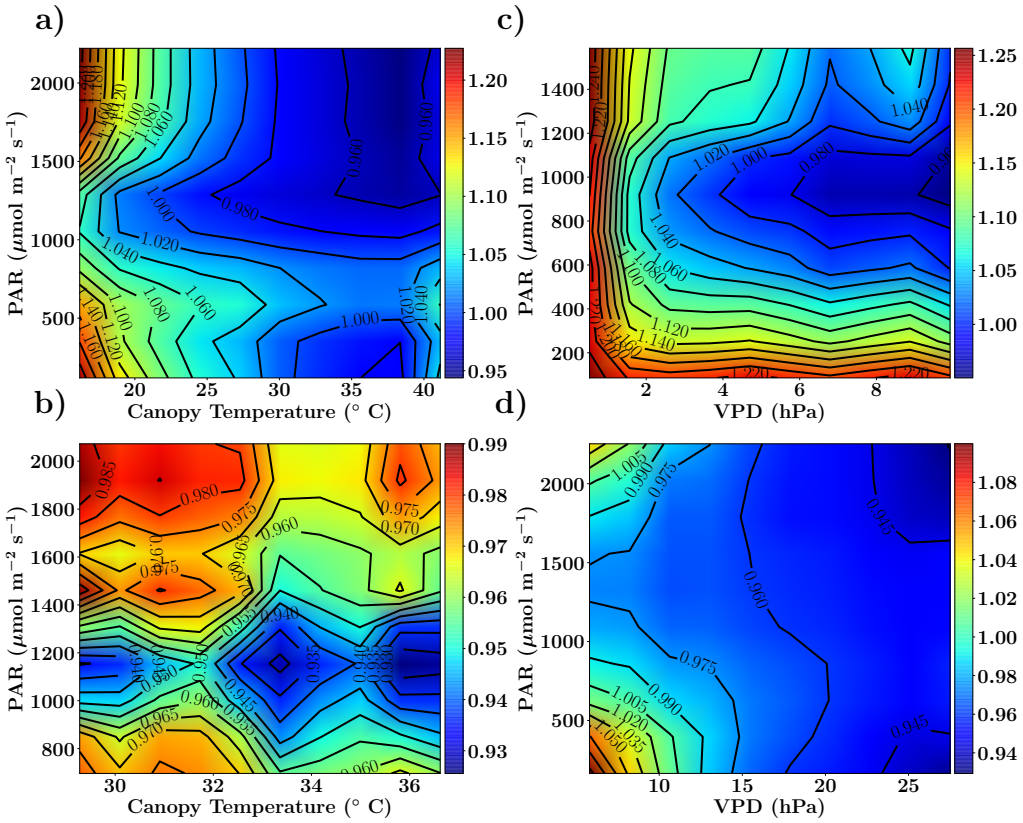

Figure 2. Figure showing the ratio of old and new SCOPE GPP ($f_{GPP} = \frac{GPP_{new}}{GPP_{old}}$) simulations as a function of PAR, canopy temperature and VPD for the C_3 species. The Missouri Ozark fluxnet site comprising of deciduous broadleaf forests for the year 2009 is used and the SCOPE simulations are driven with identical forcings and parameters for both the new and old simulations, the only difference being the implementation of Photosynthesis and its temperature dependence (see text). The left column shows f_{GPP} as a function of PAR and canopy temperature with data points in the low VPD range of 10-15 hPa (panel-a) and high VPD range of 25-30 hPa (panel-b). The right column shows f_{GPP} as a function of PAR and VPD with data points in the low temperature range of 10-15 °C (panel-c) and moderate temperature range of 25-30 °C (panel-d).

f_{GPP} values are close to 1 (except for very low PAR/VPD values and with a maximum of about 4-6% increase) which can be explained by almost identical V_{cmax} response at lower temperatures in Fig. 1. At high PAR values with higher temperatures (25-30°C) and low VPD values (panel d) we find that GPP increases by about 6-14% which can be directly explained by the new increased V_{cmax} response in that temperature range as indicated in Fig. 1.

[..[65]]

[65]removed: Figure showing the ratio of old and new SCOPE GPP ($f_{GPP} = \frac{GPP_{new}}{GPP_{old}}$) simulations as a function of PAR, canopy temperature and VPD for the C_4 species. The Nebraska Mead-1 site with corn growing for the year 2009 is used and the SCOPE simulations are driven with identical forcings and

[..[66]]

[..[67]]

[..[68]]The results for a similar comparative study with C_4 species is presented in the supplementary information Section S1. Overall, we find that the new model implementation of photosynthesis and its temperature dependence as well as $A - C_i$ iterations works well and only result in moderate, yet noticeable changes. It also underlines that tabulated model parameters can only be optimized for a specific model implementation, which is not necessarily universally transferable to other carbon cycle models.

3 Formulation of Inverse Problem

The problem of ecosystem flux computation (e.g. GPP, Latent Energy, etc) from meteorological variables (e.g. VPD, air temperature, relative humidity etc) and other ecosystem parameters can be represented as:

$$Y = \mathcal{F}(X') + \epsilon \tag{1}$$

where, $\mathcal{F}() : X' \longrightarrow Y$ is a functional representation of the model, which maps the model input and parameter space (X') quantitatively to the space of ecosystem fluxes (Y), and ϵ represents the residual error which includes the precision error, the model error and random errors. In our case, SCOPE represents the forward model $\mathcal{F}()$, which is complex and moderately non-linear, representing a range of physics and canopy physiological processes. We can further represent our forward problem as:

$$Y = \mathcal{F}(X; p) + \epsilon \tag{2}$$

parameters for both the new and old simulations, the only difference being the implementation of photosynthesis and its temperature dependence (see text). The left column shows f_{GPP} as a function of PAR and canopy temperature with data points in the low VPD range of 10-15 hPa (panel-a) and high VPD range of 25-30 hPa (panel-b). The right column shows f_{GPP} as a function of PAR and VPD with data points in the low temperature range of 10-15 °C (panel-c) and high temperature range of 30-35 °C (panel-d).

[66]removed: Figure **??** shows similar plots and comparisons as described above in terms of f_{GPP} but for corn (C_4) crop grown at the Mead-1 Ameriflux site in Nebraska Lincoln (see section 6.3.1 for some more site information). It appears from the results that there is only a decrease in canopy GPP for the new SCOPE both in the space of PAR-Canopy Temperature and PAR-VPD by about 5-30%, which can be attributed to photosynthesis being limited by light instead of rubisco at higher temperatures. As mentioned previously, there is uncertainty associated with these contour diagrams although these are quite small ($< 10\%$) and it is found that these patterns are also nearly the same (not shown).

[67]removed: Figure showing the comparison of the tower observed vs modeled canopy GPP for new and old Photosynthesis implementations in the SCOPE model. The results are shown for both the C_3 (left) and C_4 (right) species. The model simulations for the C_3 species are for the Missouri Ozark Site comprising of Deciduous Broadleaf Forests, the C_4 simulations are for the Nebraska Mead-1 site with corn growing both for the year 2009.

[68]removed: Figure **??** shows the modeled vs observed comparison for new (as per CLM4.5) and old (previous) implementation of photosynthesis in SCOPE for both the C_3 and C_4 species . We select a set of points (time indices) from the new SCOPE simulations at various PAR ranges whose modeled GPP fluxes are very close to the tower observed values. The points corresponding to the same time indices from the old SCOPE simulations are then selected for comparing the modeled GPP. It is found that for C_3 species there is not much change but for C_4 species the new SCOPE GPP values are generally reduced. This result is also in agreement with the contour plots as presented earlier

where X represents the state vector of parameters to be retrieved, p ($X, p \subset X'$ and $X' = X \cup p$) is a vector of parameters which represents those quantities that influence the measurement, are known to some accuracy but not to be retrieved. We call these parameters the forward functional parameters. In our example p represents the set of all fixed model (SCOPE) parameters not involved in the retrieval. The error term ϵ represents the measurement noise (e.g. noise or errors in the flux measurements). Given a set of measurements Y, the optimal state vector $\hat{X}$ can be obtained by a generalized inverse method $\mathbf{R}$ represented as:

$$\hat{X} = \mathbf{R}(Y, \hat{p}, X_a, c)\,, \tag{3}$$

where $\hat{p}$ represents the best estimate of the forward function parameters. The parameters X_a and c represents the parameters that do not appear in the forward function but they do affect the retrieval and are associated with uncertainties. X_a represents the prior estimate of X and c represents any other parameters in the retrieval scheme as a catch-all for anything else that is used in the retrieval method, which also includes the convergence criteria.

4 Linearization of the Forward Model

A basic prerequisite for inverting the forward model is to compute its sensitivity with respect to input parameters, i.e. the partial derivatives with respect to all the state vector elements (Jacobi matrix). For linear models, the Jacobians are independent of the actual state. In our case, the SCOPE forward model is moderately non-linear and its Jacobians need to be computed numerically as analytical methods are currently lacking and hard to implement given some peculiarities in the FvCB equations.

With the Jacobian matrix and a simple forward model call, we can thus write a first order Taylor expansion for the forward model

$$F(X;p) = F(X;p)_{X=X_l} + \left.\frac{\delta F}{\delta X}\right|_{X=X_l} (X - X_l)\,, \tag{4}$$

where X_l is an arbitrary linearization point, $\frac{\delta F}{\delta X}$ is the partial derivative or Jacobian at the point $X = X_l$.

5 Iterative Retrieval Algorithm Setup

In the remainder of the paper, we will omit the vector of forward model parameters p which are not a part of the retrieval framework. For the non-linear problem we use the maximum a-posteriori approach. The Bayesian solution for the non-linear inverse problem where the forward model is a general function of the state, the measurement error is Gaussian (S_ϵ) and with a prior estimate of the state (X_a) with a Gaussian uncertainty in the prior state (S_a) (Rodgers, 2000) can be represented as:

$$-2\ln P(X|Y) = [Y - F(X)]^T S_\epsilon^{-1} [Y - F(X)] + [X - X_a]^T S_a^{-1} [X - X_a] + c'\,, \tag{5}$$

where c' is a constant. Our aim is to find the best estimate of the state vector $\hat{X}$ (denoted as X henceforth) and an error characterization that describes the posterior *pdf*. The Gauss-Newton iteration steps for determining the state vector is given by:

$$X_{i+1} = X_i + (S_a^{-1} + K_i^T S_\epsilon^{-1} K_i)^{-1}[K_i^T S_\epsilon^{-1}[Y - F(X_i)] - S_a^{-1}[X_i - X_a]] \tag{6}$$

[..[69]]where, K_i is the Jacobi matrix, a brief derivation of Eqn. 6 is presented in appendix C, for a more in-depth treatment the reader is referred to (Rodgers, 2000).

5.1 Levenberg Marquardt Method

In general, the Gauss-Newton iterations discussed previously finds the minimum in one step if the cost function is quadratic with respect to X. However, in our case the cost function is not perfectly quadratic and the initial guess potentially far away from the solution, thus requiring multiple iterations. In addition, the non-linearity of the problem sometimes results in steps that would actually increase rather than decrease the fit quality. In order to overcome this issue Levenberg (1944) (Levenberg, 1944) and Marquardt (1963) (Marquardt, 1963) proposed the following iteration for non-linear least squares problem:

$$X_{i+1} = X_i + (KK^T + \gamma_i D)^{-1} K^T [Y - F(X_i)] \tag{7}$$

where, γ_i is chosen at each step to minimize the cost function and D is a diagonal scaling matrix to scale the elements of the state vector. It can be noted that for $\gamma_i \to 0$, leads to a Gauss-Newton iteration step and for $\gamma_i \to \infty$ tends to steepest descent and further the step size tends to 0. It is also expected that the cost function will decrease corresponding to the decrease in γ_i from infinity to zero. The value of γ_i is sequentially updated at each iteration by evaluating the change in cost function. Here, we follow the general recommendations as outlined in (Marquardt, 1963; Rodgers, 2000).

The guidance for choosing the scaling matrix D is that it must be positive definite. For the current problem we choose it to be S_a^{-1} (as in (Rodgers, 2000)) and apply the Levenberg Marquardt (LM) modification to the Gauss-Newton method (iteration equation C8), resulting in the following iterative inversion scheme:

$$X_{i+1} = X_i + [(1+\gamma)S_a^{-1} + K_i^T S_\epsilon^{-1} K_i]^{-1}\{K_i^T S_\epsilon^{-1}[Y - F(X_i)] - S_a^{-1}[X_i - X_a]\} \tag{8}$$

5.2 A Moving Window Set up of the Inversion Problem Using Flux Tower Observations

Figure 3 top row shows the SCOPE model simulations of GPP, LE, H and SIF for one day (August 3, 2010) in the growing season for C_4 corn using data from the Nebraska Mead-1 flux tower site with parameter values $V_{cmax} = 50$ μ mols m^{-2} s^{-1}, $BB_{slope} = 7$ and LAI = 4. The second, third and fourth rows from the top shows the numerically computed partial derivatives

[69] removed: A

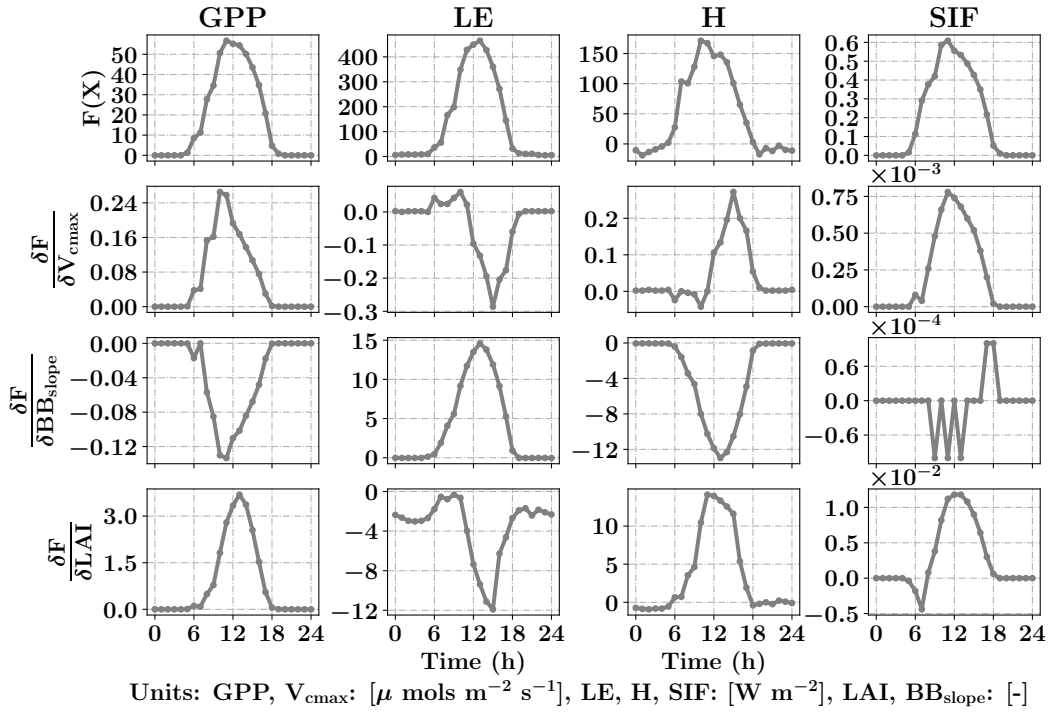

Figure 3. Diurnal variability of GPP, LE, H and SIF from SCOPE model simulations (top row) for a typical day in the growing season (August 3, 2010) for C_4 corn using data from the Nebraska Mead-1 flux tower site with parameter values $V_{cmax} = 50$ μ mols m^{-2} s^{-1}, $BB_{slope} = 7$ and LAI = 4. Second, third and fourth rows from the top shows the diurnal variability in the gradient of GPP, LE, H and SIF with respect to the parameters using SCOPE with positive perturbations $\delta V_{cmax} = 5$ μ mols m^{-2} s^{-1}, $\delta BB_{slope} = 1$ and δLAI = 0.5 which constitutes the Jacobian matrix for the inversions. It can be observed that the Jacobian matrix is non-linear with maximum values near the mid-day period. Our retrieval framework uses concatenated 3-day GPP and LE fluxes (modeled and observed) and their gradients successively within a 3-day window.

of GPP, LE, H and SIF with respect to the parameters using SCOPE with positive perturbations $\delta V_{cmax} = 5$ μ mols m^{-2} s^{-1}, $\delta BB_{slope} = 1$ and δLAI = 0.5. Each column of figure 3 represents a row of Jacobian matrix used for the inversions. The figure clearly demonstrates the influence of each of the parameter variables in the state vector (X) on the modeled fluxes ($F(X)$). We can observe the counteracting nature of variables and the fluxes from the Jacobian. For example, for LE flux, BB_{slope} has a positive gradient but LAI has a negative gradient. The decrease in LE is attributed to less radiation reaching the soil and corresponding increase in soil aerodynamic resistance. In this case the canopy resistance goes up but does not compensate for the decreased soil evaporation and results in low sensitivities. Similarly we find V[..[70]]$_{cmax}$ has positive [..[71]]gradient for GPP but negative for LE which may again be attributed to the soil evaporation responding to soil

[70] removed: $_{cmax}$ has positive gradient for GPP but negative for LE and likewise for GPP fluxes, V

[71] removed: gradients but BB_{slope} has negative gradient

temperature. It can be noted that the nature of these [..[72]]sensitivities at the canopy level are sometimes counter-intuitive from their leaf-level mechanisms and may vary depending on environmental conditions, such as incoming PAR as well as air temperature and vapor pressure deficit. This also creates diversity in the Jacobians over the diurnal cycle, which allows us to derive more than 2 parameters from 2 sets of measurements (GPP and LE). In Figure 3, we have not only shown derivatives of GPP and LE but also H and SIF (not used here). In this manuscript, we outline the general framework of parameter inversion, which can easily be modified to make use of more measurements such as H, SIF, reflectance or thermal emissions, all of which can be modeled with SCOPE.

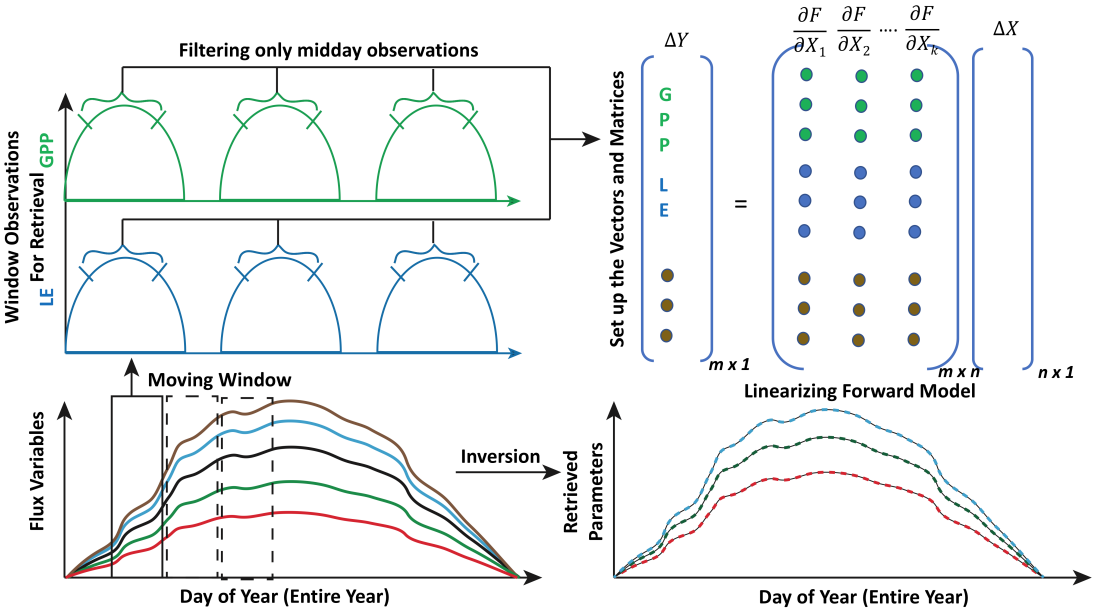

Figure 4. Illustration of moving window inversion retrieval setup. The bottom left part illustrates the annual ecosystem time series flux variables used for driving the SCOPE model. A [..[73]]3-day time window is selected for each retrieval in the yearly growing season and a time filter is implemented for concatenating the measurement vector (flux tower observations, with each color representing a different observation variable) of length m in the retrieval windows. The top right shows the vector and matrix setup and the linearization of the forward model. ΔY represents the difference between concatenated observation and modeled vector and ΔX represents the corresponding change in the state vector comprising of n-variables (parameters). The bottom right shows the retrieved model parameters after implementing the moving window approach.

For setting up the observation vector $Y_{m\times 1}$ (see Eqn. 8), we use observations of carbon and latent energy fluxes from eddy covariance tower time series records. The observational error matrix ($S_{\epsilon[m\times m]}$) is assumed to be a diagonal matrix and computed using noise standard deviation as 10% of the [..[74]]half hourly to hourly observations (Leuning et al., 2012). We use an initial prior state value of the state vector ($X_{a[n\times 1]}$) as well as the prior error covariance matrix ($S_{a[n\times n]}$). As mentioned

[72]removed: gradients

[74]removed: observations. We assume

previously, the Jacobian matrix $K_{m\times n}$ is computed numerically by a small perturbation to the value of the state vector $X_i + \delta$ (see Fig. 3) at a particular iteration step. The observed (Y) and modeled ($F(X)$) fluxes in the inversion framework are set up as a long concatenated vector as shown in Fig 4. The concatenation of different flux variables are done using a time filter to represent the part of the day we wish to include in the retrieval framework as illustrated in Fig. 4. This is logical as we have already demonstrated in Fig. 3 that the gradients are variable throughout the day. Ideally, the time filter applied for concatenating the data should capture the maxima and a range of variations in the gradients, but at the same time reduce the data points to make the retrieval computationally efficient and further tend towards providing stable solutions (retrievals) of the parameter values. Further, the time filter helps to eliminate the night time anomalies in the observations for accurate parameter estimation. For other observations such as spectral reflectance a daily noon time average is suitable for concatenation in the observations Y. The assumptions behind the long term (seasonal) retrieval of important ecosystem and plant physiological parameters is that these parameters change significantly over the growing season but at a slower rate compared to and in response to the environmental and meteorological forcing. Thus, the ecosystem parameters can be assumed to be constant over some finite time window. We implement this assumption to set up our inverse parameter retrieval framework for finite [..[75]]N-day contiguous moving windows over the entire growing season (Fig 4). We extend the one-day diurnal set up of Y, $F(X)$ and K as shown in Fig. 3 to multiple days for setting up the [..[76]]N-day windows as illustrated by color coding in Fig. 4. After computing the necessary vectors and matrices for the [..[77]]N-day window, iterations are performed by applying the LM algorithm until convergence to obtain the posterior estimation of the state vector. The retrieval window is moved over to the contiguous next [..[78]]N-days and the process is repeated. The retrieval thus proceeds for the entire length of the growing season (Fig 4). For our retrieval example, we choose a 3-day moving window which seems optimal for the plant response in terms of the photosynthesis parameters (V_{cmax}, BB_{slope} and LAI) towards the change in environmental drivers.

5.3 Error Characterization and Convergence Criteria for the Retrievals

As mentioned in section 5.1, we have selected a convergence criteria for the parameter retrievals in each of the moving windows based on the ratio of the true error to the expected error for each of the iteration steps. [..[79]]The total error minimized for the retrieval is given by $[Y - F(X_i)]^T S_\epsilon^{-1}[Y - F(X_i)] + [X - X_a]^T S_a^{-1}[X - X_a]$. However for testing the convergence within each iteration step, we use the method suggested by Rodgers, 2000, which adapts the Levenberg-Marquardt parameter depending on the non-linearity of the forward model.

[..[80]][[..[81]]][..[82]]

[75] removed: n
[76] removed: n
[77] removed: n
[78] removed: n
[79] removed: For each iteration step, the error (mismatch between observations and modeled values) (χ^2) can be represented as:

[..[83]]

[..[84]][[..[85]]][..[86]]

[..[87]]

[..[88]][[..[89]]][..[90]]

[..[91]]

[..[92]]

[..[93]]

After convergence, the posterior error covariance matrix for the retrieved state vector $\hat{X}$ can be computed as:

$$S = [S_a^{-1} + K_i^T S_\epsilon^{-1} K_i]^{-1} \tag{9}$$

The reduction in error is defined as:

$$\zeta_i = 1 - \left(\frac{S_{jj}}{S_{a_{jj}}}\right)^{0.5} \tag{10}$$

Where S_{jj} and $S_{a_{jj}}$ represent the diagonal elements in the posterior and prior error covariance matrices respectively. In our LM retrieval process, we use the retrieved state vector $\hat{X}$ of the previous window as first guess (but not prior) for the current window. This saves computational cost and is based on the assumption that our state vector varies smoothly in time.

6 Results for Implementing the Inversion Framework in SCOPE

In this section, we discuss the results of optimal parameter estimation by applying the Bayesian inversion framework to three different ecosystems. The aim is to demonstrate the applicability for the retrieval [..[94]](as well as capturing the seasonal variability) of canopy structural and photosynthesis parameters using carbon and water fluxes, [..[95]]and to further compare and

[83] removed: The expected reduction in the error (χ^2_E) which is computed after the inversion retrieval step and an expected value of the new state vector and without making update to either X or γ can be represented as:

[87] removed: The true reduction in the error (χ^2_T) which is computed using a forward model run after the inversion retrieval stepand using the updated value of state vector without actually making the update to either X or γ can be represented as:

[91] removed: Finally, the ratio (R) of the true to expected change in error reads:

[93] removed: A few additional filters are implemented to ensure that the updated state vector is always within a physically meaningful space (e. g. $R < 0$ indicates negative X and hence the state vector is not updated instead the γ value is increased).

[94] removed: of canopy

[95] removed: to demonstrate the seasonality of retrieved parameters

contrast the results across the [..[96]]different ecosystems. In order to demonstrate greater potential of SCOPE in modeling spectrally resolved reflectance (not found in other general carbon cycle models) and versatility of the inversion framework we have also incorporated MODIS satellite reflectance bands in the retrievals. We further demonstrate how reflectance and fluxes are able to better constrain parameters such as V_{cmax}, BB_{slope} and LAI compared to just using flux tower observations.

6.1 Data Filtering Criteria in the Moving Window Retrievals

Apart from the overall algorithmic steps as described previously, we apply the following filter criteria on the results and the data for a computationally efficient retrieval.

1. In constructing the observation vector Y we apply a time of the day filter (e.g. data between 9 am and 4 pm and so on) for the initial forward SCOPE model.

2. For computing the Jacobians, a PAR based threshold (PAR > 100 μ mols m^{-2} s^{-1}) to ensure sensitivity of the measurement vector with respect to state vector variations and to minimize the occurrence of unreasonable fluxtower data (high fractional errors).

3. A filter is implemented to check and ensure that the state vector remains positive at every iteration. If somehow due to a small enough γ the state vector is negative, the γ value is adjusted in an iterative manner to keep it within bounds.

6.2 MODIS Satellite Reflectance Data

We use the daily Moderate Resolution Imaging Spectrometer (MODIS) MCD43A reflectance product in this study (Schaaf and Wang, 2015). The spatial resolution of the dataset is 500m and bands 1 and 2 (red and NIR) centered at 620 nm and 841 nm respectively were used in the inversion. This data is adjusted using a bidirectional reflectance distribution function to model the values as if they were collected from a nadir view. Figure 5 shows the distinct seasonality in greenness which is represented by NDVI over the two sites. SCOPE models the full Nadir VSWIR spectral reflectance (400 to 2500 nm) from which values corresponding to the two MODIS reflectance bands are extracted and used concurrently with the observations in the inversion framework.

6.3 Retrieval Results for the Nebraska Mead-1 site

6.3.1 Site Description

The Nebraska Mead-1 site is a part of the Ameriflux network located in Lincoln, Nebraska and is one of the three cropland sites at the University of Nebraska Agricultural Research and Development Center[..[97]], with continuous data records from 2001 till present (Suyker et al., 2005). This site is a continuously irrigated corn (C_4 species) crop site, with mean annual precipitation

[96] removed: sites.

[97] removed: . The site has

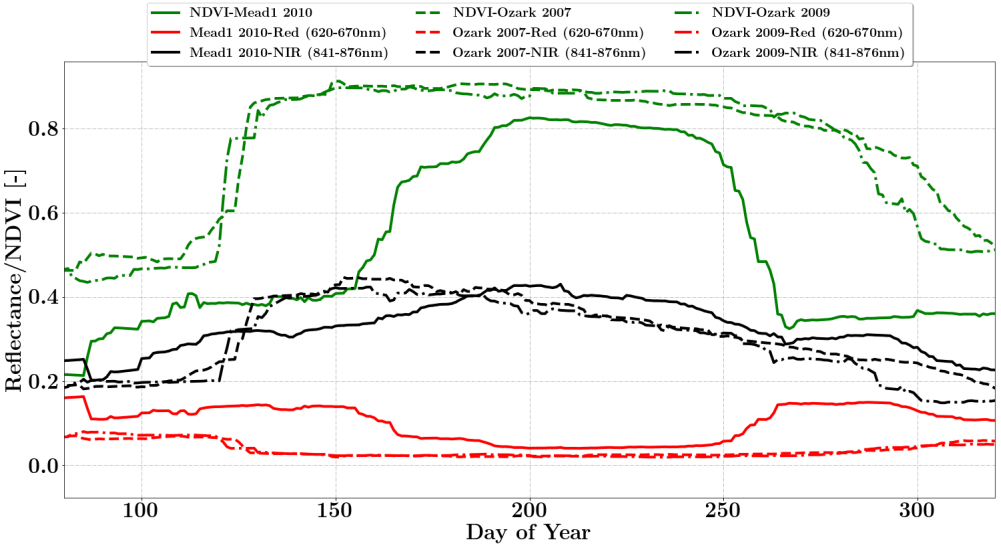

Figure 5. Figure showing the seasonal variability of Red, NIR MODIS Nadir Reflectance and NDVI for the Nebraska Mead1 and Missouri Ozark Site. This dataset is used in SCOPE model inversions in conjunction with fluxes of carbon and water for retrieval of ecosystem parameters.

of 790 mm and mean annual temperature of 10.07 °C. We choose the year 2010 and an hourly time resolution for the analysis. The site meteorology and forcing variables relevant to the SCOPE inversion retrievals are shown in Figure 6. The top two panels show the environmental forcing variables which are used as input (except precipitation) in the SCOPE simulations. The bottom panel represents carbon (GPP) and energy (LE, H) fluxes, which are used to construct the observation vector Y. [..[98]]The figure indicates that the growing season extends from around June through September, coinciding with high temperature, VPD and net radiation. We focus on the retrieval of the parameters V_{cmax}, BB_{slope} and LAI during this entire growing season.

	Prior State Vector			Prior Error (σ)			
Site	V_{cmax}	BB_{slope}	LAI	V_{cmax}	BB_{slope}	LAI	Duration (hrs)
Mead-1 (C_4)	50	[..[99]]7	4	30	5	[..[100]]3	9 - 16
Missouri Ozark (C_3)	[..[101]]50	4	2	20	5	1	10 - 14
Niwot Ridge (C_3)	80	4	3.8	20	5	10^{-5}	9 - 16

Table 1. Prior Values for LM Inversion (Units: V_{cmax}: [μ mols m^{-2} s^{-1}], BB_{slope}, LAI: [-]

[98] removed: We can clearly see

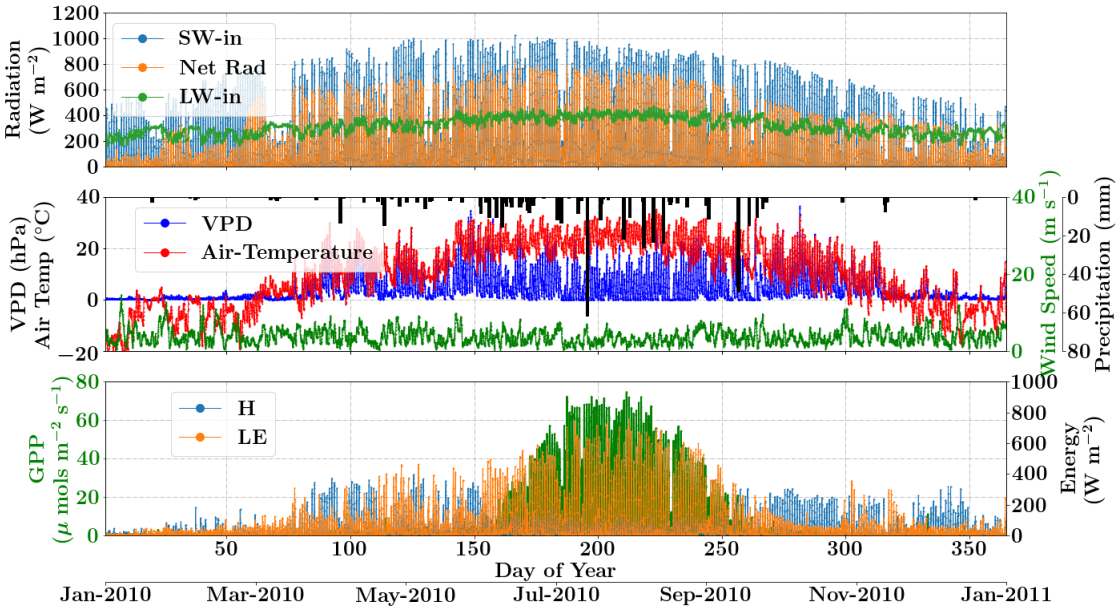

Figure 6. Figure showing the diurnal and seasonal variability of important environmental and meteorological forcings together with the tower observed fluxes of carbon and energy used in SCOPE model inversions for the Nebraska Mead flux tower site. The variables in the top and middle panels are used as inputs to the SCOPE model and the variables in bottom panel is used as a target in a moving window retrieval approach.

6.3.2 Inversion Parameters and Results

For each of the retrieval windows, the prior value of the state vector along with prior errors and day time duration, which is used for filtering the GPP and LE observations, are shown in Table 1. Here, we use a purely diagonal prior error covariance matrix, with zero off-diagonal elements. Figure 7 shows the retrievals of parameters V_{cmax}, BB_{slope} and LAI. The grey time series of GPP and LE values in the background are the actual filtered values used for constructing the observation (Y) [..[102]]vector corresponding to each retrieval window. The dashed lines indicate the retrieved parameters using only GPP and LE fluxes. The solid lines indicate the retrieved parameters using the fluxes together with MODIS reflectance. The brown (with fluxes only) and orange (with fluxes and MODIS red and NIR reflectance) lines show the result of posterior simulations of fluxes with the optimized parameters. These lines represent the absolute daily average posterior simulation errors ($\Delta = |\text{Observed} - \text{Posterior}|$) in the fluxes with and without the use of MODIS reflectance along with the flux observations in the inversions.

[102]removed: and modeled ($F(X)$) vectors

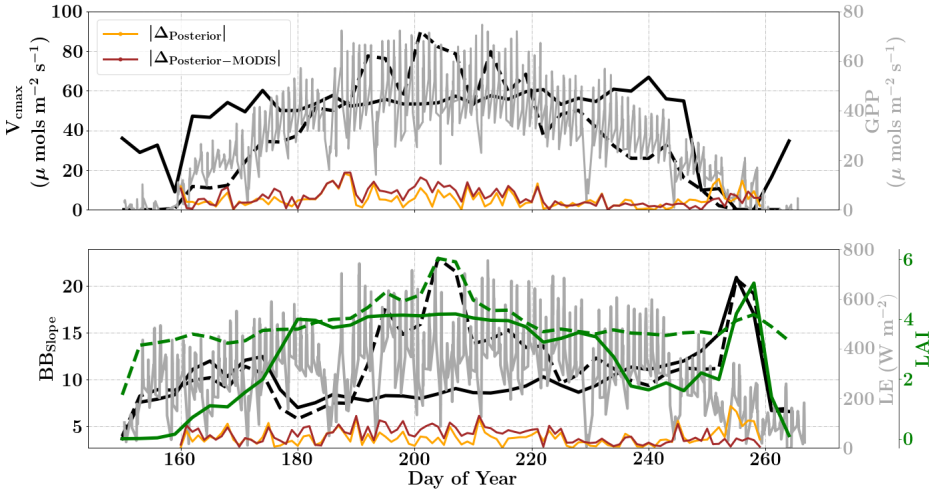

Figure 7. Figure showing the seasonal variability in retrieved parameter values of V_{cmax}, BB_{slope} and LAI for the Nebraska Mead-1 site using a 3-day moving window inversion approach for the year 2010. The actual points in the time series (grey lines) of the GPP and LE fluxes used as the target observations (Y) for the moving window inversion approach are shown in the background. The figure shows the comparison of the retrieved parameters using only GPP and LE fluxes (shown as dashed lines) as well as using a combination of fluxes and MODIS reflectance (shown as solid lines). The results show reasonable trends in the retrieved parameters along with their sensitivity to GPP and LE fluxes across the growing season.

We find a seasonal variability in the retrieved parameters, which follow a similar pattern in GPP or LE. [..[103]]In particular, the retrieved LAI as well as V_{cmax} shows a [..[104]]similar seasonality as GPP. There is also [..[105]]some variability in retrieved BB_{slope}[..[106]], which is correlated with LE observations. We found that including MODIS reflectance places better constraints on the parameters during the peak of the growing season, with much less variability in retrieved LAI and V_{cmax}.

As expected, the optimized parameters using just flux observations (dashed lines) are quite sensitive to the variation in GPP and LE, for example around DOY 190, 210 where there is sudden dip in the [..[107]]retrieved V_{cmax}. Including the MODIS reflectance (solid lines) in the inversions alleviates most of these large variability due to fluctuations in the observed fluxes or meteorology. Moreover, with this additional MODIS reflectance constraint the range of variability for all the three parameters V_{cmax}, BB_{slope} and LAI is more realistic. The comparison of posterior simulations (brown and orange lines)

[103] removed: The retrieved

[104] removed: very strong seasonality with

[105] removed: a considerable seasonality in

[106] removed: and LAI. The values during the growing season for the corn crop are found to be reasonable and realistic for all parameters. The LAI increases steadily from 2 to about 6 and then declines gradually.

[107] removed: fluxes. The large variability

indicate the net errors in the prediction of fluxes are almost similar in both cases (with and without MODIS reflectance) with the difference between the two, $\delta_\Delta \leq 15\%$ during the middle of the growing season. This may indicate that in this example there is an equifinality in the posterior simulation of fluxes with the retrieved parameters, which gets alleviated with the reflectance data. We find that the MODIS reflectance better constrains LAI during the beginning of the growing season between DOY 160 and 180. The unexpectedly large increases in BB_{slope} and LAI around DOY [..[108]]250-260 may be partially attributed to the largest rainfall events (see Fig. 6). Part of [..[109]]this variability and correlation between BB_{slope} and LAI may also be due to the diminishing role of soil evaporation (parameterized by a single resistance in SCOPE) with increasing LAI. Another part may be due to evaporation from the wet canopies which is not currently represented in SCOPE. This may cause the inversion to overestimate BB_{slope}, [..[110]]even though it would not represent the gas exchange [..[111]]through the stomata. From the inversion results it is clear that all three parameters V_{cmax}, BB_{slope} and LAI are much better constrained (with more realistic values and better seasonal variability) with the assimilation of reflectance data together with fluxes in the optimal estimation framework.

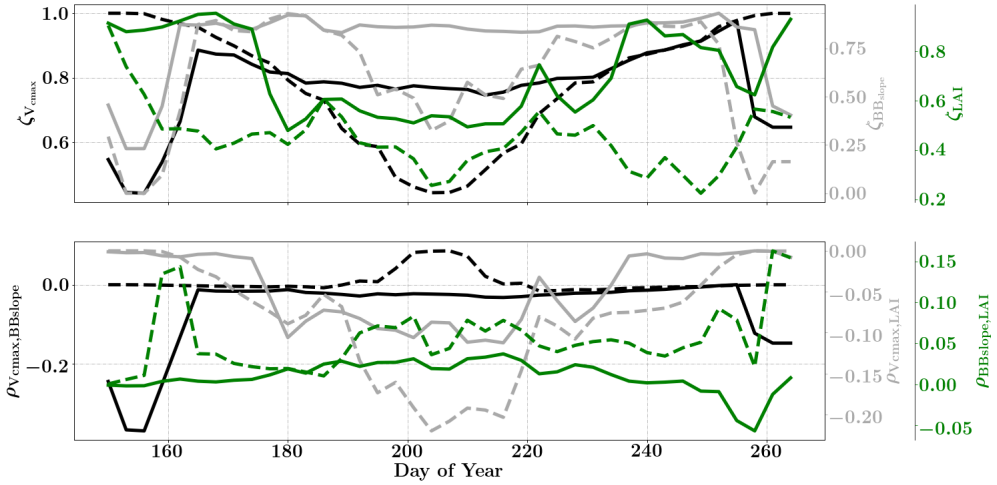

Figure 8. Figure showing the seasonal variability of the posterior error reduction (ζ) and correlation coefficient of the retrieved parameter values of V_{cmax}, BB_{slope} and LAI for the Nebraska Mead -1 site using a 3-day moving window inversion approach for the year 2010. The top panel shows the $\zeta_{V_{cmax}}$, $\zeta_{BB_{slope}}$ and ζ_{LAI} for the entire growing season and the bottom panels shows the correlation coefficients (normalized off-diagonal elements of posterior error covariance matrix) among these variables. The results of retrievals using only GPP and LE fluxes are shown as dashed lines and the results using a combination of fluxes and MODIS reflectance are shown as solid lines. Both the ζ and correlation coefficients are computed using the final Jacobian matrix at the end of each retrieval window.

[108] removed: 200 and DOY 260
[109] removed: the
[110] removed: but it may
[111] removed: between the stomataand the leaf surface

Figure 8 (top panel) shows the final posterior error reduction (ζ_i-eqn. 10) of the retrieval iterations for each moving window. The dashed lines indicate retrieval results using GPP, LE observations only and the solid lines shows retrievals that use reflectance observations in addition. The value of ζ_i is computed from the diagonal elements of the posterior error covariance matrix. We find a significant reduction in the posterior errors of the variables in the state vector. There is a strong seasonality in $\zeta_{\mathrm{V_{cmax}}}$ and [..[112]]ζ_{LAI} values and moderate to none for the [..[113]]$\zeta_{\mathrm{BB_{slope}}}$. It can be clearly seen that the posterior error reduction is significantly greater ($\sim 50\%$) when combining the reflectance data with the flux observations. The error reduction provides more confidence in the retrieved parameters, which are also more realistic. The posterior error covariance matrix also indicates whether the retrieved parameters are truly independent (as in the case of a diagonal matrix) or whether they co-vary (indicated by significant off-diagonal elements). The error correlation is given by [..[114]]$\rho_{x,y} = \frac{COV(x,y)}{\sigma_x \sigma_y}$ and should be considered when interpreting co-variations of retrieved parameters as the nature and magnitude of the associations between the variable pairs are true for the retrievals only and may or may nor represent the behavior of the variable pairs in nature due to different environmental conditions. Figure 8 (bottom panel) shows the growing season error correlation patterns between the three parameters from the retrievals. From the results which includes reflectance data with flux observations, it can be seen that during the peak growing season [..[115]]$\rho_{\mathrm{BB_{slope}},\mathrm{LAI}}$ and $\rho_{\mathrm{V_{cmax}},\mathrm{LAI}}$ have opposite signs indicating slightly positive and negative association between the variable pairs in the retrievals. These trends are also true when only flux data are used for the retrievals. However, in comparison [..[116]]$\rho_{\mathrm{V_{cmax}},\mathrm{BB_{slope}}}$ is mostly zero but has opposite signs with and without reflectance data and thus indicate both favorable and competing effects during the [..[117]]middle of the growing season. [..[118]]

[..[119]]

[112]removed: $\zeta_{\mathrm{BB_{slope}}}$

[113]removed: ζ_{LAI}. The

[114]removed: $r^2_{x,y} = \frac{COV(x,y)}{\sigma_x \sigma_y}$, it can be either positive or negative indicating whether the parameters move in the same or opposite direction. In general, high correlations indicate that we cannot fit these parameters independently.

[115]removed: $r^2_{\mathrm{BB_{slope}},\mathrm{LAI}}$ is positive indicating they are changing in sync and

[116]removed: $r^2_{\mathrm{V_{cmax}},\mathrm{LAI}}$ is negative indicating the counteracting influence of these variable pairs . However, $r^2_{\mathrm{V_{cmax}},\mathrm{BB_{slope}}}$ is positive until DOY 220 thereafter it is negative indicating

[117]removed: different parts

[118]removed: The error correlations $r^2_{\mathrm{BB_{slope}},\mathrm{LAI}}$ and $r^2_{\mathrm{V_{cmax}},\mathrm{LAI}}$ are stronger than $r^2_{\mathrm{V_{cmax}},\mathrm{BB_{slope}}}$. It is also found that the error correlations increase during the peak growing season.

[119]removed: Figure showing the evolution of the Jacobian Matrix for one retrieval window(DOY 213-216) for the Nebraska Mead-1 site in 2010. The normalized mismatch Y_{error} between the observation and modeled vector (observed minus modeled) for the 3-day window composed of GPP (indices 1-24) and LE (indices 25-48) time series concatenated together for each retrieval iteration is shown in panel (a). The normalized gradients of the forward model (SCOPE) with respect to the variables in the state vector after each update step of the LM algorithm are shown in the panels (b), (c) and (d) respectively. The gradient decreases with each iteration and the observations of GPP are weighed more for $\mathrm{V_{cmax}}$, Observations of LE more for $\mathrm{BB_{slope}}$ and both for the LAI retrievals.

[..[120]]Finally, Figure 9 demonstrates the net improvement in canopy GPP and LE fluxes due to the optimized state vector using flux observations only over their prior values. The first column represents the diurnal and seasonal variability in the time series of GPP and LE fluxes with optimized and unoptimized parameters and further its comparisons with flux tower values. The right column represents the one-to-one comparisons of the same. We find a significant improvement in the estimation of GPP (R^2 = 0.94) and the optimized parameters are able to capture the growing seasonal variability well as measured by flux tower observations (slope = 1.04). The improvement in modeling the fluxes with the posterior over the prior value of the state vector is also captured by the χ^2 error statistic ($\chi^2 = \sum_{i=0}^{k}((y_i - F(x_i))/\sigma_i)^2$) for the prior (unoptimized) and posterior (optimized) simulations. The corresponding values are $\chi^2_{GPP-opt} = 9382$, $\chi^2_{GPP-unopt} = 10728$, $\chi^2_{LE-opt} = 19235$ and $\chi^2_{LE-unopt} = 20554$.

[..[121]]

6.4 Retrieval Results for the Missouri Ozark site

6.4.1 Site Description

The Missouri Ozark site is also a part of the Ameriflux network and is located in the University of Missouri Baskett Wildlife Research area, situated in the Ozark region of central Missouri. It is uniquely located in the ecologically important transitional zone between the central hardwood region and the central grassland region of the US (Gu et al., 2006). This site has a mean annual precipitation of 986 mm and a mean annual temperature of 12.11 °C and has continuous data [..[122]]records from 2004 till present. It is a deciduous broadleaf forest site [..[123]]comprised of C_3 plant species. We use [..[124]]half hourly datasets from the year [..[125]]2007 and 2009 in the present analysis. The site meteorology and forcing variables relevant to the SCOPE inversion retrievals [..[126]]are shown in [..[127]]Figures S4 and S5 in the supplementary information. From the meteorological

[120]removed: Figure **??** shows the evolution of the Jacobian matrix for a typical retrieval window represented by DOY 213-216. The lines in the top panel (a) represent the concatenated normalized errors between the observation and modeled vector. It is found that the errors decrease monotonically with each retrieval iteration. The panels (b), (c) and (d) (Fig. **??**) represent the normalized gradients with respect to each variable in the state vector corresponding to each iteration step of the LM inversion approach in the retrieval window. The indices 1-24 on the x-axis represents the concatenated and filtered 3-day GPP and indices 25-48 represents the LE. We find that the gradients are not constant, decrease with each iteration step and has a somewhat diurnal structure to it, indicating the non-linear nature of the problem. Further, the influence of gradient values are higher in terms of V_{cmax} for GPP and BB_{slope} for LE and the values are very small for the vice-versa cases (also see Fig. 3). LAI appears to have interesting competing behavior with positive gradients for GPP and slightly negative for LAI although it varies with different iterations. Finally, figure 9 represents

[121]removed: Figure showing the diurnal and seasonal variability of important environmental and meteorological forcings together with the tower observed fluxes of carbon and energy used in SCOPE model inversions for the Missouri Ozark flux tower site. The variables in the top and middle panels are used as inputs to the SCOPE model and the variables in bottom panel is used as a target in a moving window retrieval approach.

[122]removed: record

[123]removed: comprising

[124]removed: the half hourly time resolution

[125]removed: 2010

[126]removed: for the year 2010

[127]removed: Figure **??**. The top two panels show the environmental forcing variables which (except precipitation) are used as input in the SCOPE model simulations. The bottom panel represents the observations of carbon (GPP) and energy (LE, H) fluxes which are used to construct the observation vector Y (composed of

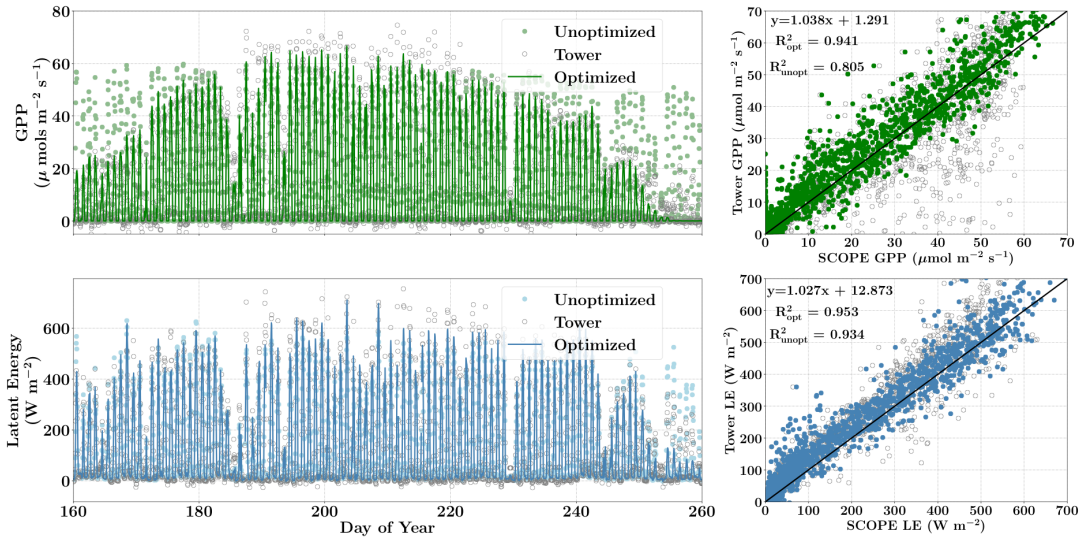

Figure 9. Figure showing the improvement in diurnal and seasonal variability in modeling the GPP and LE fluxes with optimized parameters over prior values using SCOPE for the Nebraska Mead-1 site for the year 2010. The figure also shows the one-to-one comparison (indicated by black-line) with the observed flux tower values. The optimization of the photosynthetic parameters improves the accuracy of computing the carbon and water fluxes as indicated by the R^2 value and the equation of the regression line.

data it can be seen that the year 2009 was a normal wet year and the year 2007 was a year with a midsummer drought around DOY 250. This is also reflected in observed GPP and LE [..[128]]fluxes with two distinct peaks in the growing season, caused by a late-summer drought and associated low productivity around DOY 250. This decrease in productivity is not distinguishable from the MODIS reflectance data in Fig. 5, which indicates that plants maintain greenness during this time, making this a unique test case for our inversion setup as the V_{cmax} fits reflect the a stress-factor as well, which is usually applied to downscale the physiological V_{cmax} during environmental stress. We focus on the retrieval of the parameters V_{cmax}, BB_{slope} and LAI during this entire [..[129]](longer) growing season. For both the years we demonstrate the parameter retrievals using GPP and LE fluxes only as well as compare our retrievals using additional constraints of MODIS red and NIR reflectances (Fig. 5).

[128]removed: data concatenated together) for each of the windowed inversions. We find that the growing seasonis longer for this site from around March, when the air temperatures starts to become positive and slightly warmer, till around November when the trees lose leaves and there is onset of the fall season. Site temperatures are quite high with high VPD around June and July. Again, we

[129]removed: longer

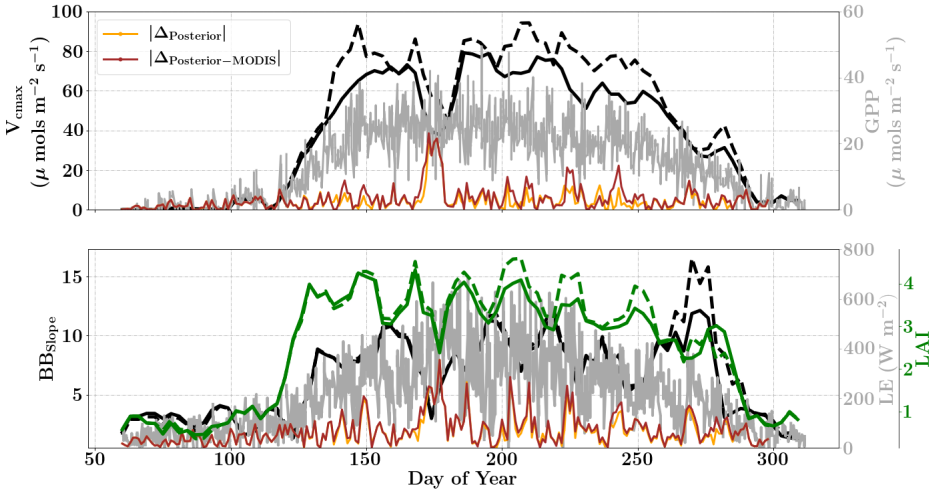

Figure 10. Figure showing the seasonal variability in retrieved parameter values of V_{cmax}, BB_{slope} and LAI for the Missouri Ozark site using a 3-day moving window inversion approach for the year [..[130]]2009. The actual points in the time series (grey lines) of the GPP and LE fluxes used as the target observations (Y) for the moving window inversion approach are shown in the background. The figure shows the comparison of the retrieved parameters using only GPP and LE fluxes (shown as dashed lines) as well as using a combination of fluxes and MODIS reflectance (shown as solid lines). The results show reasonable trends in the retrieved parameters along with their sensitivity to GPP and LE fluxes across the growing season.

6.4.2 Inversion Parameters and Results - Year 2009

The assumed prior value of the state vector[..[132]], prior errors and day time duration which is used for filtering the GPP and LE observations for the retrieval windows are shown in Table 1. [..[133]]Compared to Mead, the retrieval for this site is [..[134]]carried out over a much longer duration, covering almost the entire year.

[..[135]]Figure 10 (like Mead-1, Fig. 7) shows the comparison of parameter retrievals V_{cmax}, BB_{slope} and LAI using (i) only flux observations and (ii) flux observations combined with two MODIS reflectance bands. We find an overall strong

[132] removed: and

[133] removed: As for the Mead-1 site in the LM retrievals we have assumed the prior error covariance to be zero, along with the same assumptions for the initial guess of the state vector. Figure 10 shows the results for the retrieval of parameters V_{cmax}, BB_{slope} and LAI. The grey time series of GPP and LE values in the background are the actual values used for constructing the observation vector Y corresponding to each retrieval window for parameter retrieval. As indicated earlier the Ozark dataset is half hourly resolution therefore we have more number of observations to match the modeled fluxes in each of the retrieval windows. The retrieval for

[134] removed: also

[135] removed: Similar to the previous site, we find a strong seasonal variability in

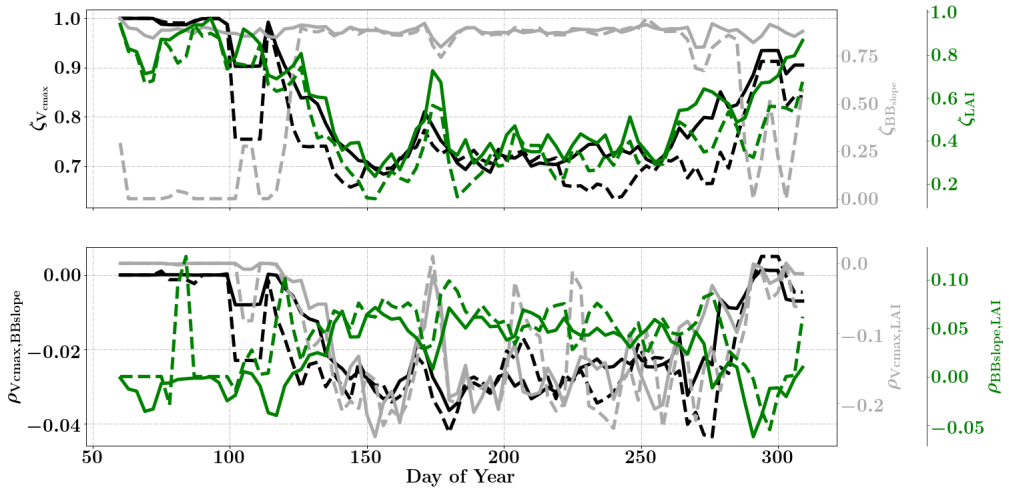

Figure 11. Figure showing the seasonal variability of the posterior error reduction (ζ) and correlation coefficient of the retrieved parameter values of V_{cmax}, BB_{slope} and LAI for the Missouri Ozark site using a 3-day moving window inversion approach for the year [..[131]]2009. The top panel shows the $\zeta_{V_{cmax}}$, $\zeta_{BB_{slope}}$ and ζ_{LAI} for the entire growing season and the bottom panels shows the correlation coefficients (normalized off-diagonal elements of posterior error covariance matrix) among these variables. The results of retrievals using only GPP and LE fluxes are shown as dashed lines and the results using a combination of fluxes and MODIS reflectance are shown as solid lines. Both the ζ and correlation coefficients are computed using the final Jacobian matrix at the end of each retrieval window.

seasonality with realistic values of V_{cmax}, BB_{slope} and LAI, following the patterns in GPP and LE. [..[136]]The beginning (and end) of the growing season shows increasing (decreasing) trends in V_{cmax} and LAI retrievals, which coincide well with the increase (decrease) in MODIS NDVI observations (Fig. 5). The [..[137]]retrieved LAI variability helps to explain the rapid appearance of new leaves in the spring [..[138]](March-April) and their disappearance around fall (October-November). The MODIS reflectance data helps to better constrain LAI and V_{cmax}, which is specifically evident around DOYs 140-150 and 200-250. The sharp increase in retrieved V_{cmax} when using just the flux observations around DOY 148 may be attributed to the sharp peaks in GPP, however the reflectance observations clearly help to better constrain the state vector. There are some issues with the retrieval for windows around DOY 175 and 275 (BB_{slope}), this may again correspond to the large precipitation (see supplementary information Fig. 4) events (e.g. overestimation of BB_{slope}) around these windows as well as sharp fluctuations in GPP and LE, respectively. This error in prediction of fluxes ($\Delta = |\text{Observed} - \text{Posterior}|$) is also

[136]removed: We also find a steady increase in BB_{slope} until it becomes constant with small fluctuations towards the middle of the year. The increasing trend in BB_{slope} around DOYs 160, 175, 230 and 250 may all be associated with individual (comparatively large) rainfall events around these days (see Fig. **??**

[137]removed: LAI evolves from near zero rapidly to around 4-5 in the March-April time frame, which indicate

[138]removed: time. The LAI also further remains nearly constant for most part of the growing season from around DOY 100 to 300. This can be explained by the fact that after the leaves are fully developed the LAI of the deciduous forest stand reaches its maximum value. It is observed that the inversion framework captures the seasonal variability in LAI

revealed by posterior simulations represented by brown and orange lines. Comparing the posterior simulations with and without the MODIS reflectance constraints with the prior reveals the net error to be of similar magnitude in both cases with $\delta_\Delta \leq 15\%$ during the growing season and indicating equifinality in the predicted fluxes with the parameter combinations. [..[139]]

[..[140]]Figure 11 shows the final posterior error reduction of the retrieval iterations for each moving window. It is found that there is significant reduction in the posterior errors for BB_{slope}[..[141]]. We find that $\zeta_{V_{cmax}}$ and [..[142]]ζ_{LAI} has the same trend and seasonality as that of retrieved V_{cmax} and LAI respectively. The evolution of the retrieval error correlations is again interesting and [..[143]]comparison with the Mead Corn-C_4 site using flux observations only show shows it is similar for $\rho_{V_{cmax},LAI}$ and $\rho_{BB_{slope},LAI}$ (negative and positive respectively) and different for $\rho_{V_{cmax},BB_{slope}}$ The correlations $\rho_{V_{cmax},BB_{slope}}$ and $\rho_{V_{cmax},LAI}$ are both negative indicating counteracting effects of these [..[144]]variables in the retrieval. In comparison[..[145]], $\rho_{BB_{slope},LAI}$ is positive for the retrievals indicating in-sync [..[146]]behavior. The error correlations $\rho_{V_{cmax},LAI}$ are highest among the three in the middle of the growing season[..[147]].

Finally, [..[148]]there is a significant improvement in the estimation of both GPP and LE fluxes [..[149]](see supplementary information Fig. S6) (R^2 = 0.7) with the optimized state vector over [..[150]]the prior values. The [..[151]]optimized state vector is able to capture the growing seasonal variability well (slope of regression lines: GPP = 0.97 and LE = 1.02). The un-optimized prior values severely under-predict both fluxes. The corresponding error measures $\chi^2_{GPP-opt} = 12975$, $\chi^2_{GPP-unopt} = 30070$, $\chi^2_{LE-opt} = 17260$ and $\chi^2_{LE-unopt} = 32283$ indicates that the inversion framework is able to retrieve the seasonal dynamics in the photosynthetic and canopy structural parameters for accurate prediction of the fluxes.

6.4.3 Inversion Results for Year 2007

The year 2007 for the Missouri Ozark site is an interesting example because the forest experiences a late summer drought and decrease in productivity, which is captured by the flux observations but not with phenology or greenness (see supplementary information Fig. S5, Fig. 12 and Fig. 5). The inversion setup, meteorological data resolution, initial guess

[139] removed: Figure showing the improvement in diurnal and seasonal variability in modeling the GPP and LE fluxes with optimized parameters over prior values using SCOPE for the Missouri Ozark site for the year 2010. The figure also shows the one-to-one comparison (indicated by black-line) with the observed flux tower values. The optimization of the photosynthetic parameters improves the accuracy of computing the carbon and water fluxes as indicated by the R^2 value and the equation of the regression line.

[140] removed: Figure **??**

[141] removed: and V_{cmax}

[142] removed: $\zeta_{BB_{slope}}$

[143] removed: very different from what we found for the Mead corn-C_4 case. The correlations $r^2_{V_{cmax},BB_{slope}}$ and $r^2_{V_{cmax},LAI}$

[144] removed: variable pairs

[145] removed: $r^2_{BB_{slope},LAI}$ is positive

[146] removed: or similar behaviortowards either positive or negative change. Both the error correlations $r^2_{V_{cmax},BB_{slope}}$ and $r^2_{V_{cmax},LAI}$ are high

[147] removed: with the later an order of magnitude higher, indicating the necessity for jointly optimizing this parameter pair. The error in LAI is high after around DOY 250, and so is its correlation with BB_{slope} indicating increased uncertainty for the period.

[148] removed: Figure **??** represents the net improvement in canopy

[149] removed: due to

[150] removed: their

[151] removed: left column represents the diurnal and seasonal variability in the time series of

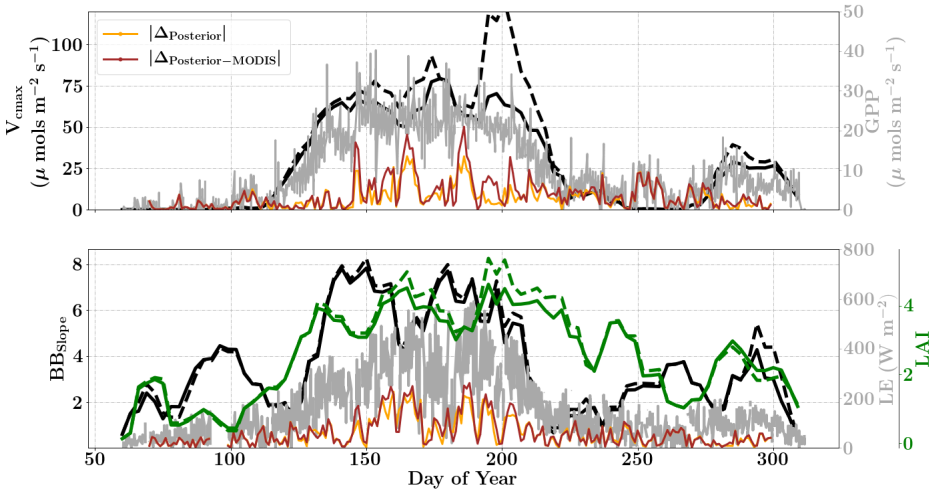

Figure 12. Figure showing the seasonal variability in retrieved parameter values of V_{cmax}, BB_{slope} and LAI for the Missouri Ozark site using a 3-day moving window inversion approach for the year 2007. The actual points in the time series (grey lines) of the GPP and LE fluxes used as the target observations (Y) for the moving window inversion approach are shown in the background. The figure shows the comparison of the retrieved parameters using only GPP and LE fluxes (shown as dashed lines) as well as using a combination of fluxes and MODIS reflectance (shown as solid lines). The results show reasonable trends in the retrieved parameters along with their sensitivity to GPP and LE fluxes across the growing season.

and prior errors for the year 2007 are similar to that of 2009. Figure 12 shows the results for the retrieval of parameters V_{cmax}, BB_{slope} and LAI from the inversion framework using (i) observations of GPP and LE fluxes ([..[152]]dashed line) and (ii) flux observations with MODIS reflectance bands (solid lines). The overall seasonality of the retrieved parameters reveals that the inversion framework is able to capture the late-summer drought. The mid season drought around DOY 230-250 is well captured by decreases in photosynthesis (V_{cmax}) and stomatal conductance (BB_{slope}). These parameters again increase from around DOY 260 after the drought recovery and also correlates well with the flux observations. However, the V_{cmax} variations shouldn't be confused with actual changes in Rubisco concentrations. Like many other carbon cycle models, the only way to impose environmental stress (apart from VPD and temperature) in SCOPE is to scale V_{cmax} with a stress-factor between 0-1. Our retrieved effective V_{cmax} is the product of a stress factor and the physiological V_{cmax}, which explains the large variations during drought here.

In contrast, the change in retrieved LAI during the period from DOY 240 to 300 is fairly gradual and reflects the phenology only. The addition of MODIS reflectance data constrains LAI (and in conjunction V_{cmax}) much better than than just the flux observations, which is clearly evident from the V_{cmax} retrievals around DOY 200. This large change in V_{cmax}

[152]removed: R^2 = 0.79) with optimized and unoptimized parameters and further its comparisons with flux tower values. The right column represents the one-to-one comparisons of the same. We find there is a significant improvement in the estimation of both

(when using just constraining flux observations) also corresponds to the single largest rainfall event of the season (see supplementary information Fig. S5) as well as a corresponding concurrent spike in productivity. The MODIS red and NIR reflectance unlike GPP and LE fluxes [..[153]]were insensitive to this short drought and provides better constraints on the LAI and V_{cmax} retrievals during this period. A comparison of modeled red and NIR reflectance from the SCOPE model with optimized parameters shows that it matches well with the observations (see supplementary information Fig. S8). There is excellent match in the red reflectance throughout the season, the NIR reflectance also matches well with the observations during the early-middle of the growing season (DOYs 130-250), during the post drought recovery phase the increase may be attributed to the increase in retrieved LAI. Apart from the drought period, the range and variability of all three parameters correspond well with the retrievals for the same site for the year 2009 presented earlier.

The posterior simulations excluding and including the MODIS observations (represented as orange and brown lines respectively in Fig. 12) indicate similar improvement in prediction of fluxes over their priors with $R^2_{GPP-opt}$ = [..[154]]0.7, $R^2_{GPP-unopt}$ = [..[155]]0.2, R^2_{LE-opt} = 0.5 and $R^2_{LE-unopt} = 0.1$. For the year 2007 it is also found that the posterior error reduction $\zeta_{V_{cmax}}$ and ζ_{LAI} is similar or slightly better compared to the year 2009 (See supplementary information Fig. S7). This again provides more confidence in the retrieved parameters and their temporal dynamics. As expected, the posterior error reduction is slightly better for all three parameters with the reflectance constraints during the middle of the growing season. The error correlations $\rho_{V_{cmax},BB_{slope}}$ and $\rho_{V_{cmax},LAI}$ for 2007 are both negative and similar in magnitude to that of year 2009. The error correlation structure for the year 2007 is different compared to the wet year 2009, especially during the middle of the growing season and may be attributed to the change in interaction between the state vector elements due to imposed drought stresses. We note that our moving window inversion setup using different observational streams is able to capture the [..[156]]ecosystem dynamics over the entire growing season as well as capture in season drought dynamics, which are not possible using traditional one-step seasonal or annual inversion approaches. Inversions like this will also help guide model parameterizations of stress impacts on the dynamic down-regulation of photosynthesis as a response to, e.g., changes in the soil matric potential.

Finally, we performed a sensitivity analyses of the newer temperature dependence implementation in SCOPE on the inversion retrieval results for the Ozark site [see supplementary section S2.1.2]. It is found that with the newer temperature dependence implementation and optimized parameters SCOPE is able to well capture V_{cmax} variations due to changes in the average canopy temperatures. There is a clear difference between the retrieved V_{cmax} with and without temperature dependence and the changes correlate with the implemented temperature response functions [see supplementary section S2.1.2]. The results of the posterior simulation on GPP and LE fluxes also indicate improvement with $\delta\chi^2$ error reduction of 3415 and 2104 for GPP and LE respectively.

[153]removed: with the optimized parameters. The optimized state vector is able to capture the growing seasonal variability well (slope of regression lines : GPP

[154]removed: 0.84 and LE

[155]removed: 0.98). The un-optimized prior values severely under-predict both fluxes. The optimal inversion method

[156]removed: seasonal dynamics in the photosynthetic and canopy structural parameters for accurate prediction of the fluxes

[..[157]]

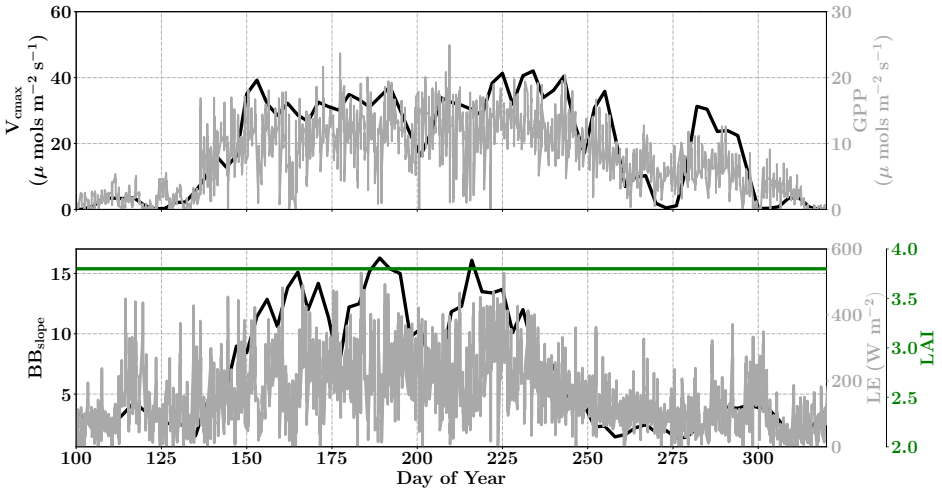

Figure 13. Figure showing the seasonal variability in retrieved parameter values of V_{cmax}, BB_{slope} and LAI for the Niwot Ridge site using a 3-day moving window inversion approach for the year 2010. The actual points in the time series (grey lines) of the GPP and LE fluxes used as the target observations (Y) for the moving window inversion approach are shown in the background. The results show reasonable trends in the retrieved parameters along with their sensitivity to GPP and LE fluxes across the growing season.

6.5 Retrieval Results for the Niwot Ridge Site

6.5.1 Site Description

The Niwot Ridge site is also a part of the Ameriflux network located in a subalpine forest ecosystem just below the continental divide near Nederland, Colorado. The average elevation of this site is 3050 m and is one of the high alpine evergreen needleleaf forests with C_3 plant species (Burns et al., 2016). This ecosystem is nearly 100 years old, thus very different from the Mead and the Ozark sites (Monson et al., 2002). This site has a mean annual precipitation of 800 mm and a mean annual temperature of 1.5 °C and has continuous data record from 1998 till present. This site is thus the coldest and driest among the three. [..[158]]We choose the year 2010 for the current analysis[..[159]], using half hourly flux data. The site meteorology and forcing variables relevant to the SCOPE inversion retrievals for the year 2010 are [..[160]]presented in the supplementary information Figure S10. The snow-cover at this site affects the energy exchanges and GPP for a large fraction of the year. The trees are evergreen and there is no [..[161]]well defined growing season but we find that [..[162]]most photosynthetic activity occurs in

[158]removed: Once again we

[159]removed: and we have used dataset at an half hourly time resolution

[160]removed: shown in Figure **??** which is very different from the previous two sites. The top two panels show the environmental forcing variables which (except precipitation) are used as input in the SCOPE model simulations. The bottom panel represents the observations of carbon (GPP) and energy (LE, H) fluxes which are used to construct the observation vector Y (composed of GPP and LE data concatenated together) for each of the windowed inversions

[161]removed: growing season although

[162]removed: the photosynthetic activity and fluxes of GPP are increasing

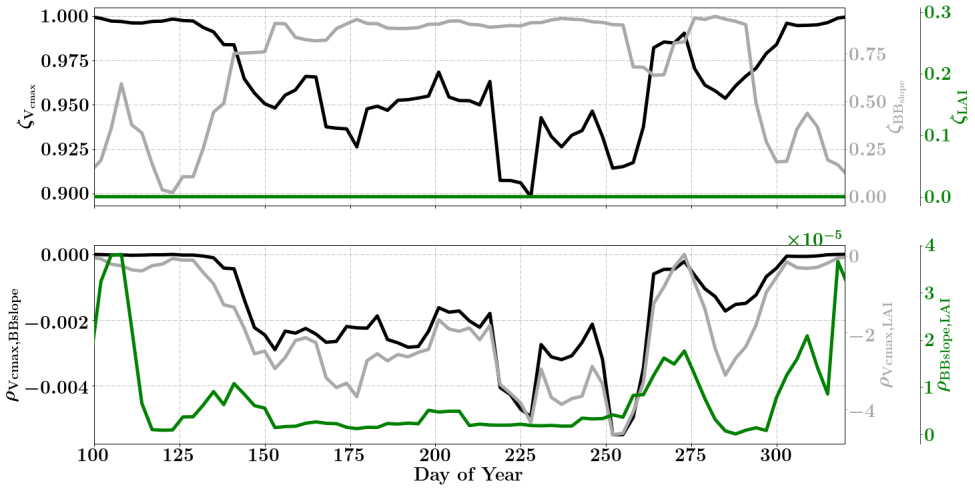

Figure 14. Figure showing the seasonal variability of the posterior error reduction (ζ) and correlation coefficient of the retrieved parameter values of V_{cmax}, BB_{slope} and LAI for the Niwot Ridge site using a 3-day moving window inversion approach for the year 2010. The top panel shows the $\zeta_{V_{cmax}}$, $\zeta_{BB_{slope}}$ and ζ_{LAI} for the entire growing season and the bottom panels shows the correlation coefficients (normalized off-diagonal elements of posterior error covariance matrix) among these variables. Both the ζ and correlation coefficients are computed using the final Jacobian matrix at the end of each retrieval window.

the period between May and October[..[163]], with a smaller flux magnitude compared to either the Mead or Ozark sites. The sensible heat at the site is also larger during this period compared to the latent heat fluxes. [..[164]]Since the LAI for the site does not really change over the year, we focus on the retrieval of the parameters V_{cmax} [..[165]]and BB_{slope} [..[166]]only from constraining GPP and LE fluxes, fixing the LAI.

6.5.2 Inversion Parameters and Results

For the retrievals the prior value of the state vector along with prior errors and day time duration used in the retrieval windows are shown in table 1. [..[167]]For this evergreen site, we [..[168]]assumed a prior value of LAI equal to 3.8 [..[169]](Monson et al.,

[163]removed: . Although the magnitudes are much smaller
[164]removed: We will focus on this period for
[165]removed: ,
[166]removed: and LAI from
[167]removed: Same as the earlier examples for the LM retrievals we have assumed the prior error covariance to be zero.
[168]removed: have
[169]removed: from previous literature (Monson et al., 2009) and assumed the prior error on LAI to be very small. This way, we set the LAIvalues to remain constant for the retrieval windows in the inversion framework

2009) with very low variance, effectively fixing the LAI, which improves the retrieval of the other state vector parameters [..[170]]as it reduces error co-variations.

Figure 13 shows the results for the retrieval of parameters V_{cmax}, BB_{slope} and LAI. The grey time series of GPP and LE in the background are the actual values used for constructing the observation vector Y corresponding to each retrieval window for parameter retrieval. [..[171]]The V_{cmax} values again follow [..[172]]similar trends as the GPP fluxes across the entire active season and the inversion captures the rise and fall in the GPP trends extremely well. The slight dip and rise in the 190-210 day period follows the GPP observational data and may be attributed to [..[173]]temperature and precipitation fluctuations. The BB_{slope} seems to closely follow [..[174]]variations in LE fluxes and captures the seasonality well. However, we should note that changes in soil evaporation might alias into the retrieval of the BB_{slope}, especially at Niwot Ridge.

Figure 14 shows the final posterior error reduction of the retrieval iterations for each moving window. [..[175]]The posterior error reductions for BB_{slope} and V_{cmax} are [..[176]]high throughout the year, likely attributable to a constant LAI used for this example (e.g. at vanishing LAI in winter for deciduous ecosystems, the Jacobians of fluxes with respect to physiological parameters will be meaningless and vanish as well, thereby reducing error reductions). The evolution of the error correlations follows similar [..[177]]trends as in the [..[178]]Missouri Ozark C_3 site. We find [..[179]]$\rho_{V_{cmax},BB_{slope}}$ and $\rho_{V_{cmax},LAI}$ are both negative and [..[180]]$\rho_{BB_{slope},LAI}$ is positive. There is a sharp discontinuity around DOY 250-260 in terms of $\zeta_{BB_{slope}}$ and [..[181]]$\rho_{V_{cmax},LAI}$, $\rho_{V_{cmax},BB_{slope}}$, probably due to quality and/or discontinuity in the observational fluxes and environmental forcings. The prior and posterior simulations (with unoptimized and optimized parameters respectively) show overall net improvement of the flux predictions when compared to tower observations with $R^2_{GPP-opt}$ = 0.85, $R^2_{GPP-unopt}$ = 0.79, R^2_{LE-opt} = 0.52 and $R^2_{LE-unopt} = 0.49$. The corresponding error measures are $\chi^2_{GPP-opt} = 38971$, $\chi^2_{GPP-unopt} = 22085$, $\chi^2_{LE-opt} = 63865$ and $\chi^2_{LE-unopt} = 68463$. The high χ^2 values for posterior GPP over the prior may indicate that the posterior simulation may not capture some periods in the simulation where the observed fluxes are higher than average (which were probably captured with high prior value of V_{cmax}). This may also be due to model structural issues where stress induced due to snow processes are not accurately represented in SCOPE (with a stress factor in V_{cmax}). Further, we have an additional constraint of near constant LAI, while we have found that GPP is very sensitive to LAI. In this case the inversion has to fit GPP by mainly varying the V_{cmax}, which gives it less degrees of

[170] removed: . In the future, other observables such as near-infrared reflectance could be used to add constraints on LAI, which will help decouple correlated errors

[171] removed: As indicated earlier the LAI value is maintained constant by setting a very low prior error in the inversion framework.

[172] removed: the similar trend

[173] removed: consecutive cloudy days. The trends in

[174] removed: the

[175] removed: It is found that the posterior error reduction

[176] removed: significantly high and almost zero for the LAI (as expected).We find that V_{cmax} has a similar trend in error reduction and correlation with both BB_{slope} and LAI , although they are two orders of magnitude different. This is attributed to very low prior error on LAI used for this example

[177] removed: trend

[178] removed: previous

[179] removed: $r^2_{V_{cmax},BB_{slope}}$ and $r^2_{V_{cmax},LAI}$

[180] removed: $r^2_{BB_{slope},LAI}$

[181] removed: $r^2_{V_{cmax},LAI}$, $r^2_{V_{cmax},BB_{slope}}$ this is

freedom and may not yield the most optimal solution. For instance, changes in the fraction of direct vs. diffuse light is not fully represented in our model (apart from changing PAR) but could affect the overall PAR value incident at the top of canopy as well as the overall light interception, as there are considerable gaps between canopies.

7 Discussion and Conclusion

Our results demonstrate the feasibility of a moving window inversion approach for [..[182]]the retrieval of key ecosystem parameters [..[183]]using eddy covariance flux tower observations. In addition, we also demonstrated that red and NIR spectral reflectance observation from satellites adds better constraints on LAI, and thereby also improves the retrievals of V_{cmax} and BB_{slope} by reducing interferences in retrieved parameters. The moving window retrieval approach is [..[184]]specifically useful for dynamic changes in ecosystem parameters, such as the response to environmental stress due to water stress, which we observed during a summer drought at the Ozark flux tower site.

There is strong evidence from measurements that under normal conditions both LAI and photosynthetic parameters have seasonal variability (Wang et al., 2008; Wilson and Baldocchi, 2000; Wilson et al., 2000), which correlate with [..[185]]energy fluxes. Our model inversion results are in alignment and agree well with these [..[186]]findings. From our results, we find considerable seasonal variability in V_{cmax} and BB_{slope} (to some extent). Previously, many studies have reported measured V_{cmax} values of similar ranges such as, 0-70 μ mols m^{-2} s^{-1} (Wilson et al., 2000) for deciduous trees and 0-80 μ mols m^{-2} s^{-1} as annual variability in tall Japanese red pine forests (Han et al., 2004). In addition, most of the V_{cmax} variability is found in systems, which have seasonally variable or constant Nitrogen (N) content (Wilson et al., 2000). These changes may be mostly attributed to substantial in-season changes in the fraction of total N allocated to Rubisco as well as changes in leaf mass per area (Wilson et al., 2000). In addition, most models including SCOPE have no other method of imposing environmental stress than reducing V_{cmax} by a stress factor [0,1]. The effect of reductions in V_{cmax} are a reduction in assimilation, which also suppresses transpiration. Thus, we are fitting an *'effective'* V_{cmax} parameter, which factors in effects from true changes in Rubisco content as well as the impact of environmental stress. It has been shown that there is also possibility to have large seasonality variability in BB_{slope} (15 to 25) values (Wolf et al., 2006). The SCOPE model handles both the C_3 and C_4 photosynthetic pathways and could thus be applied to study a wide variety of ecosystems. We demonstrate the approach here for climate and productivity gradients across agricultural, deciduous broadleaf forest and sub-alpine evergreen forest ecosystems.

[182] removed: successful

[183] removed: by constraining the SCOPE modeled carbon and water fluxes with

[184] removed: a novel method for the retrieval of the seasonal parameter variability. The SCOPE model handles both the C_3 and C_4 photosynthetic pathways and could thus be applied to study a wide variety of ecosystems. We demonstrate the approach here for climate and productivity gradients across agricultural, deciduous broadleaf forest and sub-alpine evergreen forest ecosystems

[185] removed: observations of

[186] removed: observations.

[..[187]]The framework demonstrates the feasibility of the approach in parameter retrievals using suitable apriori uncertainty on state vector and observation noise. The uncertainty in surface energy balance closure has been generally reported to be around 10-30% (Wilson et al., 2002; von Randow et al., 2004; Sánchez et al., 2010) and is found to be dependent on time-scales due to differences in energy storage terms in ecosystems (Reed et al., 2018). Apart from observations, it should also be noted that filtering and quality control may be necessary for the meteorological and/or forcing fluxes as artifacts in the data can influence the inversion and optimization and greatly affects the results.

[..[188]]In the current implementation, the inversion approach may not properly retrieve the key parameters for ecosystems for which the underlying forward model (SCOPE) may have deficiencies in process representation. For example, there are competing optimality theories between whether the BB_{slope} (Van der Tol et al., 2008b, a; MÄKELÄ et al., 1996) or V_{cmax} (Xu and Baldocchi, 2003) is most affected by drought during growing season. An improvement in the current framework in the form of better process representation (and parameterization) of the soil moisture status in the stomatal conductance model within SCOPE may improve the results and could serve as a test-bed for improvements in process representations. In this case, it could be through the implementation of leaf water potential (Tuzet et al., 2003) or an optimality approach between water loss and carbon gain (Medlyn et al., 2011; Katul et al., 2009).

While this paper focuses on the conceptual inversion framework, demonstrating a novel approach for estimating important ecosystem parameters in short time windows for modeling the dynamics of coupled carbon and water fluxes across ecosystems[..[189]], there are opportunities for improving the overall inversion approach to better estimate the parameters. SCOPE allows us to ingest a variety of other [..[190]]observables to constrain the parameters space, including spectrally resolved reflectance (which can constrain LAI and chlorophyll content) as well as thermal emissions (which constrain LE) and SIF (which constrains APAR and V_{cmax}). [..[191]]Global time series of SIF observations, which provide a direct probe into photosyn-

[187] removed: The developed Bayesian optimal inversion framework in SCOPE is flexible to incorporate other constraining fluxes and variables as well as other elements in the state vector to be optimized. SIF and visible to shortwave reflectance data are examples of such constraining observations, which are also obtained from SCOPE model simulations. Global time series of SIF observations, which provide a direct probe into photosynthetic machinery are becoming available from space based (Frankenberg et al., 2014; Guanter et al., 2014; Frankenberg et al., 2011) and ground based observations (Frankenberg et al., 2016). Further, the retrieval framework could also be used to retrieve the photosynthetic temperature dependency parameters such as entropies and activation energies, which are even harder to measure directly but might be crucial, especially as the modeling of the ecosystem response to a warming climate mostly neglects potential changes in temperature dependencies of V_{cmax}. Our ongoing and future research efforts aims to address these questions by incorporating these newer observations(Zhang et al., 2014) with carbon and water fluxes in the inversion framework. The Jacobians from our inversion results indicate that the optimal estimation is non-linear and therefore requires an iterative solution. Our Bayesian non-linear estimation allows us to compute accurate posterior uncertainty estimates.

[188] removed: It should be mentioned that our study

[189] removed: . However

[190] removed: observable

[191] removed: In addition, in the current implementation the inversion approach may not optimize and retrieve the key parameters well for ecosystems undergoing drought with limited soil water availability. An example is a typical mid-summer drought leading to a stomatal closure or productivity maximums being reached in the early morning hours which has a large phase difference with the diurnal PAR forcing. We hypothesize these may be due to some deficiencies in the process representation in SCOPE. There are competing optimality theories between whether the BB_{slope} (Van der Tol et al., 2008b, a; MÄKELÄ et al., 1996) or V_{cmax} (Xu and Baldocchi, 2003) is most affected by drought during growing season. An improvement in the current frameworkcould be better process representation of the soil moisture status in the stomatal conductance model within SCOPE either through implementation of leaf water potential

thetic machinery are now available from space based (Frankenberg et al., 2014; Guanter et al., 2014; Frankenberg et al., 2011) and ground based observations (Frankenberg et al., 2016). It will also be important to quantify the respective information content for the observables within the framework, which can vary depending on the state vector itself as the Jacobians from our inversion results indicate that the inverse system is non-linear.

Our Bayesian inversion framework is highly flexible in terms of allowing an arbitrary number of prior and retrieval parameters, which could be tuned for better estimation of the key ecosystem parameters with accurate posterior uncertainty estimates. The step-wise [..[192]]LM optimization framework with the SCOPE model also automatically weighs the carbon and water fluxes towards optimal state vector estimation without any predefined [..[193]]constraints (Wolf et al., 2006) for particular parameters. [..[194]]Further, the Bayesian retrieval framework could also be used to retrieve the photosynthetic temperature dependency parameters such as entropies and activation energies, which are even harder to measure directly but might be crucial, especially as the modeling of the ecosystem response to a warming climate mostly neglects potential changes in temperature dependencies of V_{cmax}. Our ongoing and future research efforts aims to utilize the developed framework to address these questions by incorporating newer observations and making use of the full potential of SCOPE.

Code and data availability. The authors thank the AmeriFlux team for making the eddy-covariance flux data available for this study. The FLUXNET2015 datasets used in this study have been downloaded from the FLUXNET community data portal (http://fluxnet.fluxdata.org/data/fluxnet2015-dataset/). The version of SCOPE model used in this study can be obtained from https://github.com/Christiaanvandertol/SCOPE.

Appendix A: Modeling Photosynthesis in SCOPE

The biochemical module is at the center of energy balance computations within SCOPE. This module computes the net assimilation (photosynthesis), stomatal conductance and the chlorophyll fluorescence of a leaf. This module is thus extremely important because the coupled photosynthesis and stomatal conductance regulates the latent heat flux which in turn affects the net energy balance and the leaf temperature, which in turn again affects the leaf photosynthesis and subsequently the energy balance. SCOPE computes the leaf temperature and the overall energy balance iteratively such that they there is closure in energy balance. As such the leaf temperature and its regulation of photosynthesis forms an extremely important component

(Tuzet et al., 2003) or optimality approach between water loss and carbon gain (Medlyn et al., 2011). Our inversion framework which jointly constrains both parameters may then be able to provide a better solution in drought conditions which is a subject for future investigation

[192] removed: optimization approach within SCOPE

[193] removed: constraining measures (Wolf et al., 2006) towards

[194] removed: The developed method also emphasizes the need to be able to compute the Jacobian matrices numerically for complex biophysical models, perhaps as an auxiliary but important output for general carbon cycle and terrestrial ecosystem modeling paradigms, which could facilitate inversions and error characterization on a global scale.

of the overall energy balance of the canopy. [..[195]]We have adapted photosynthetic model together with coupled temperature dependence of the photosynthetic parameters according to the implementation in CLM4.5. This includes both the temperature dependence functions and the high temperature inhibition of the parameters. The model includes exclusive pathways both for the C_3 and C_4 plant species and is represented as follows:

The net photosynthesis (assimilation) after accounting for respiration (R_d) is given as:

$$A_n = \min(A_c, A_j, A_p) - R_d \tag{A1}$$

Further, the rate limiting steps are represented as follows:

The RuBP carboxylase (Rubisco) limited rate of carboxylation A_c is given by:

$$A_c = \begin{cases} \frac{V_{cmax}(C_i - \Gamma^*)}{C_i + K_c(1+O_i/K_o)}, & \text{for } C_3 \text{ species.} \\ V_{cmax}, & \text{for } C_4 \text{ species.} \end{cases} \tag{A2}$$

The light-limited rate of carboxylation (governed by the capacity to regenerate RuBP) A_j is given by:

$$A_j = \begin{cases} \frac{J(C_i - \Gamma^*)}{4(C_i + 2\Gamma^*)}, & \text{for } C_3 \text{ species.} \\ \alpha(4.6\phi), & \text{for } C_4 \text{ species.} \end{cases} \tag{A3}$$

Finally the product limited carboxylation rate for C_3 plants and the PEP-carboxylase-limited rate of carboxylation for the C_4 plants A_p is given by:

$$A_p = \begin{cases} 3T_p, & \text{for } C_3 \text{ species.} \\ k_p C_i, & \text{for } C_4 \text{ species.} \end{cases} \tag{A4}$$

For the above equations A2, A3, A4, we have the assimilation rates $A_{c,j,p}$ in the units of μmols m^{-2} s^{-1}, C_i is the internal CO_2 concentration of the leaf (units of ppm) and V_{cmax} is the maximum rate of carboxylation. For the C_3 species, K_c and K_o are the Michelis-Menten constants for CO_2 and O_2 respectively (units of μmols m^{-2} s^{-1}), Γ^* is the CO_2 compensation point (units are ppm), J is the potential electron transport rate (units of μmols m^{-2} s^{-1}) and T_p is the triose phosphate utilization rate. For the C_4 plants, ϕ is the absorbed PAR in the units of Wm^{-2} and the factor 4.6 converts it to PPFD in units of μmol m^{-2} s^{-1} (for SCOPE biochem module the PAR is already in PPFD units), α is the quantum efficiency (0.05 mol CO_2 mol^{-1} photon), and k_p is the initial slope of the C_4 CO_2 response curve.

[195]removed: In this study we have made changes to the biochemical module of SCOPE to make it consistent with the widely used CLM4.5.

For the C_3 plants, the potential electron transport rate J depends on the PAR absorbed by a leaf, which is obtained as the smaller root of the two roots of the equation:

$$\Theta_{PSII}J^2 - (I_{PSII} + Jmax)J + I_{PSII}J_{max} = 0 \tag{A5}$$

Where, J_{max} is the maximum electron transport rate (μmols m^{-2} s^{-1}), I_{PSII} is the light used in photosystem II (μmols m^{-2} s^{-1}) which is given by eqn. A6 and Θ_{PSII} is a curvature parameter.

$$I_{PSII} = 0.5\Phi_{PSII}(4.6\phi) \tag{A6}$$

The term Φ_{PSII} in eqn. A6 is the quantum yield of photosystem II and 0.5 represents half electron transfer to each of the photosystems I and II. The overall gross photosynthesis rate is computed as a co-limitation (Collatz et al., 1991a, 1992) and is computed as the smaller root of the equations:

$$\begin{aligned}&\Theta_{cj}A_i^2 - (A_c + A_j)A_i + A_cA_j = 0\\ &\Theta_{ip}A^2 - (A_i + A_p)A + A_iA_p = 0\end{aligned} \tag{A7}$$

The parameters Θ_{cj} and Θ_{ip} control the smoothness of the light response curve between light limited and enzyme/product limiting rates. The values of the different parameters at optimum temperature (mostly as a function of V_{cmax25} here the optimum temperature, is assumed as $25°C$) used in the photosynthesis model are presented in Table A1

Parameter	$\mathbf{C}_3$	$\mathbf{C}_4$
R_d^{opt}	$0.015V_{cmax}^{opt}$	$0.025V_{cmax25}$
J_{max}^{opt}	$1.97V_{cmax}^{opt}$	-
K_c^{opt}	404.9	-
K_o^{opt}	278.4	-
Γ_{opt}^*	$\frac{0.5OV_oK_c}{V_cK_c}$	-
T_p^{opt}	$0.1182V_{cmax}^{opt}$	-
Θ_{PSII}	0.7	-
Φ_{PSII}	0.85	-
k_p^{opt}	-	$20000V_{cmax}^{opt}$
Θ_{cj}	0.98	0.80
Θ_{ip}	0.95	0.95

Table A1. Functional forms of photosynthesis equation parameters

Appendix B: Temperature Dependence of Photosynthetic Parameters

The photosynthesis model parameters for both the C_3 and C_4 pathways described in the previous section and shown in Table A1 have temperature dependent variations and need to be adjusted for specific leaf temperature before implementing them in the photosynthesis model. The temperature dependence of photosynthetic parameters for the C_3 species can be broadly decomposed into two parts (i) the temperature response and (ii) the high temperature inhibition. The functional form of these are as follows:

$$
\begin{aligned}
f(T_v) &= exp\left[\frac{H_a}{RT_0}(1-\frac{T_0}{T_v})\right] \\
f_H(T_v) &= \frac{1+exp\left(\frac{S_vT_0-H_d}{RT_0}\right)}{1+exp\left(\frac{S_vT_v-H_d}{RT_v}\right)}
\end{aligned}
\tag{B1}
$$

Where, H_a is the activation energy, H_d is the deactivation energy, S_v is the entropy term, T_o is the optimum temperature and T_v is the leaf temperature. The functional relationship of the different photosynthetic parameters in the C_3 pathway are as follows:

$$
\begin{aligned}
V_{cmax} &= V_{cmax}^{opt} f(T_v) f_H(T_v) \\
J_{max} &= J_{max}^{opt} f(T_v) f_H(T_v) \\
T_p &= T_p^{opt} f(T_v) f_H(T_v) \\
R_d &= R_d^{opt} f(T_v) f_H(T_v) \\
K_c &= K_c^{opt} f(T_v) \\
K_o &= K_o^{opt} f(T_v) \\
\Gamma^* &= \Gamma^*_{opt} f(T_v)
\end{aligned}
\tag{B2}
$$

The temperature dependence of photosynthetic parameters for the C_4 species are given by the following relationships:

$$
\begin{aligned}
V_{cmax} &= V_{cmax}^{opt}\left[\frac{f(Q_{10})}{f_U(T_v)f_L(T_v)}\right] \\
f(Q_{10}) &= Q_{10}^{(T_v-T_0)/10} \\
f_U(T_v) &= 1+exp(s_1(T_v-s_2)) \\
f_L(T_v) &= 1+exp(s_3(s_4-T_v))
\end{aligned}
\tag{B3}
$$

$$
R_d = R_d^{opt}\left[\frac{f(Q_{10})}{f_U(T_v)}\right] \tag{B4}
$$

$$k_p = k_p^{opt} f(Q_{10}) \tag{B5}$$

The Q_{10} temperature coefficient is a measure of the rate of change of a biological or chemical system as a consequence of increasing the temperature by 10°C. The values of the temperature dependence functional parameters for both C_3 and C_4 species used in the present study are provided in tables B1 and B2 respectively.

Parameter	H_a (J mol^{-1})	H_d (J mol^{-1})	S_v (J mol^{-1} K^{-1})	T_0 (K)
V_{cmax}	65330	14920	485	298
J_{max}	43540	152040	495	298
T_p	65330	14920	485	298
R_d	46390	150650	490	298
K_c	79430	-	-	298
K_o	36380	-	-	298
Γ^*	37830	-	-	298

Table B1. C_3 Temperature dependence functional parameters

Parameter	Q_{10} (-)	s_1 (K^{-1})	s_2 (K)	s_3 (K^{-1})	s_4 (K)
V_{cmax}	2	0.3	313.15	0.2	288.15
R_d	2	1.3	328.15	-	-
k_p	2	-	-	-	-

Table B2. C_4 Temperature dependence functional parameters

The temperature dependence parameters (activation, deactivation and entropy) is variable between different plant species (Leuning, 2002) as such its formulation in the newer implementation of the SCOPE model allows us to use appropriate values depending on the ecosystem we study.

B1 A-Ci-g_s Iterations

The final solution for photosynthesis requires an iterative solution of the coupled equations representing (i) the Farquhar, von Caemmerer and Berry (FvCB) model (Farquhar et al., 1980) for the photosynthesis rate (A), (ii) Fick's law of diffusion (Eqn. B6) for internal (C_i) and leaf surface (C_s) CO_2 concentration and (iii) Ball-Berry stomatal conductance model (Ball et al., 1987) (Eqn. B7) for stomatal conductance (g_s) to obtain stable converging solutions.

$$C_i = C_s - 1.6\frac{A}{g_s}, \quad \text{(from Fick's Law)} \tag{B6}$$

$$g_s = g_0 + BB_{slope}\frac{Ar_h}{C_s}, \quad \text{(Ball-Berry model)} \tag{B7}$$

In Eqn. B7, BB_{slope} represents the Ball-Berry slope, r_h the relative humidity and g_0 the Ball-Berry intercept. In the absence of an initial specification of C_i, we make the assumption that $g_0 = 0$ in Eqn. B7, then combining equations B6, B7, the initial estimate of C_i is given as:

$$C_i = \max(f_{Ci}^{min} C_s, C_s - 1.6\frac{C_s r_h}{BB_{slope}}) \tag{B8}$$

where f_{Ci}^{min} is the assumed minimum fractional leaf boundary layer CO_2 (assumed as 0.3 for C_3 and 0.1 for C_4 species). This initial estimate of C_i is used to again estimate the photosynthesis based on the FvCB model (Farquhar et al., 1980), followed by estimation of stomatal conductance using the Ball-Berry model Eqn. B7. Finally, the Newton-Raphson method is used to obtain a forward estimation of the new value of internal CO_2 concentration (Sun et al., 2012; Ivanov et al., 2008). The updated C_i is further used in the $A - g_s - C_i$ until convergence.

Appendix C: Derivation of Iterative Retrieval Algorithm

For deriving the maximum probability state X ($\hat{X}$) we equate the derivative of the equation 5 to zero to obtain:

$$\nabla_X\{-2\ln P(X|Y)\} = -[\nabla_X F(X)]^T S_\epsilon^{-1}[Y - F(X)] + S_a^{-1}[X - X_a] = 0 \tag{C1}$$

It can be noted here that the gradient ∇_X of the above vector valued function is a matrix valued function and the Jacobian matrix is represented as: $K(X) = \nabla_X F(X)$ and which results in the following implicit equation for $\hat{X}$:

$$-K^T(X)S_\epsilon^{-1}[Y - F(X)] + S_a^{-1}[X - X_a] = 0 \tag{C2}$$

We have to now use any general root finding method for finding the solutions of equation C2. If the problem is not too non-linear we can use the Newton and Gauss-Newton iterative methods (Hartley, 1961). In general for any vector equation $G(X) = 0$, we can write the Newton iteration as follows:

$$X_{i+1} = X_i - [\nabla_X G(X_i)]^{-1} G(X_i) \tag{C3}$$

For our problem we can assume the derivative of the cost-function $G(X)$ to be the LHS of equation C1, therefore the gradient of $G(X)$ (∇G) also known as the Hessian is given by:

$$\nabla_X G(X) = S_a^{-1} + K^T S_\epsilon^{-1} K - [\nabla_X K^T] S_\epsilon^{-1}[Y - F(X)] \tag{C4}$$

The Hessian in equation C4 involves the Jacobian K and both the first and second derivatives of the forward model. The second derivative is complicated because it is a vector whose elements are matrices and further this term is post multiplied by the factor $S_\epsilon^{-1}[Y - F(X)]$. The third term in the RHS of equation C4 is thus computationally expensive and further for moderately linear problems this term is small, as such this term can be ignored (also called small-residual problems in numerical methods). When we ignore this term, we get the Gauss-Newton iteration scheme by substituting equations C2 and C4 in equation C3:

$$X_{i+1} = X_i + (S_a^{-1} + K_i^T S_\epsilon^{-1} K_i)^{-1}[K_i^T S_\epsilon^{-1}[Y - F(X_i)] - S_a^{-1}[X_i - X_a]] \tag{C5}$$

where, $K_i = K(X_i)$, we can substitute $F(X)$ from equation 4 in equation C2 to get:

$$-K^T(\hat{X})S_\epsilon^{-1}[Y - F(X)_{X=X_l} + \nabla_X F(X)_{X=X_l}(X - X_l)] + S_a^{-1}[\hat{X} - X_a] = 0 \tag{C6}$$

Again, representing $K_l = \nabla_X F(X)_{X=X_l}$, $F_l = F(X)_{X=X_l}$ we can further simplify and rearrange equation C6 as:

$$\begin{aligned} &S_a^{-1}[\hat{X} - X_a] + K_l^T S_\epsilon K_l(\hat{X} - X_a) = K_l S_\epsilon^{-1}[Y - F_l + K_l(X_l - X_a)] \\ &\hat{X} = X_a + (S_a^{-1} + K_l^T S_\epsilon^{-1} K_l)^{-1} K_l S_\epsilon^{-1}[Y - F_l + K_l(X_l - X_a)] \end{aligned} \tag{C7}$$

In the above equations, if we change the interpretation of the subscript l from 'linearization' to 'iteration counter', we obtain the following equation:

$$X_{i+1} = X_a + (S_a^{-1} + K_i^T S_\epsilon^{-1} K_i)^{-1} K_i S_\epsilon^{-1}[Y - F(X_i) + K_i(X_i - X_a)] \tag{C8}$$

If we express X_{i+1} as a departure from X_i rather than X_a we obtain the same expression for the iteration steps as equation C5 or 6.

Competing interests. The authors declare no competing interests.

Acknowledgements. AmeriFlux site Missouri Ozark (US-MOz) is supported by the US Department of Energy (DOE), Office of Science, Office of Biological and Environmental Research Program, through Oak Ridge National Laboratory's Terrestrial Ecosystem Science-Science Focus Area; ORNL is managed by UT-Battelle, LLC, for DOE under contract DE-AC05-00OR22725.

The research was carried out, in part, at the Jet Propulsion Laboratory, California Institute of Technology, under a contract with the National Aeronautics and Space Administration. California Institute of Technology. Government sponsorship is acknowledged. ©2018. All rights reserved.

References

Baldocchi, D.: An analytical solution for coupled leaf photosynthesis and stomatal conductance models, Tree Physiology, 14, 1069–1079, 1994.

Baldocchi, D., Valentini, R., Running, S., Oechel, W., and Dahlman, R.: Strategies for measuring and modelling carbon dioxide and water vapour fluxes over terrestrial ecosystems, Global change biology, 2, 159–168, 1996.

Baldocchi, D., Kelliher, F. M., Black, T. A., and Jarvis, P.: Climate and vegetation controls on boreal zone energy exchange, Global Change Biology, 6, 69–83, 2000.

Baldocchi, D., Falge, E., Gu, L., Olson, R., Hollinger, D., Running, S., Anthoni, P., Bernhofer, C., Davis, K., Evans, R., et al.: FLUXNET: A new tool to study the temporal and spatial variability of ecosystem–scale carbon dioxide, water vapor, and energy flux densities, Bulletin of the American Meteorological Society, 82, 2415–2434, 2001.

Ball, J. T., Woodrow, I. E., and Berry, J. A.: A model predicting stomatal conductance and its contribution to the control of photosynthesis under different environmental conditions, in: Progress in photosynthesis research, pp. 221–224, Springer, 1987.

Beerling, D. and Quick, W.: A new technique for estimating rates of carboxylation and electron transport in leaves of C3 plants for use in dynamic global vegetation models, Global Change Biology, 1, 289–294, 1995.

Bernacchi, C. J., Singsaas, E. L., Pimentel, C., Portis Jr, A. R., and Long, S. P.: Improved temperature response functions for models of Rubisco-limited photosynthesis, Plant, Cell & Environment, 24, 253–259, 2001.

Bonan, G. B., Lawrence, P. J., Oleson, K. W., Levis, S., Jung, M., Reichstein, M., Lawrence, D. M., and Swenson, S. C.: Improving canopy processes in the Community Land Model version 4 (CLM4) using global flux fields empirically inferred from FLUXNET data, Journal of Geophysical Research: Biogeosciences, 116, 2011.

Burns, S. P., Maclean, G. D., Blanken, P. D., Oncley, S. P., Semmer, S. R., and Monson, R. K.: The niwot ridge subalpine forest US-NR1 ameriflux site–part 1: Data acquisition and site record-keeping, Geoscientific Instrumentation, Methods and Data Systems, 2016.

Chen, J. M., Rich, P. M., Gower, S. T., Norman, J. M., and Plummer, S.: Leaf area index of boreal forests: Theory, techniques, and measurements, Journal of Geophysical Research: Atmospheres, 102, 29 429–29 443, 1997.

Collatz, G., Ball, J., Grivet, C., and Berry, J. A.: Physiological and environmental regulation of stomatal conductance, photosynthesis and transpiration: a model that includes a laminar boundary layer, Agricultural and Forest Meteorology, 54, 107 – 136, https://doi.org/https://doi.org/10.1016/0168-1923(91)90002-8, http://www.sciencedirect.com/science/article/pii/0168192391900028, 1991a.

Collatz, G. J., Ball, J. T., Grivet, C., and Berry, J. A.: Physiological and environmental regulation of stomatal conductance, photosynthesis and transpiration: a model that includes a laminar boundary layer, Agricultural and Forest meteorology, 54, 107–136, 1991b.

Collatz, G. J., Ribas-Carbo, M., and Berry, J.: Coupled photosynthesis-stomatal conductance model for leaves of C4 plants, Functional Plant Biology, 19, 519–538, 1992.

Cox, P. M., Pearson, D., Booth, B. B., Friedlingstein, P., Huntingford, C., Jones, C. D., and Luke, C. M.: Sensitivity of tropical carbon to climate change constrained by carbon dioxide variability, Nature, 494, 341, 2013.

Cramer, W., Bondeau, A., Woodward, F. I., Prentice, I. C., Betts, R. A., Brovkin, V., Cox, P. M., Fisher, V., Foley, J. A., Friend, A. D., et al.: Global response of terrestrial ecosystem structure and function to CO2 and climate change: results from six dynamic global vegetation models, Global change biology, 7, 357–373, 2001.

Dai, Y., Dickinson, R. E., and Wang, Y.-P.: A two-big-leaf model for canopy temperature, photosynthesis, and stomatal conductance, Journal of Climate, 17, 2281–2299, 2004.

Dutta, D., Wang, K., Lee, E., Goodwell, A., Woo, D. K., Wagner, D., and Kumar, P.: Characterizing Vegetation Canopy Structure Using Airborne Remote Sensing Data, IEEE Transactions on Geoscience and Remote Sensing, 55, 1160–1178, 2017.

Falkowski, P., Scholes, R., Boyle, E., Canadell, J., Canfield, D., Elser, J., Gruber, N., Hibbard, K., Högberg, P., Linder, S., et al.: The global carbon cycle: a test of our knowledge of earth as a system, science, 290, 291–296, 2000.

Farquhar, G. v., von Caemmerer, S. v., and Berry, J.: A biochemical model of photosynthetic CO2 assimilation in leaves of C3 species, planta, 149, 78–90, 1980.

Flexas, J., Escalona, J. M., Evain, S., Gulías, J., Moya, I., Osmond, C. B., and Medrano, H.: Steady-state chlorophyll fluorescence (Fs) measurements as a tool to follow variations of net CO2 assimilation and stomatal conductance during water-stress in C3 plants, Physiologia plantarum, 114, 231–240, 2002.

Frankenberg, C., Fisher, J. B., Worden, J., Badgley, G., Saatchi, S. S., Lee, J.-E., Toon, G. C., Butz, A., Jung, M., Kuze, A., et al.: New global observations of the terrestrial carbon cycle from GOSAT: Patterns of plant fluorescence with gross primary productivity, Geophysical Research Letters, 38, 2011.

Frankenberg, C., O'Dell, C., Berry, J., Guanter, L., Joiner, J., Köhler, P., Pollock, R., and Taylor, T. E.: Prospects for chlorophyll fluorescence remote sensing from the Orbiting Carbon Observatory-2, Remote Sensing of Environment, 147, 1–12, 2014.

Frankenberg, C., Drewry, D., Geier, S., Verma, M., Lawson, P., Stutz, J., and Grossmann, K.: Remote sensing of solar induced Chlorophyll Fluorescence from satellites, airplanes and ground-based stations, in: Geoscience and Remote Sensing Symposium (IGARSS), 2016 IEEE International, pp. 1707–1710, IEEE, 2016.

Friedlingstein, P., Cox, P., Betts, R., Bopp, L., von Bloh, W., Brovkin, V., Cadule, P., Doney, S., Eby, M., Fung, I., et al.: Climate–carbon cycle feedback analysis: results from the C4MIP model intercomparison, Journal of climate, 19, 3337–3353, 2006.

Gu, L., Meyers, T., Pallardy, S. G., Hanson, P. J., Yang, B., Heuer, M., Hosman, K. P., Riggs, J. S., Sluss, D., and Wullschleger, S. D.: Direct and indirect effects of atmospheric conditions and soil moisture on surface energy partitioning revealed by a prolonged drought at a temperate forest site, Journal of Geophysical Research: Atmospheres, 111, 2006.

Guanter, L., Zhang, Y., Jung, M., Joiner, J., Voigt, M., Berry, J. A., Frankenberg, C., Huete, A. R., Zarco-Tejada, P., Lee, J.-E., et al.: Global and time-resolved monitoring of crop photosynthesis with chlorophyll fluorescence, Proceedings of the National Academy of Sciences, 111, E1327–E1333, 2014.

Han, Q., Kawasaki, T., Nakano, T., and Chiba, Y.: Spatial and seasonal variability of temperature responses of biochemical photosynthesis parameters and leaf nitrogen content within a Pinus densiflora crown, Tree physiology, 24, 737–744, 2004.

Hartley, H. O.: The modified Gauss-Newton method for the fitting of non-linear regression functions by least squares, Technometrics, 3, 269–280, 1961.

Heimann, M. and Reichstein, M.: Terrestrial ecosystem carbon dynamics and climate feedbacks, Nature, 451, 289, 2008.

Houborg, R., Soegaard, H., and Boegh, E.: Combining vegetation index and model inversion methods for the extraction of key vegetation biophysical parameters using Terra and Aqua MODIS reflectance data, Remote Sensing of Environment, 106, 39–58, 2007.

Ivanov, V. Y., Bras, R. L., and Vivoni, E. R.: Vegetation-hydrology dynamics in complex terrain of semiarid areas: 1. A mechanistic approach to modeling dynamic feedbacks, Water Resources Research, 44, 2008.

Jacquemoud, S., Baret, F., Andrieu, B., Danson, F., and Jaggard, K.: Extraction of vegetation biophysical parameters by inversion of the PROSPECT+ SAIL models on sugar beet canopy reflectance data. Application to TM and AVIRIS sensors, Remote sensing of environment, 52, 163–172, 1995.

Katul, G., Manzoni, S., Palmroth, S., and Oren, R.: A stomatal optimization theory to describe the effects of atmospheric CO2 on leaf photosynthesis and transpiration, Annals of Botany, 105, 431–442, 2009.

Knorr, W. and Heimann, M.: Uncertainties in global terrestrial biosphere modeling: 1. A comprehensive sensitivity analysis with a new photosynthesis and energy balance scheme, Global Biogeochemical Cycles, 15, 207–225, 2001.

Knorr, W. and Kattge, J.: Inversion of terrestrial ecosystem model parameter values against eddy covariance measurements by Monte Carlo sampling, Global Change Biology, 11, 1333–1351, 2005.

Kucharik, C. J., Foley, J. A., Delire, C., Fisher, V. A., Coe, M. T., Lenters, J. D., Young-Molling, C., Ramankutty, N., Norman, J. M., and Gower, S. T.: Testing the performance of a dynamic global ecosystem model: water balance, carbon balance, and vegetation structure, Global Biogeochemical Cycles, 14, 795–825, 2000.

Lawrence, D. M., Oleson, K. W., Flanner, M. G., Thornton, P. E., Swenson, S. C., Lawrence, P. J., Zeng, X., Yang, Z.-L., Levis, S., Sakaguchi, K., et al.: Parameterization improvements and functional and structural advances in version 4 of the Community Land Model, Journal of Advances in Modeling Earth Systems, 3, 2011.

Leuning, R.: Temperature dependence of two parameters in a photosynthesis model, Plant, Cell & Environment, 25, 1205–1210, 2002.

Leuning, R., Van Gorsel, E., Massman, W. J., and Isaac, P. R.: Reflections on the surface energy imbalance problem, Agricultural and Forest Meteorology, 156, 65–74, 2012.

Levenberg, K.: A method for the solution of certain non-linear problems in least squares, Quarterly of applied mathematics, 2, 164–168, 1944.

Liu, J., Bowman, K. W., Schimel, D. S., Parazoo, N. C., Jiang, Z., Lee, M., Bloom, A. A., Wunch, D., Frankenberg, C., Sun, Y., et al.: Contrasting carbon cycle responses of the tropical continents to the 2015–2016 El Niño, Science, 358, eaam5690, 2017.

Mackay, D. S., Ewers, B. E., Loranty, M. M., Kruger, E. L., and Samanta, S.: Bayesian analysis of canopy transpiration models: a test of posterior parameter means against measurements, Journal of Hydrology, 432, 75–83, 2012.

MÄKELÄ, A., BERNINGER, F., and HARI, P.: Optimal control of gas exchange during drought: theoretical analysis, Annals of Botany, 77, 461–468, 1996.

Marquardt, D. W.: An algorithm for least-squares estimation of nonlinear parameters, Journal of the society for Industrial and Applied Mathematics, 11, 431–441, 1963.

McGuire, A., Sitch, S., Clein, J. S., Dargaville, R., Esser, G., Foley, J., Heimann, M., Joos, F., Kaplan, J., Kicklighter, D., et al.: Carbon balance of the terrestrial biosphere in the twentieth century: Analyses of CO2, climate and land use effects with four process-based ecosystem models, Global Biogeochemical Cycles, 15, 183–206, 2001.

McGuire, A., Wirth, C., Apps, M., Beringer, J., Clein, J., Epstein, H., Kicklighter, D., Bhatti, J., Chapin Iii, F., De Groot, B., et al.: Environmental variation, vegetation distribution, carbon dynamics and water/energy exchange at high latitudes, Journal of Vegetation Science, 13, 301–314, 2002.

Medlyn, B. E., Duursma, R. A., Eamus, D., Ellsworth, D. S., Prentice, I. C., Barton, C. V., Crous, K. Y., De Angelis, P., Freeman, M., and Wingate, L.: Reconciling the optimal and empirical approaches to modelling stomatal conductance, Global Change Biology, 17, 2134–2144, 2011.

Monson, R., Turnipseed, A., Sparks, J., Harley, P., Scott-Denton, L., Sparks, K., and Huxman, T.: Carbon sequestration in a high-elevation, subalpine forest, Global Change Biology, 8, 459–478, 2002.

Monson, R. K., Prater, M. R., Hu, J., Burns, S. P., Sparks, J. P., Sparks, K. L., and Scott-Denton, L. E.: Tree species effects on ecosystem water-use efficiency in a high-elevation, subalpine forest, Oecologia, 162, 491–504, 2009.

Monteith, J. and Unsworth, M.: Principles of environmental physics, Academic Press, 2007.

Myneni, R. B., Ramakrishna, R., Nemani, R., and Running, S. W.: Estimation of global leaf area index and absorbed PAR using radiative transfer models, IEEE Transactions on Geoscience and remote sensing, 35, 1380–1393, 1997.

Oleson, K., Lawrence, D., Bonan, G., Drewniak, B., Huang, M., Koven, C., Levis, S., Li, F., Riley, W., Subin, Z., et al.: Technical description of version 4.5 of the Community Land Model (CLM), 420 pp., doi: 10.5065, 2013.

Oleson, K. W., Lawrence, D. M., Gordon, B., Flanner, M. G., Kluzek, E., Peter, J., Levis, S., Swenson, S. C., Thornton, E., Feddema, J., et al.: Technical description of version 4.0 of the Community Land Model (CLM), 2010.

Pappas, C., Fatichi, S., Leuzinger, S., Wolf, A., and Burlando, P.: Sensitivity analysis of a process-based ecosystem model: Pinpointing parameterization and structural issues, Journal of Geophysical Research: Biogeosciences, 118, 505–528, 2013.

Quaife, T., Lewis, P., De Kauwe, M., Williams, M., Law, B. E., Disney, M., and Bowyer, P.: Assimilating canopy reflectance data into an ecosystem model with an Ensemble Kalman Filter, Remote Sensing of Environment, 112, 1347–1364, 2008.

Reed, D. E., Frank, J. M., Ewers, B. E., and Desai, A. R.: Time dependency of eddy covariance site energy balance, Agricultural and Forest Meteorology, 249, 467–478, 2018.

Reichstein, M., Rey, A., Freibauer, A., Tenhunen, J., Valentini, R., Banza, J., Casals, P., Cheng, Y., Grünzweig, J. M., Irvine, J., et al.: Modeling temporal and large-scale spatial variability of soil respiration from soil water availability, temperature and vegetation productivity indices, Global biogeochemical cycles, 17, 2003.

Ricciuto, D. M., Davis, K. J., and Keller, K.: A Bayesian calibration of a simple carbon cycle model: The role of observations in estimating and reducing uncertainty, Global biogeochemical cycles, 22, 2008.

Rodgers, C. D.: Inverse methods for atmospheric sounding: theory and practice, vol. 2, World scientific, 2000.

Rogers, A., Medlyn, B. E., Dukes, J. S., Bonan, G., Caemmerer, S., Dietze, M. C., Kattge, J., Leakey, A. D., Mercado, L. M., Niinemets, Ü., et al.: A roadmap for improving the representation of photosynthesis in Earth system models, New Phytologist, 213, 22–42, 2017.

Running, S. W. and Coughlan, J. C.: A general model of forest ecosystem processes for regional applications I. Hydrologic balance, canopy gas exchange and primary production processes, Ecological modelling, 42, 125–154, 1988.

Sánchez, J., Caselles, V., and Rubio, E.: Analysis of the energy balance closure over a FLUXNET boreal forest in Finland, Hydrology and Earth System Sciences, 14, 1487–1497, 2010.

Schaaf, C. and Wang, Z.: MCD43A4 MODIS/Terra+ Aqua BRDF/Albedo Nadir BRDF Adjusted RefDaily L3 Global 500 m V006, NASA EOSDIS Land Processes DAAC, https://doi.org/10.5067/MODIS/MCD43A4.006, 2015.

Schimel, D. S.: Terrestrial ecosystems and the carbon cycle, Global change biology, 1, 77–91, 1995.

Schulze, E., Kelliher, F. M., Korner, C., Lloyd, J., and Leuning, R.: Relationships among maximum stomatal conductance, ecosystem surface conductance, carbon assimilation rate, and plant nitrogen nutrition: a global ecology scaling exercise, Annual Review of Ecology and Systematics, 25, 629–662, 1994.

Simioni, G., Gignoux, J., Le Roux, X., Appé, R., and Benest, D.: Spatial and temporal variations in leaf area index, specific leaf area and leaf nitrogen of two co-occurring savanna tree species, Tree Physiology, 24, 205–216, 2004.

Sitch, S., Smith, B., Prentice, I. C., Arneth, A., Bondeau, A., Cramer, W., Kaplan, J., Levis, S., Lucht, W., Sykes, M. T., et al.: Evaluation of ecosystem dynamics, plant geography and terrestrial carbon cycling in the LPJ dynamic global vegetation model, Global Change Biology, 9, 161–185, 2003.

Sitch, S., Huntingford, C., Gedney, N., Levy, P., Lomas, M., Piao, S., Betts, R., Ciais, P., Cox, P., Friedlingstein, P., et al.: Evaluation of the terrestrial carbon cycle, future plant geography and climate-carbon cycle feedbacks using five Dynamic Global Vegetation Models (DGVMs), Global Change Biology, 14, 2015–2039, 2008.

Sitch, S., Friedlingstein, P., Gruber, N., Jones, S., Murray-Tortarolo, G., Ahlström, A., Doney, S. C., Graven, H., Heinze, C., Huntingford, C., et al.: Recent trends and drivers of regional sources and sinks of carbon dioxide, Biogeosciences, 12, 653–679, 2015.

Sun, Y., Gu, L., and Dickinson, R. E.: A numerical issue in calculating the coupled carbon and water fluxes in a climate model, J. Geophys. Res., 117, n/a–n/a, 2012.

Suyker, A. E., Verma, S. B., Burba, G. G., and Arkebauer, T. J.: Gross primary production and ecosystem respiration of irrigated maize and irrigated soybean during a growing season, Agricultural and Forest Meteorology, 131, 180–190, 2005.

Tanaka, K., Kosugi, Y., and Nakamura, A.: Impact of leaf physiological characteristics on seasonal variation in CO2, latent and sensible heat exchanges over a tree plantation, Agricultural and Forest Meteorology, 114, 103–122, 2002.

Tuzet, A., Perrier, A., and Leuning, R.: A coupled model of stomatal conductance, photosynthesis and transpiration, Plant, Cell & Environment, 26, 1097–1116, 2003.

Van der Tol, C., Dolman, A., Waterloo, M., and Meesters, A.: Optimum vegetation characteristics, assimilation, and transpiration during a dry season: 2. Model evaluation, Water resources research, 44, 2008a.

Van der Tol, C., Meesters, A., Dolman, A., and Waterloo, M.: Optimum vegetation characteristics, assimilation, and transpiration during a dry season: 1. Model description, Water resources research, 44, 2008b.

van der Tol, C., Verhoef, W., Timmermans, J., Verhoef, A., and Su, Z.: An integrated model of soil-canopy spectral radiances, photosynthesis, fluorescence, temperature and energy balance, Biogeosciences, 6, 3109–3129, 2009.

Verhoef, W., Jia, L., Xiao, Q., and Su, Z.: Unified optical-thermal four-stream radiative transfer theory for homogeneous vegetation canopies, IEEE Transactions on Geoscience and Remote Sensing, 45, 1808–1822, 2007.

von Randow, C., Manzi, A. O., Kruijt, B., De Oliveira, P., Zanchi, F., Silva, R., Hodnett, M., Gash, J., Elbers, J., Waterloo, M., et al.: Comparative measurements and seasonal variations in energy and carbon exchange over forest and pasture in South West Amazonia, Theoretical and Applied Climatology, 78, 5–26, 2004.

Wang, Q., Iio, A., Tenhunen, J., and Kakubari, Y.: Annual and seasonal variations in photosynthetic capacity of Fagus crenata along an elevation gradient in the Naeba Mountains, Japan, Tree physiology, 28, 277–285, 2008.

Wang, Y.-P. and Leuning, R.: A two-leaf model for canopy conductance, photosynthesis and partitioning of available energy I:: Model description and comparison with a multi-layered model, Agricultural and Forest Meteorology, 91, 89–111, 1998.

Wilson, K., Goldstein, A., Falge, E., Aubinet, M., Baldocchi, D., Berbigier, P., Bernhofer, C., Ceulemans, R., Dolman, H., Field, C., et al.: Energy balance closure at FLUXNET sites, Agricultural and Forest Meteorology, 113, 223–243, 2002.

Wilson, K. B. and Baldocchi, D. D.: Seasonal and interannual variability of energy fluxes over a broadleaved temperate deciduous forest in North America, Agricultural and Forest Meteorology, 100, 1–18, 2000.

Wilson, K. B., Baldocchi, D. D., and Hanson, P. J.: Spatial and seasonal variability of photosynthetic parameters and their relationship to leaf nitrogen in a deciduous forest, Tree Physiology, 20, 565–578, 2000.

Wolf, A., Akshalov, K., Saliendra, N., Johnson, D. A., and Laca, E. A.: Inverse estimation of Vc max, leaf area index, and the Ball-Berry parameter from carbon and energy fluxes, Journal of Geophysical Research, 111, 1–18, 2006.

Wramneby, A., Smith, B., Zaehle, S., and Sykes, M. T.: Parameter uncertainties in the modelling of vegetation dynamics?effects on tree community structure and ecosystem functioning in European forest biomes, Ecological Modelling, 216, 277–290, 2008.

Wu, X., Luo, Y., Weng, E., White, L., Ma, Y., and Zhou, X.: Conditional inversion to estimate parameters from eddy-flux observations, Journal of Plant Ecology, 2, 55–68, 2009.

Wullschleger, S. D.: Biochemical limitations to carbon assimilation in C3 plants—a retrospective analysis of the A/Ci curves from 109 species, Journal of Experimental Botany, 44, 907–920, 1993.

Xu, L. and Baldocchi, D. D.: Seasonal trends in photosynthetic parameters and stomatal conductance of blue oak (Quercus douglasii) under prolonged summer drought and high temperature, Tree physiology, 23, 865–877, 2003.

Xu, T., White, L., Hui, D., and Luo, Y.: Probabilistic inversion of a terrestrial ecosystem model: Analysis of uncertainty in parameter estimation and model prediction, Global Biogeochemical Cycles, 20, 2006.

Zaehle, S., Sitch, S., Smith, B., and Hatterman, F.: Effects of parameter uncertainties on the modeling of terrestrial biosphere dynamics, Global Biogeochemical Cycles, 19, 2005.

Zhang, Y., Guanter, L., Berry, J. A., Joiner, J., Tol, C., Huete, A., Gitelson, A., Voigt, M., and Köhler, P.: Estimation of vegetation photosynthetic capacity from space-based measurements of chlorophyll fluorescence for terrestrial biosphere models, Global change biology, 20, 3727–3742, 2014.